DEPOSITION AND DIAGENESIS OF THE LOWER CRETACEOUS ANTLERS SANDSTONE ON THE YOUNG RANCH, NOLAN COUNTY, TEXAS

by

LEONARD WAYNE WOOD, B.S.

A THESIS

IN

GEOSCIENCE

Submitted to the Graduate Faculty
of Texas Tech University in
Partial Fulfillment of
the Requirements for
the Degree of

MASTER OF SCIENCE

Approved

Chairperson of the Committee

Accepted

Dean of the Graduate School

December, 2001

ACKNOWLEDGEMENTS

I would like to express my appreciation to Dr. George B. Asquith for his constant guidance, assistance, and encouragement during my tenure at Tech. He has been a second father to me and a great teacher; his influence has truly shaped my life. I am also grateful to my graduate committee, Dr. Tom Lehman and Dr. Moira Ridley, for their assistance and review of my thesis. I would like to thank R.T. Winn, Jason Slayden, Cindy Welch, and Lee Wood (my father) for their assistance in the field. Thank you to the Young family for allowing me access and the opportunity to work on their beautiful ranch. I would also like to thank Mike Gower for his help in preparing thin sections, and his assistance with any other questions I had. His help was greatly appreciated. Thank you to Dr. Mark Grimson for his assistance in the SEM lab and to the Department of Biological Sciences at Texas Tech University for providing access to the Electron Microscopy Laboratory.

I would like to dedicate this thesis to my parents and grandparents, the people that have influenced my life the most. I am glad they all stayed around long enough to see this. Finally, I would like to thank my wife Tamera for her support (emotional and financial) to help me see this through. Without her, this would not have been possible.

TABLE OF CONTENTS

ABSTRACT

The Lower Cretaceous Antlers Sandstone on the Young Ranch is the time equivalent to the Twin Mountains, Glen Rose, and Paluxy Formations of the Cretaceous Trinity Group. The Antlers represents the initial deposition of sediment onto the Wichita Paleoplain unconformity of North and West-Central Texas. The Antlers on the Young Ranch is interpreted as a bed-load channel deposit consisting of sandstone and gravelly sandstone. On the Young Ranch, the Antlers Sandstone is a discontinuous sandstone that is only present where post-depositional cementation by quartz and microquartz has occurred, or where the sandstone is overlain by uneroded limestones of the Walnut Formation. The silicification is similar to silcretes (quartz cemented soils) found in other Mesozoic and Cenozoic sediments. Petrographic analysis of the Antlers silcrete on the Young Ranch reveals large amounts of syntaxial overgrowths on detrital quartz grains. Microquartz cement is also observed, although it is not present in the large volumes like the quartz overgrowths. Syntaxial quartz overgrowths were observed when using the SEM, as well as the small euhedral and subhedral crystals characteristic of microquartz.

The reconstruction of the diagenetic history of the Antlers Sandstone on the Young Ranch indicates that the Antlers most resembles a groundwater silcrete. The maximum depth of burial that the Antlers could have undergone (< 160 ft.) excludes deep burial (>3 km), therefore silicification must have formed under shallow burial conditions (diagenetic quartzarenite or silcrete). Moreover, the multicolored nature of the Antlers in outcrop indicates shallow silicification (silcrete). The predominance of quartz overgrowths (~70%) compared to mircoquartz cement (~30%) indicates a groundwater silcrete as opposed to a pedogenic silcrete. The absence of numerous soil features also supports the interpretation of the Antlers being primarily a groundwater silcrete.

The silicification of the Antlers sandstone probably occurred penecontemporaneous with Antlers deposition, but could have occurred during post-Edwards exposure. Fluctuations in the water table on the Young Ranch are the likely mechanism for silicification, which transported silica liberated from intraformational sources such as dissolutioned chert and polycrystalline quartz grains. This accumulation of silica from internal sources aids in the interpretation of the Antlers Sandstone on the Young Ranch being classified as a paleosilcrete horizon.

LIST OF TABLES

LIST OF FIGURES

CHAPTER I

INTRODUCTION

Location of Study

Field work and sampling for this study was limited to the four contiguous sections of the Young Ranch in Nolan County, Texas. The ranch is located approximately 5 miles southeast of Roscoe, Texas (Fig. 1.1). The topography of the ranch consists of rolling hills and valleys, with numerous outcrops of Antlers Sand. Other rock units exposed on the ranch vary from Permian to Tertiary in age.

Purpose of Study

The Antlers Formation (Lower Cretaceous, Trinity Group) is a fluvial sand, silt, and gravel deposit (Brothers, 1984) that outcrops throughout north Texas and southern Oklahoma. Previous work has focused primarily on the stratigraphic relationship between the Antlers Sand and its Trinity age equivalent sediments to the east. More detailed work has identified sedimentary facies (Boone, 1972; Hobday et al.,1981) in the Antlers, as well as evidence for paleopediment horizons (Murray, 1985). However, little work has been done to study this sandstone in west-central Texas. This project was undertaken with two purposes: (1) to describe the

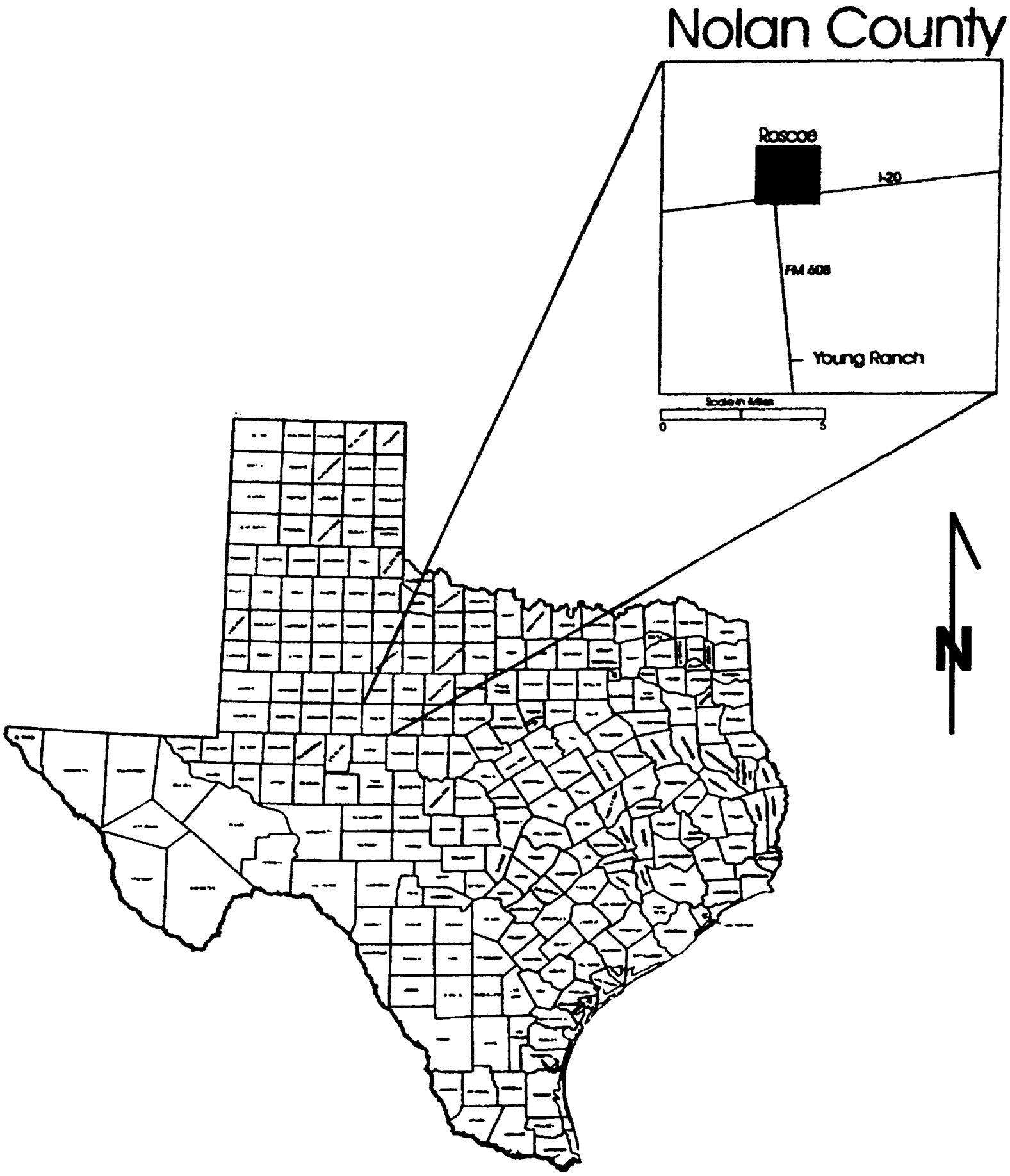

Figure 1.1. Location of Young Ranch in Nolan County, Texas.

depositional history of the Antlers, and (2) to determine diagenetic history of post-depositional silicification by varieties of silica cement.

Previous Work and Antlers Nomenclature

The name Antlers sand was first used by Hill (1891) for sand exposures near Antlers (Pushmataha County), Oklahoma. The term Antlers was later applied by Hill (1901) to a 200 foot thick sand section at the base of the Comanchean Series in northern Parker County, Texas. In this area, Hill (1901) observed the pinching out of the Glen Rose Limestone (Fig. 1.2) which allowed the lower Trinity sand (now known as the Twin Mountains Formation) and the Paluxy Sand to become an undifferentiable single "Antlers" unit (Fig. 1.3).

Later work on Trinity age sands focused on describing unconformable contacts in north Texas between Antlers-Paluxy type sands and the overlying Walnut Clay Formation (Scott and Armstrong, 1932). The problem of proper age of the Antlers was not aided by work in southern Oklahoma and north Texas by Forgotson (1957) and Atlee (1962) which placed the Paluxy sand in the Fredricksburg group as a Walnut Clay time-equivalent. Frederickson et al. (1965) stated that the formation of the Antlers Sand was contemporaneous with the basal Trinity sands, the

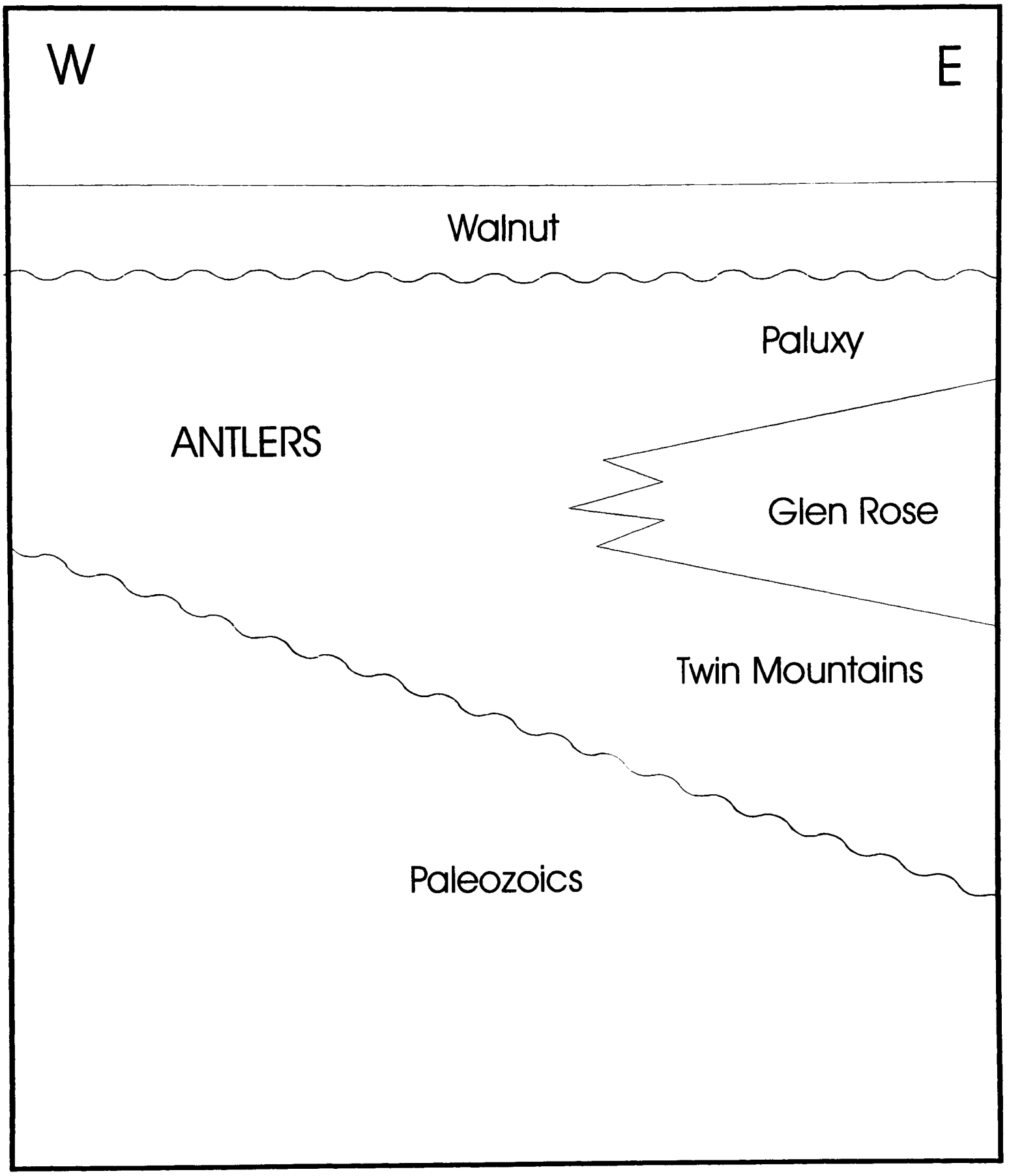

Figure 1.2. Cross section showing relationship of Antlers to the Paluxy,Glen Rose, and Twin Mountains Formations.

	HILL (1901)		FISHER ET AL (1966)		BROTHERS (1984)	
FREDERICKSBURG						
	Walnut Clay		Walnut Clay		Walnut Clay	
TRINITY	Paluxy	Antlers Sand	Paluxy	Antlers Sand	Paluxy	Antlers Sand
	Glen Rose		Glen Rose		Glen Rose	
	Travis Peak		Twin Mountains		Twin Mountains	

Figure 1.3. Historical Development of Antlers Nomenclature.

Paluxy, the Glen Rose, and the Walnut Clay based on Hill's original definition; meaning the term Antlers only applies updip of the Glen Rose pinch-out. Fisher and Rodda (1966) adopted the original definition of the Antlers used by Hill (1901) and later by Frederickson (1965) as the correct nomenclature for all sand found from the base of the Cretaceous up to the base of the Fredericksburg where the Glen Rose Formation is absent.

Boone (1972) studied Antlers outcrops in west-central Texas from Eastland County over to the Big Spring area in Howard County. Based on his studies, Boone was able to describe several sedimentary depositional environments and eight lithofacies including point bar, flood basin, delta, coastal plain, marine bar, bay-lagoon, terrigenious shallow shelf, and open marine carbonate: all representative of a fining upward transgressive sequence. He concluded the deposition of the Antlers was associated with a major drainage system that emptied into a broad embayment, which was progressively drowned during westward transgression.

Hobday et al. (1981) identified several non-marine clastic facies of the Antlers in north Texas (Cooke, Grayson, Denton, and Collin counties) and evaluated it for uranium mineralization potential. From their study, paleogeographic intrepretations were made noting that the presence of a tectonically active mountain belt and coastal lowlands in the area greatly

influenced stream flow during deposition. They also noted that evidence of both braided and meadering river in some Antlers facies made depositional environment interpretation difficult.

Brothers (1984) studied outcrops of Antlers just to the west of Hobday et al. (1981). In his work, Brothers divided the Antlers into three distinct units: upper, middle, and lower Antlers based on differences in stratigraphy and depositional environment. He interpreted the lower Antlers to be of fluvial origin; the middle Antlers to be of fluvial, deltaic, and shallow-marine origin; and the upper Antlers to represent the return of fluvial conditions which preceeded the deposition of clays and limestone that ended Antlers deposition. He noted that the three units are clearly visible in the southern part of Wise County, near the up-dip limit of the Glen Rose Formation, but are indistinguishable in the northern parts of Cooke and Montague counties.

Murray (1985) reported the presence of a paleopediment horizon in the basal conglomerate of the Antlers in central Texas (Eastland, Erath, Comanche, and Callahan counties). He concluded that the cementation of the Antlers must have occurred at or near the surface, and was penecontemporaneous with deposition. Based on his work, he identified two facies of quartz cementation and noted that their relationship indicates

vadose and phreatic cementation. Data from isotope analysis also points to shallow cementation; probably by meteoric water near the surface (Murray, 1985).

Methods of Study

Initial field work included the construction of a complete stratigraphic section of the ranch and the measurement of other section to evaluate variations in thickness of the Antlers. Sections were measured using a staff with .0305m increments. A Brunton compass was used to help correctly measure covered intervals and to measure orientations of trough cross-bed sets for paleocurrent reconstruction. Samples of Antlers Sand were collected from eleven localities throughout the ranch. From these samples, thin sections were made for point-count analysis and several samples were selected for SEM analysis. A Hitachi S-570 scanning electron microscope was used to photograph SEM samples.

CHAPTER II

SILICA CEMENTATION IN SANDSTONES

General

Geologists have studied the presence of silica cement in sandstones for years. Since quartz cement is the main porosity destroyer in sandstones, the main goals of these studies have been to make predictions about a sediments depositional and diagenetic history (Worden et al., 2000). The type of basin in which a sandstone is deposited will determine whether large amounts of quartz cements could be present (Blatt, 1992). The abundance of silica cement and the factors in which it forms is a complex and detailed process. Sources and factors that influence silica cementation are numerous (see table 2.1) although some are significantly more important that others. Understanding the depositional setting, as well as regional processes that occurred since deposition are crucial to determining which factors of silica cementation are applicable. The use of petrographic and geochemical techniques is extremely useful in confirming or eliminating a silica source, as well as determining whether compaction or pressure dissolution due to deep burial has occurred.

Table 2.1. Proposed sources of silica for quartz cementation
modified after McBride (1989)

Year	Source
1880	Decomposition of feldspars
1904	Silica precipitated from descending meteoric water Silica derived from silicate minerals in zone of weathering
1920	Compaction of shales; dissolution of quartz silt grains
1929	From decomposed silicious plant material From sponge spicules in shales
1941	Precipitation from sea water on ocean floor Pressure solution at sandstone grain contacts
1955	Pressure solution at stylolites in sandstones
1957	Dissolution of opaline skeletal grains
1959	Hydration of volcanic glass
1960	Replacement of silicates by carbonates
1962	Conversion of smectite to illite in shales Dissolution of eolian quartz abrasion dust
1964	Released from natural silica complexes derived from organic acids
1967	Pressure solution of quartz in clayey siltstones Dissolution of detrital quartz grains without pressure dissolution
1971	Desorption of H4SiO4 from clays
1974	Pressure solution loss of detrital quartz silt in shales Dissolution of glacially produced abrasion dust
1975	Abrasion solution of detrital quartz grains followed by precipitation of overgrowths
1982	Accumulation of detrital amorphous alumino-silicates in sands and muds
1987	Pressure solution of quartz and other silicates in deeply buried shales undergoing low-grade metamorphism.

Sources of Silica

A debated topic among geologists is the origin of silica for quartz cementation (McBride, 1989). Since this is a broad topic, the most dominant sources can be broken down into internal and external sources. External sources are those that provide silica from outside the rock unit. These external sources can be laterally from adjacent beds or structures, as well as from shallow or deep fluids. Internal sources are focused within the rock unit, mainly from alteration, dissolution, and replacement reactions.

Internal Sources

The most common internal source of silica is usually associated with deep burial from pressure dissolution and the formation of stylolites. Pressure dissolution is local reprecipitation of quartz from nearby quartz grains, and stylolites are often formed by the alignment of interpenetrating grains due to dissolution (Worden et al., 1998). It has been reported by Pettijohn et al. (1987) that the of pressure dissolution is caused by high pressures at the contact points between quartz grains which increases the solubility of the grains and allows them to dissolve at the points of

contacts. Where the dissolution occurs, the grains have the appearance of being welded together, forming a stylolitic grain boundary. Although some authors believe this process could provide a source of silica for shallow burial sands, Bjorlykke et al. (1993) states that this source of silica would be very localized. In deeper sands (>3 km), the silica released from pressure dissolution is probably precipitated within 10m of its origin (Bjorlykke et al., 1993). This process of quartz pressure dissolution appears to be biased or at least has a preference for sandstones containing mica and clay minerals (reference, date). Pettijohn et al. (1987) noted that dissolution is most advanced at quartz grain contacts with clay coatings. The presence of clay minerals, such as illite, at grain boundaries may increase quartz dissolution (Fisher et al., 1998). Conversely, an abundance of these clays can inhibit quartz cementation by reducing the surface area on the grain where silica cement can nucleate (Fisher et al., 1998). Detrital mica grains, biotite and muscovite, appears to increase quartz dissolution. Oelkers et al. (1996) argued that quartz dissolution occurs only at grain boundaries where mica and clay minerals are present, and reported that temperature is the main controlling factor. Besides the mineralogy bias, pressure dissolution also seems to have a preference to smaller grained sandstones. The smaller the grain size, the

more susceptible the sandstone is to dissolution (Worden et al, 1998). Worden et al. (1998) also pointed out that the most common rocks that form stylolites due to pressure dissolution are siltstones and fine grain sandstones rich in micas and clays. For this dissolution to be a significant source of silica, it should occur very deep (>3 km) or be from silica released during low-grade metamorphism (Bjorlykke et al., 1993; Passchier, 1996).

Most sandstones contain some detrital feldspar, although they are more common in arkoses and litharenites. Since the majority of these feldspars have an igneous or metamorphic origin, they are usually out of equilibrium with the pressures, temperatures and fluids they are exposed to in sandstones (Worden et al., 2000). Alteration of feldspars to kaolinite that are buried only to shallow depths can occur by reactions with meteoric water. This occurs because the feldspar minerals are unstable in the presence of water (Faure, 1998). According to Faure (1998), water interaction with the feldspar favors the following reaction:

$$\underset{\text{Microcline}}{2KAlSi_3O_8} + 9H_2O + 2H^+ \rightarrow \underset{\text{Kaolinite}}{Al_2SiO_5(OH)_4} + 2K^+ + \underset{\text{Silicic Acid (Quartz in Solution)}}{4H_4SiO_4}$$

Feldspars are a good source of silica because they have high Si/Al ratios. The clay minerals that usually replace them (i.e. kaolinite, illite) have lower

Si/Al ratios, allowing the reaction to release quartz in the form of silicic acid. It is noted by Kraishan et al. (2000) the reactions in sandstones that typically liberate silica from quartz usually involve feldspar alteration to clay minerals. As feldspars and their alteration products are exposed to waters at greater depths, the formation of illite and the conversion of kaolinite to other clay minerals are more common (Morad et al., 1994). All of these conversions can generate silica. It has been noted by Leder and Park (1986) that the volume of silica released from the alteration of feldspar minerals can be quite high, depending on composition of the detrital feldspar grains. The reaction of feldspars to kaolinite is the only reaction illustrated because it occurs during early diagenesis, and would probably have the greatest influence under shallow burial conditions.

Another internal source of silica is the dissolution of opaline fossils (sponge spicules, radiolarians, and diatoms). This source is usually limited to marine sediments, and according to McBride (1989), these opaline fossils comprise more than 30% of some deep-sea oozes. Opaline silica is unstable mainly because it is much more soluble that quartz (Blatt, 1992), and can be the origin of both shallow and deep silica cementation. In addition to siliceous fossils, the alteration of volcanic glass shards in sediments can also contribute silica. These glass shards are common in

sediments of volcanic origin. However, it should be noted that there are no highly cemented quartz sandstones whose source of silica is solely from volcanic glass (McBride, 1989).

The smectite group of three layer clays varies in composition and is a possible source of silica due to partial replacements of Si^{4+} by Al^{3+}in some of their tetrahedral layers (Faure, 1998). Smectite clays found in sandstones are often altered to illite or chlorite, producing silica for cementation. Chloritization of smectites often occurs in sediments enriched in Fe oxides, Fe-Ti oxides, and Fe silicates. Illitization of smectites often occurs in sediments rich in K-Feldspar (Worden et al., 1998). These reaction usually occur at elevated temperatures (>100° C), but can occur as low as 60° C suggesting somewhat deep burial is required (Worden et al., 1998).

Dissolution of different varieties of quartz grains without deep burial or high temperatures is another possible origin of silica for quartz cementation (McBride, 1989). Polycrystalline quartz grains are more susceptible to dissolution at shallow depths than are detrital monocrystalline grains (Thiry et al., 1988; McBride et al., 2001). Although partially dissolved quartz grains may be visible throughout a sample, the volume of silica they contribute is usually insignificant (Salem et al., 1998).

External sources

Sources of silica for cementation outside of the rock unit that is cemented usually involves an internal process such as pressure dissolution or the degrading of feldspars. The liberated silica then migrates as advecting fluids or along faults, which allows the silica to precipitate some distance from its source.

Of all external sources, quartz cementation by flow of meteoric water through a rock body is often considered to be the primary contributor of silica within shallow burial conditions (Blatt, 1979). Blatt (1979) suggests that one of the reasons quartz precipitation can occur at shallow depths is due to the rate of groundwater flow. The rates of shallow groundwater flow (can range from 2m to 20m per year, depending on recharge rate) are much faster than those of deeper fluids (Blatt, 1979). Supersaturated levels with respect to silica are quite common in natural waters, and they are able to persist at high levels for long periods of time (Pettijohn et al., 1987). The high of levels of saturation can be maintained for long periods of time due to the slow precipitation time of quartz (Pettijohn et al., 1987). However, for this level of supersaturation to account for large volumes of quartz cement, extensive circulation of water through a sandstone is

required (Pettijohn et al., 1987). Pettijohn et al. (1987) states that recirculation of groundwater under shallow burial conditions is often characteristic of some alluvial sands, and that constantly moving meteoric groundwater could contribute large volumes of silica for quartz cementation. Although both laterally and vertically moving meteoric groundwater can attribute to the precipitation of quartz cement, vertically circulating groundwaters are probably more significant because of a faster flow rate (Blatt, 1979). Cementation by meteoric water is most efficient at shallow depths where the distance of flow is minimized, usually within a few hundred meters of the surface (Blatt, 1979).

Facies changes into adjacent shales and mudstones are also possible sources of generating silica. Most shales and mudstones can produce silica during diagenetic processes that affect their large clay content. Within these rock units, most of the internal dissolution and alteration processes of clays are possible sources of silica. Sullivan and McBride (1991) note that silica from adjacent shales can cement nearby sandstones through local diffusion and advection processes. Trewick and Fallick (2000) note that instead of donating silica to the system, some rock units redistribute it to other facies. Although this local transport could be

considered an internal source, silica carried between facies can be transported for tens of meters (Trewick and Fallick, 2000).

Large-scale faults are often thought of as major pathways for fluid transportation. However, work done by Fisher et al. (2000) demonstrates that quartz cement is typically not precipitated in large volumes along fault planes and other deformation structures. This suggests that local precipitation is favored, therefore large amounts of quartz cement did not originate from fluids flowing along faults (Fisher et al., 2000).

Deeper sources such as basement rocks, igneous intrusions, deeper sandstones and mudrocks can also be sources of silica (Worden et al., 2000). Pressure dissolution at depth can be an internal or external process because some rock bodies are silica importers and some are silica exporters (Bjorlykke et al., 1993). These sources are probably not significant because they require large-scale movement of fluids. Many authors (Blatt, 1979; Bjorlykke et al., 1993;Worden et al, 1998) state local enrichment by quartz cementation is a localized process, no matter what depth it occurs. The idea that large volumes of advection fluids released from deeper sources can produce well-cemented quartz sands is also disputed, because these fluids probably precipitate calcite cement (Bjorlykke et al.,1993).

Factors Influencing Cementation

Numerous factors influence or control quartz cementation in sandstones. The debate over controlling factors usually focuses on depth, pressure, and temperature as major variables. However, the problem with focusing only on depth, pressure, and temperature is that the rock composition as well as rock fabric have some effect on quartz cementation. Another factor is the composition and volume of fluid needed to support large amounts of silica for cementation. In this summary, depth will not be described as an independent variable in cementation, but directly related to changes in temperature and pressure.

Rock Composition and Fabric

Large volumes of pore filling quartz cement are usually found in sandstones whose grains are predominately quartz (Blatt, 1992). Because of this, the type of basin in which a sandstone is deposited ultimately determines if large amounts of quartz cement will be present. Less tectonically active basins, such as intracratonic and passive-margin, tend to have more quartz rich sandstones, such as quartzarenites (McBride, 1989). Basins that are more tectonically active tend to contain sandstones

with larger feldspar and lithic fractions, such as arkoses and litharenites (McBride, 1989). With the exception of shallow formed diagenetic quartzites (silcretes), only quartzarenites contain large amounts of quartz cement (McBride, 1989).

Variation in detrital quartz grains also seems to influence quartz cementation. Monocrystalline grains, either straight or undulose, are more likely to have quartz cement (James et al., 1986). Cementation by quartz also appears to have a bias between coarse and fine grains. James et al. (1986) states quartz cementation occurs more often on coarse and medium size quartz grains. McBride (1989) also notes that larger grains often show more quartz cement, and only when the coarser grains have been cemented by calcite do finer beds have abundant quartz cement.

Age of the rock unit is also a factor. Since most well cemented sands must undergo deep burial, almost all sandstones with large volumes of quartz cement range in age from Precambrian to Mesozoic (Pettijohn, 1987). With the exception of some Cenozoic sands that have undergone rapid burial, most well cemented sandstones are older (McBride, 1989).

Fluid volume and composition

As mentioned earlier, both groundwater and deep rising fluids could be possible sources of silica for quartz cementation. Several authors (Blatt, 1979; Pettijohn et al., 1987) state that repeated circulation of pore fluid through a sandstone is required for cementation. This recirculation of pore fluid makes the volume of water required for cementation very large. McBride (1989) suggests the volume of water required to precipitate and occlude 5 to 15% of the original porosity is extremely large (10^4 to 10^5 pre-cement pore volumes), and that most sandstones were probably cemented below levels of active meteoric water flow. The debate on fluid volumes will be an issue in the future and new hypotheses will continue to be tested (McBride, 1989). Along with fluid volume, several other factors can contribute to quartz cementation, such as pH, ionic content, and water density. Several authors (Krauskopf, 1955; Worden et al., 2000) note that pH can affect quartz cementation; however, they state that pH is usually not a factor unless it is above 9. When the pH value is above 9, the solubility of amorphous silica is significantly increased (Krauskopf, 1955), and when pH is over 10, quartz solubility is significantly greater (Blatt, 1992). The ionic content of the fluid that moves through a

sandstone can also affect quartz cementation (Worden et al., 2000). The presence of K^+ ions in lower than normal volumes could help initiate feldspar alteration reactions freeing silica to solution (Worden et al., 2000). Additional ions, such as Na^+, that are added with the influx of saline water in pore fluids could inhibit silica releasing reactions by the lower density of the saline water Worden et al, 2000). Silica is less soluble, and pressure dissolution is less likely to occur in pore waters of lower density (Porter et al., 1986).

Temperature

Changes in temperature may have a significant influence on quartz cementation. It is well known that high temperatures make quartz and all its polymorphs more soluble, but quartz is usually precipitated at the higher temperatures associated with deep burial (Blatt, 1992). It is noted by several authors (Bjorlykke et al., 1993; Gluyus et al., 1993; Worden et al., 2000) that the precipitation of quartz overgrowths occurs at temperatures exceeding 90-100°C. This is not to imply that temperature alone controls quartz cementation. Worden et al. (2000) states that not only does temperature affect mineralogical assemblages (quartz, feldspars, and clays) that release silica, but it also affects rates of silica dissolution,

diffusion, and precipitation. Many diagenetic reactions (such as pressure dissolution of quartz, alteration of feldspar, and conversion of clay) often occur at a faster rate with increased temperature. Precipitation also occurs over a variety of temperatures as recorded by fluid inclusion data (McBride, 1989). Cementation may occur slowly over tens of millions of years at lower temperatures (Morad et al., 1994), or may occur much faster at higher temperatures (Worden et al., 2000).

Pressure

As a sandstone is buried, the pressures and temperatures it is exposed to increases based on the rate of basinal subsidence (Pettijohn,1987). As discussed above, higher temperatures influence quartz cementation, but the amount of pressure (normal or overpressured) a sandstone is exposed to is also a variable (Worden et al., 2000). Pressure on the grains (lithostatic pressure) and pressure on the pore fluids (hydrostatic pressure) under normal conditions are predictable; however, in some situations a zone may be considered overpressured due to higher hydrostatic pressure (Pettijohn, 1987). In these overpressured zones, the amount of quartz cement is significantly less than that found in non-overpressured zones (Worden et al., 2000). This suggests that both

hydrostatic and lithostatic pressure have some influence on quartz cementation, even if it does not control pressure solution (Worden et al., 2000). Bjorkum (1996) suggests that temperature and the presence of clay grain coatings, not pressure, actually controls the process of pressure solution.

Types of Silica Cementation

Overgrowths

Quartz overgrowths are the most common form of silica cementation in ancient sediments (Pettijohn et al., 1987). According to Pettijohn et al. (1987), overgrowths are the secondary enlargement of detrital quartz grains by coatings of euhedral or interlocking mosaic crystals that grow in optical continuity with the grains. This optical continuity applies to all types of quartz (straight, undulose, and polycrystalline), with each overgrowth aligning perfectly with the grains crystal lattice. Usually, these overgrowths are connected to the grain at widely spaced points. This spacing leaves a capillary pore between the overgrowth and the detrital grain (McBride, 1989). Trapped fluids, organic matter, and various minerals can become trapped in the space between the grain and the overgrowth. These materials usually help to visually distinguish the overgrowth by forming a "dust line" or "rim" around the original detrital grain (McBride, 1989). If the

material coating the grain is thick, due to large amounts of iron oxides, clays, or other minerals, then the formation of overgrowths on grains usually does not occur (McBride, 1989). Due the occasional absence of distinguishable dust line, other techniques like luminescence petrography can be used. In luminescence petrography, electrons cause the detrital grains to luminesce due to the presence of impurities (certain trace elements). Sometimes secondary quartz overgrowths luminesce slightly, but usually do not luminesce at all. Work done by Sippel (1968) has shown that detrital grains can display several colors during luminescence; usually red, blue, and brown.

The formation of overgrowths can occur very slowly or quite rapidly, and is usually dependent on the rate of subsidence and the amount of fluid that moves through the rock unit (Blatt, 1992). According to McBride (1989), large volumes of quartz overgrowths could represent tens of millions of years of cementation; however, other strongly cemented sandstones, such as silcretes, can be indurated with large volumes of cement in less than a million years.

Microquartz Cement

Another type of quartz cement, microcrystalline quartz, is also common in some types of sandstones (Blatt, 1992). Folk (1950) originally described any authigenic quartz crystals of any size as megaquartz. Folk's megaquartz was later subdivided in microquartz and megaquartz based on size (Knauth, 1994). Fine equant crystals of quartz with widths < 20um is termed microquartz (Summerfield, 1983). Coarse equant crystals with widths >20um in now called megaquartz (Summerfield, 1983).

Microcrystalline quartz and silica cements can be represented by several quartz crystal habits and silica polymorphs. Quartz crystal habits include: a.) fibrous microquartz (chalcedony or moganite) and b.) granular microquartz (chert). Silica polymorphs include: (a) microcrystalline opal with cristobolite and/or tridymite and (b) non-crystalline opal (Graetsch, 1994; Knauth, 1994). The transformation of the silica polymorphs usually occurs from opal A to opal CT to quartz as a result of the unstable nature of opal A (Graetsch, 1994).

Opal A →Opal CT → Fibrous Quartz → Crystalline Quartz

In thin section, opal A and opal CT are isotropic and often appear as isopachus bands around grains and as pore filling (Thiry et al., 1987). Chalcedony is commonly visible as spherulitic fibrous bundles and can be optically length-fast or length-slow (Thiry et al., 1987). Chert is most

common as dark finely granular microcrystalline quartz (average crystal size~ 8um) with no structurally distinguishing features (Knauth, 1994).

Microcrystalline quartz can be deposited by both fresh water and marine systems (McBride, 1989). Many shallow marine sediments contain unstable opaline material from abundant amounts of siliceous fossil debris, and usually undergo dissolution and reprecipitation as more stable silica polymorphs, such as chalcedony and chert (Worden et al., 2000). Because many surface waters can also be extremely saturated with silica, Blatt (1992) states that sandstone cementation by opaline silica indicates that the cementation occurred within tens of meters of the surface. The presence of microcrystalline quartz indicates early cementation, usually prior to compaction (Knauth, 1994). This is also supported by Summerfield (1986), who states that the presence of microcrystalline quartz cement almost always occurs as a result of surficial diagenesis.

Silcretes

In some shallow buried sands and soil horizons, the influx of large volumes of water enriched in silica can rapidly indurate these sediments with a variety of quartz cement types (Smale, 1973). These quartz-rich sediments, or diagenetic quartzites, are commonly referred to as silcretes

and are the result of surface or near surface diagenesis (Summerfield, 1983). Silcrete can be many colors, which usually varies based on the presence of different oxide minerals (Hutton et al, 1979). Hutton et al. (1979) states silcrete can be any grain size, from silts to boulders. They are very hard, often ringing when struck with a hammer and give off a distinct pungent odor (Hutton et al., 1979).

Silcretes are often divided into two main categories: pedogenic and groundwater (Thiry et al., 1991). Pedogenic silcretes are often associated with weathering profiles in soil horizons, and typically have abundant microquartz cement (McBride, 1989). Groundwater silcretes are commonly cemented by syntaxial overgrowths that are more typical of deep burial (> 3km), with much less or no microquartz cement (Thiry et al., 1991).

Silcretes are very common in the Cenozoic (Summerfield, 1983) and due to their resistant nature, can influence modern geomorphology (Hutton et al., 1979). However, they are probably quite common in older rocks and are misidentified as rocks that were cemented at depth (Summerfield, 1983). Silcretes commonly form in arid regions (Smale, 1973), and have been identified in several localities in Africa, central Australia, Texas, and New Mexico that to have arid to semi-arid climates (Khalaf, 1988). They

are also common in areas with humid climates such as France, southern England, coastal Australia, and southern Africa (Khalaf, 1988). In arid and semi-arid environments, due to little environmental fluctuations, silcretes could form quite rapidly. Thiry et al. (1988) estimates that a quartzite lens can form in as little as 30,000 years and a completely cemented groundwater silcrete can form in as little as 200,000 years. The time it takes to form a pedogenic silcrete is unknown (McBride, 1989).

CHAPTER III

STRATIGRAPHY AND DEPOSITIONAL ENVIRONMENTS

Regional Stratigraphy

The Callahan Divide region of west-central Texas consists of remnant Cretaceous capped limestone mesas that stand high above the rolling plains, and are underlain by clastic sequences of the Paleozoic (Moore, 1969). In west-central Texas, the lower Cretaceous is divided into three major groups: the Trinity, the Fredericksburg, and Washita (Fig. 3.1; Moore, 1969). The Antlers sandstone is the lowermost unit of the Cretaceous Trinity Group exposed in the Callahan Divide area (Moore, 1969). In this area, the Antlers is indistinguishable from the other sands (Twin Mountains and Paluxy) of the Trinity Group (Brothers, 1984). The term Antlers only applies when the Glen Rose Formation pinches out (Fig. 1.2) and the Twin Mountains and Paluxy become one unit (Hill, 1901). The term Antlers was first used in Texas by Hill (1901) and entered in the stratigraphic nomenclature for Texas by Fisher and Rodda (1966).

Regional Depositional Environment

The lower Cretaceous stratigraphy of west-central Texas records the change from continental conditions to a marine environment as a shallow transgressive sea moved across the area from East Texas Basin (Fig. 3.2; Moore, 1969). At the time of deposition, the Antlers consisted of continental type

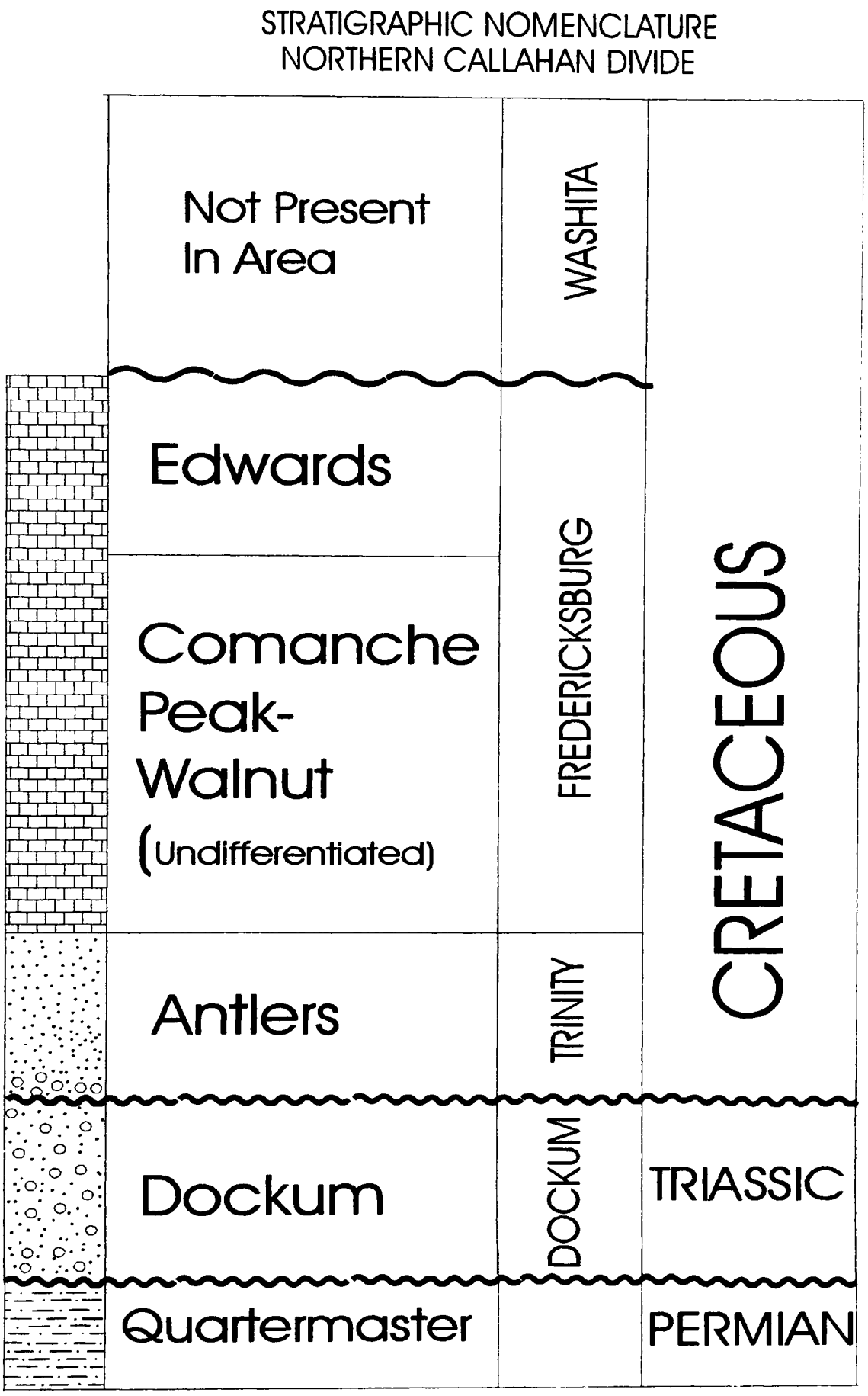

Figure 3.1. Stratigraphic Nomenclature for the Northern Callahan Divide.

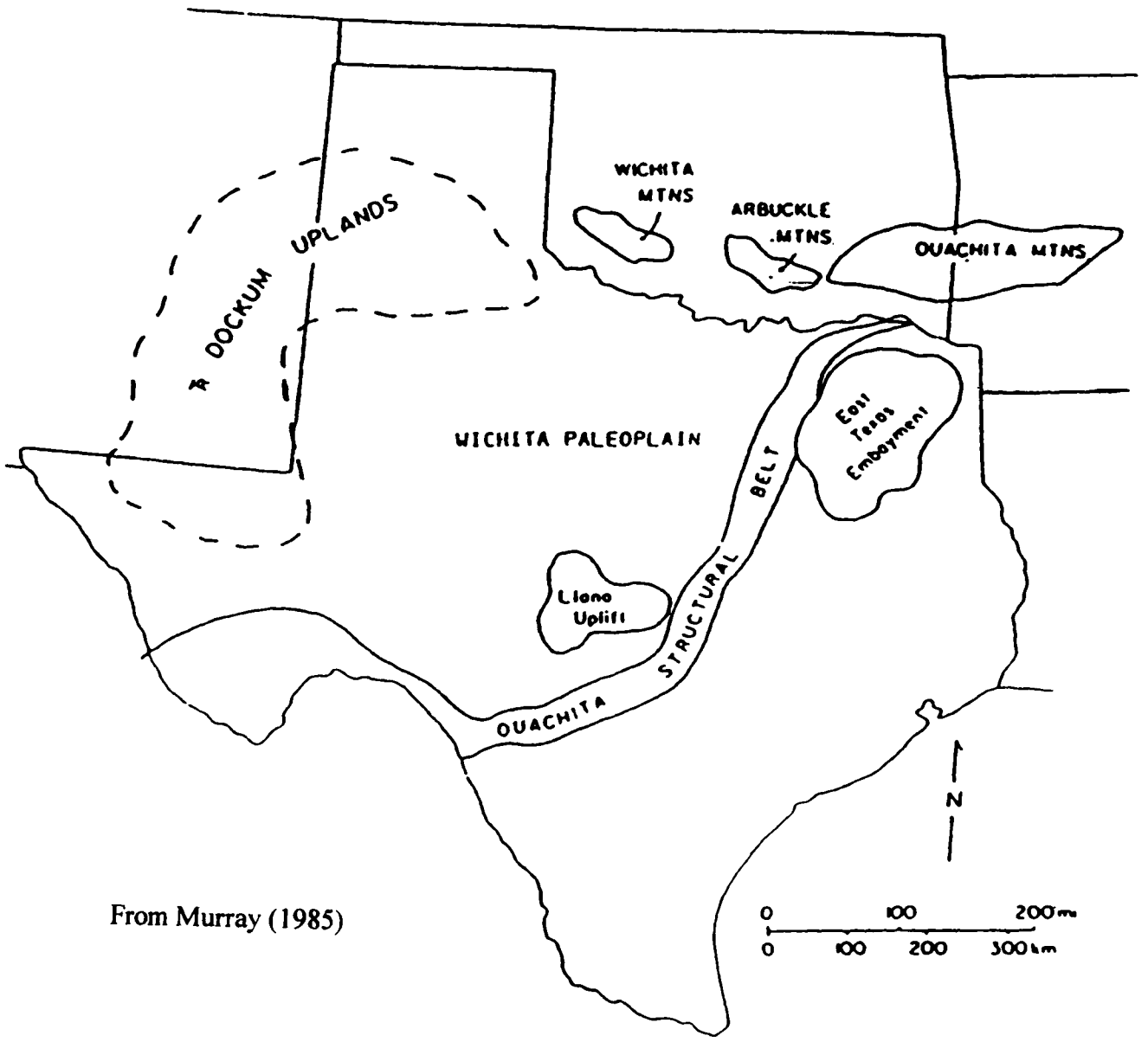

From Murray (1985)

Figure 3.2. Structural features that affected regional Antlers deposition on the Wichita Paleoplain.

sediments, characteristic of braided and meandering stream deposits plus overbank deposits (Boone, 1972). The Antlers sand varies in thickness, and reaches a maximum thickness of 120 ft. near San Angelo (Moore, 1969). As the sea began to transgress across the region, the upper Antlers developed as a fluvial to marine transitional facies. Boone (1972) notes the presence of marine bar, bay-lagoon, and shallow shelf deposits in the upper Antlers. Deposition of the Antlers was halted as marine limestones of the Fredericksburg Group were deposited during transgression (Boone, 1972).

Stratigraphy on the Young Ranch

General

On the Young Ranch, rock exposures range from Permian to Tertiary in age (Fig. 3.3). Most of the rocks are exposed naturally throughout the ranch, and some units are visible in quarries. Most rocks can be seen along the many limestone-capped hills and in creek beds. Other units are exposed along paleo-river trends (exhumed channel) due to selective silicification of channel sands. A map of the Young Ranch (Fig.3.4) shows the size of the area studied, and a composite section of the ranch (Fig. 3.5) shows the general relationship of stratigraphic units on the ranch.

STRATIGRAPHIC NOMENCLATURE
Young Ranch, Nolan County, TX

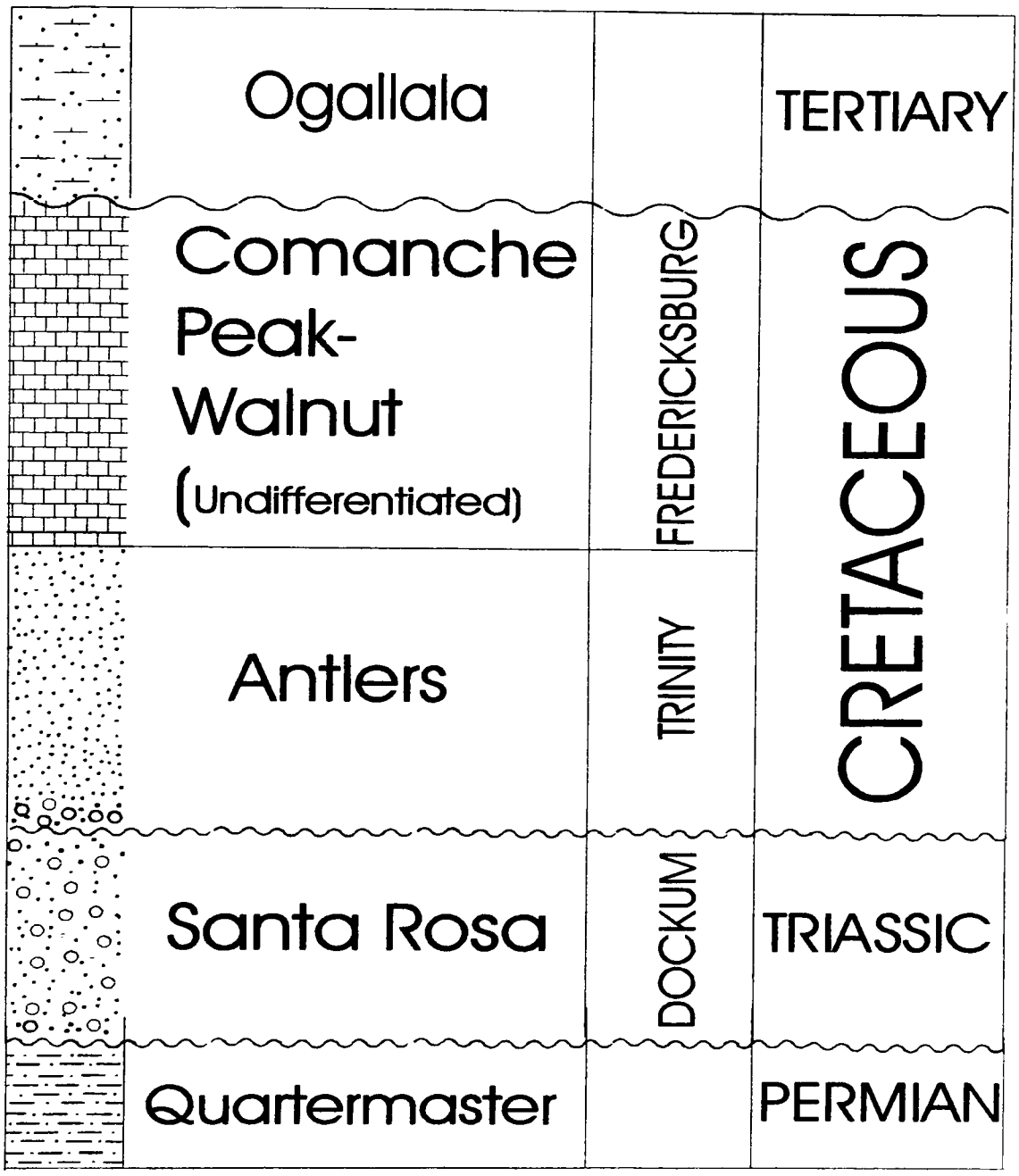

Modified after: Moore, 1969

Figure 3.3. Young Ranch Stratigraphic Nomenclature.

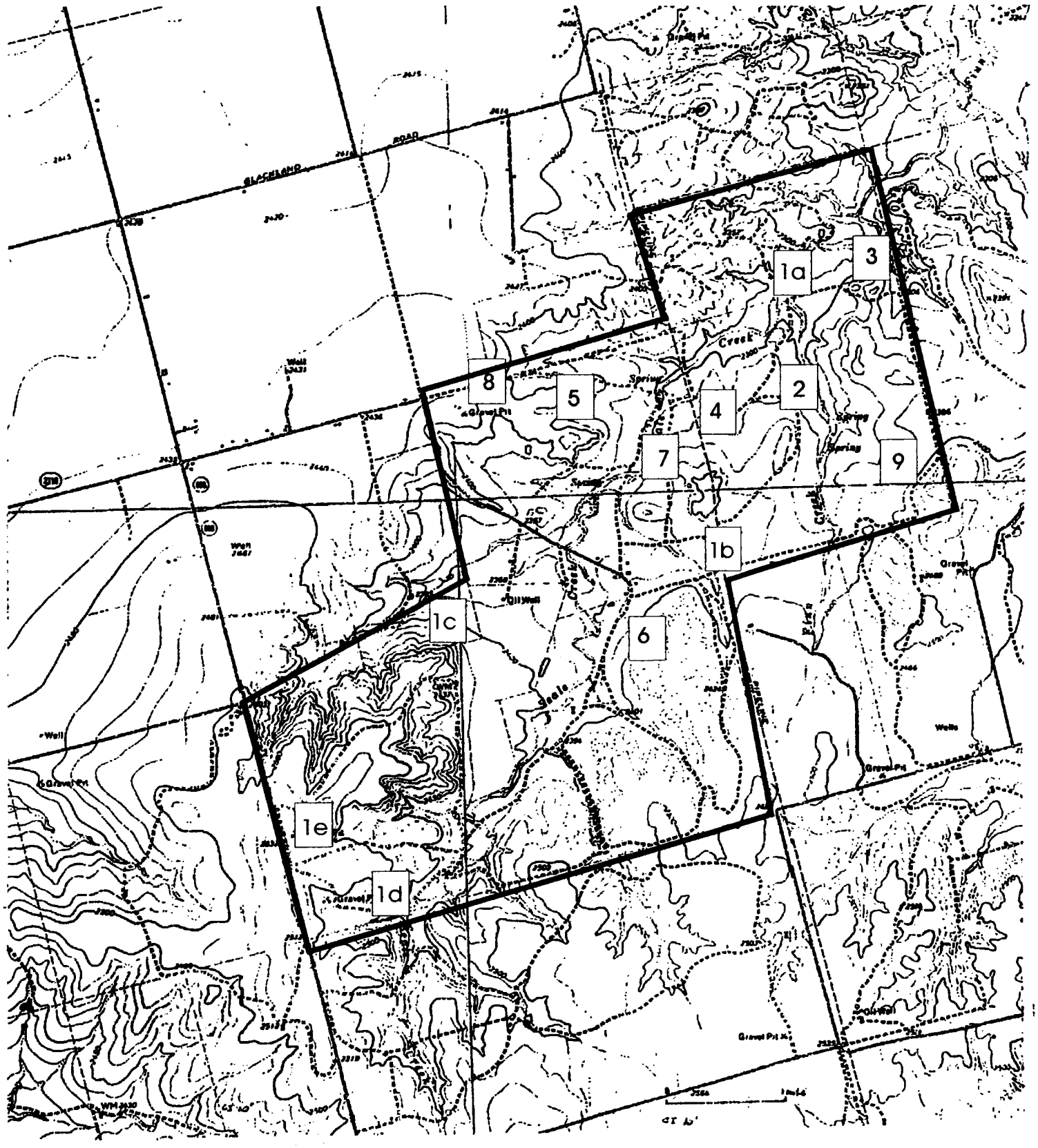

Figure 3.4. Topographic map showing locations of measured sections on the Young Ranch. The ranch boundaries are in bolded.

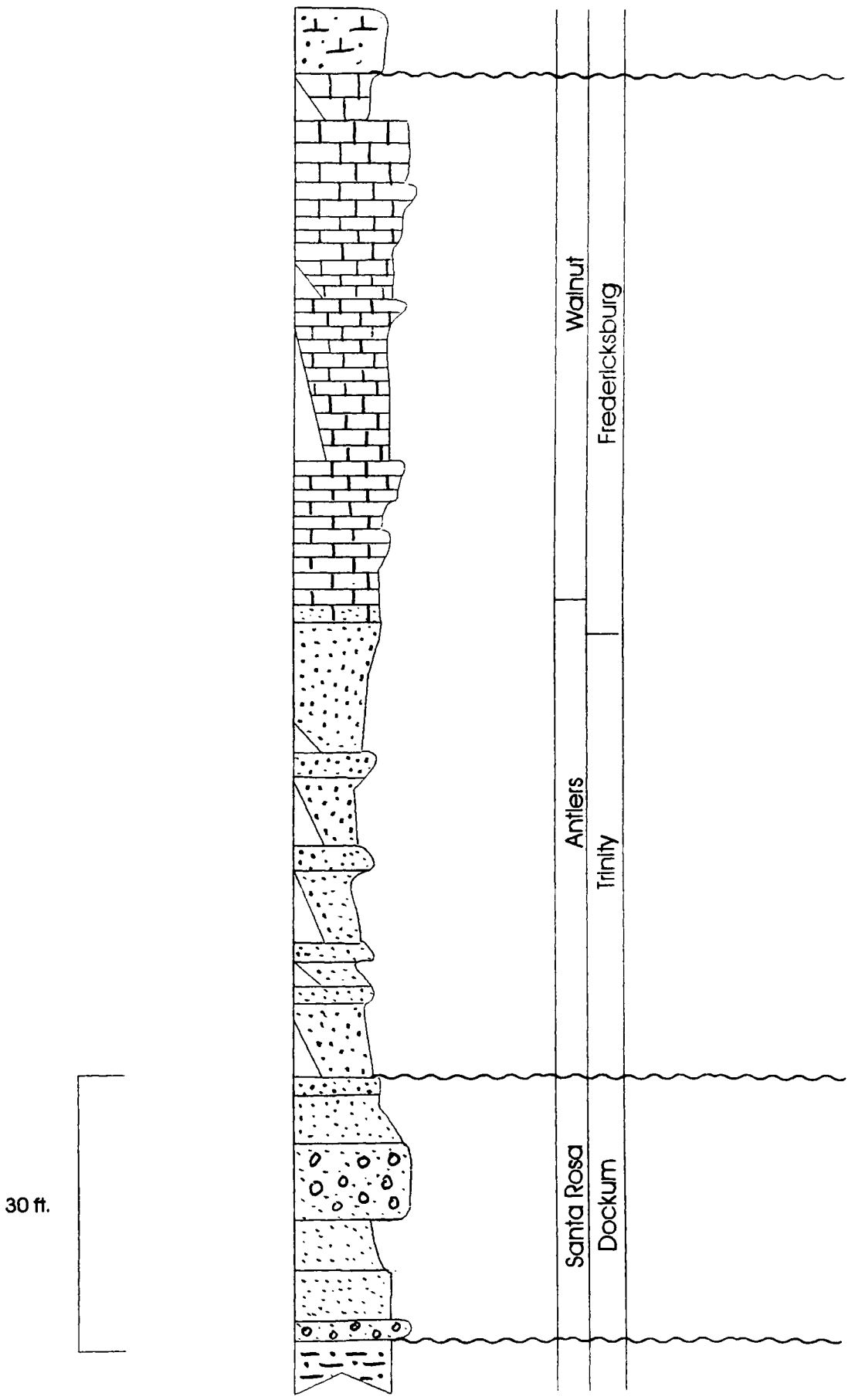

Figure 3.5. Composite stratigraphic section of the Young Ranch

Permian Quartermaster Formation

The Quartermaster Formation is the oldest unit that outcrops on the Young Ranch. It is a red and gray mottled siltstone (Figs. 3.6 and 3.7), and is overlain by the Santa Rosa Sandstone of the Triassic Dockum Group (Fig. 3.8). The Quartermaster Formation represents continental sabka-tidal flat type deposition during a dry climate (McGowen et al., 1983). The end of Permian deposition on the Young Ranch coincides with the opening of the ancestral Gulf of Mexico.

Triassic Dockum Group

The Santa Rosa Sandstone (Fig 3.9) and the Trujillo Formation (Fig. 3.10) represent the Dockum Group on the Young Ranch. The units vary from red to brown in color and range in size from fine sand to conglomerate (Figs. 3.11 and 3.12). The Dockum Group represents fluivial-deltaic-lacustrine type deposition in a humid environment (McGowen et al., 1983). The probable source for these sediments (the Santa Rosa) is from Amarillo-Wichita Mountains and the Ouachita Structural Belt to the east (Riggs et al., 1996).

Cretaceous Antlers Formation

The Antlers sandstone can be found at numerous localities throughout the ranch. Depositional environments of the Antlers will be

Figure 3.6. Unconformable contact between Permian Quartermaster and overlying Triassic Santa Rosa.

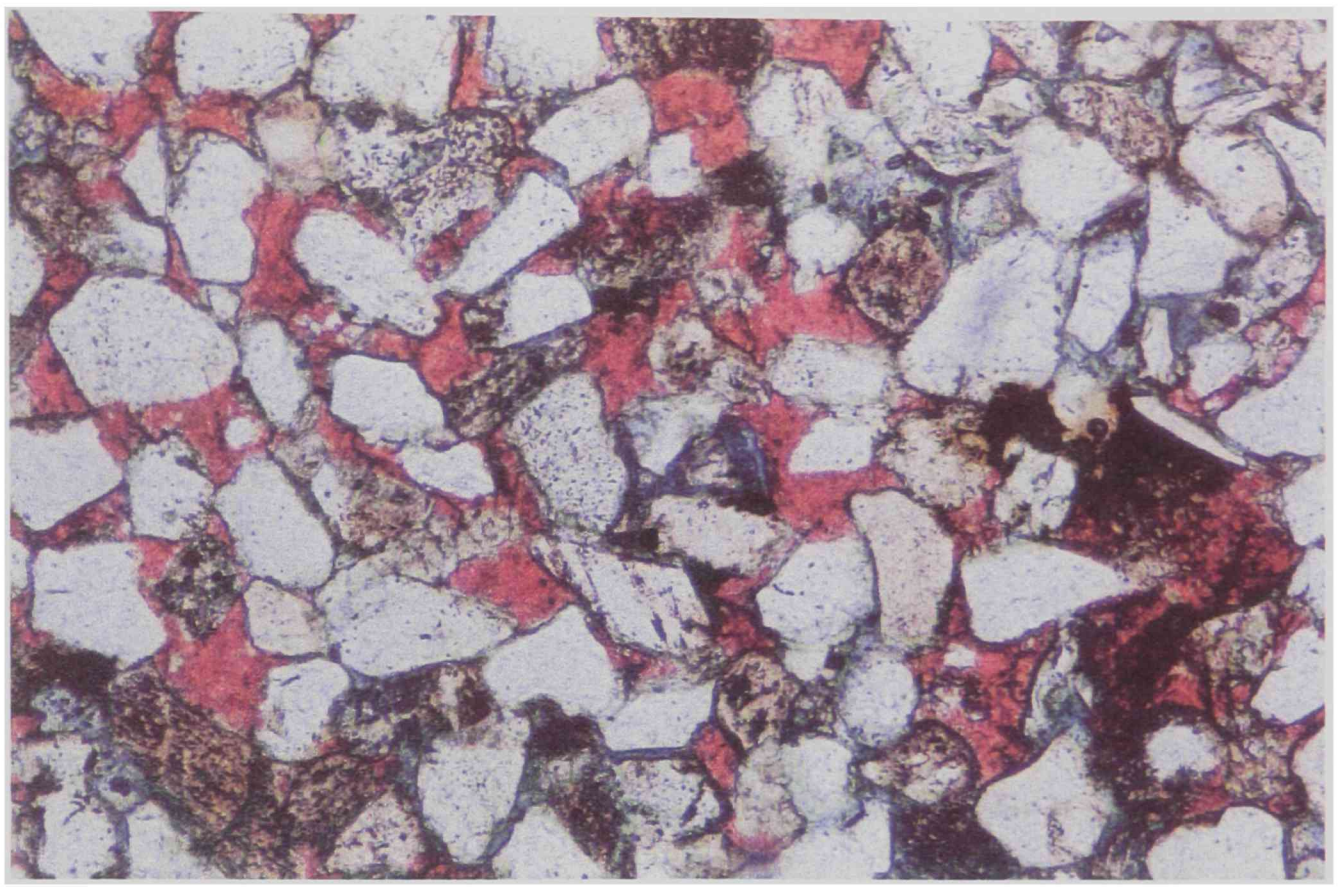

Figure 3.7. Photomicrograph of the Permian Quartermaster Formation, a calcite cemented siltstone.

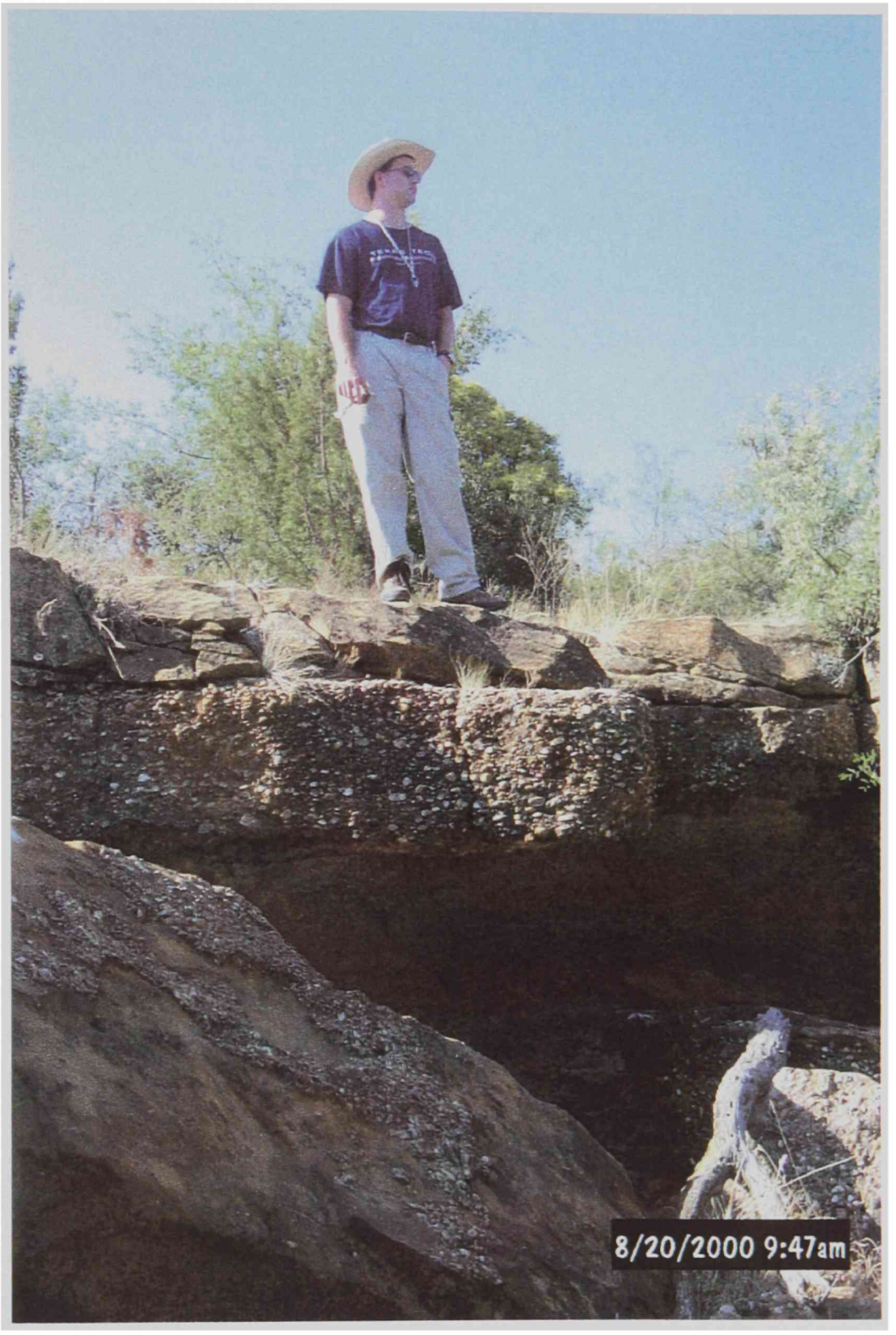

Figure 3.8 - Contact between Quartermaster and Santa Rosa.

Figure 3.9. - Gravel unit of the Santa Rosa (Dockum).

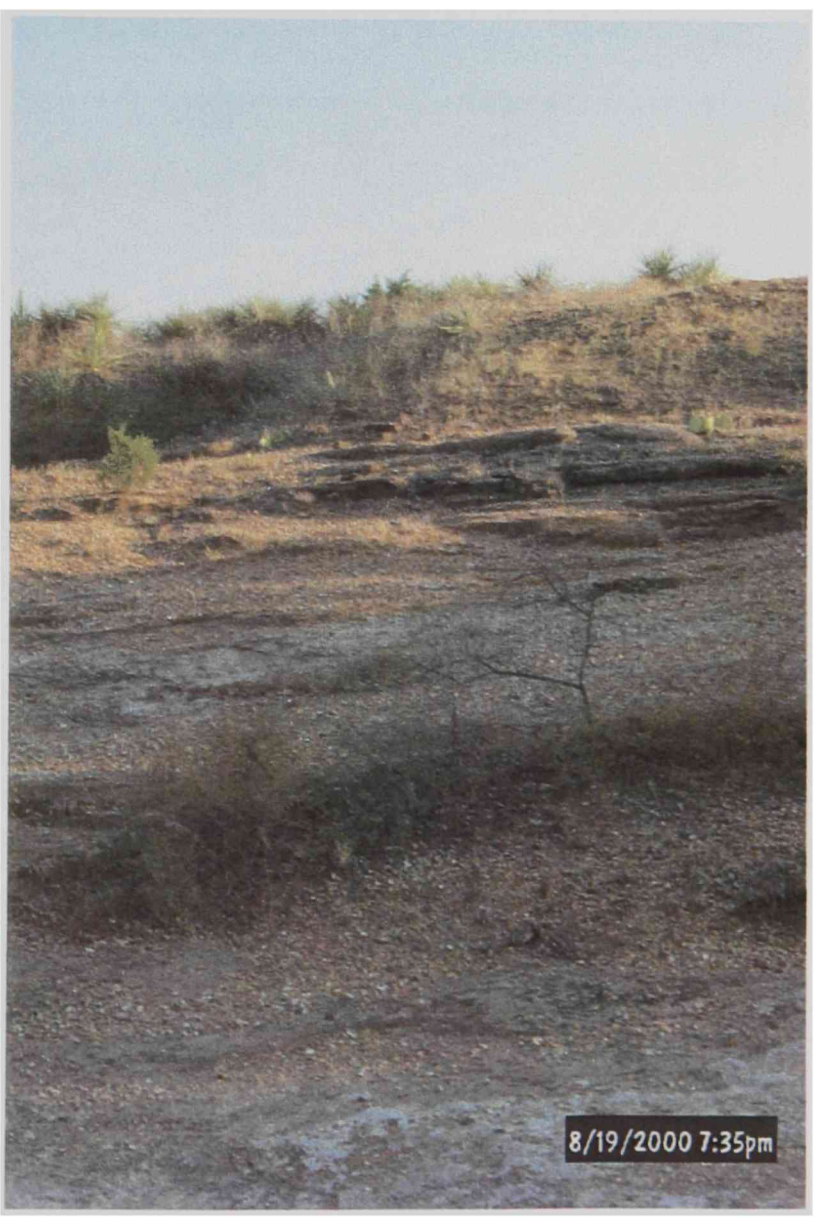

Figure 3.10. Sand and gravels of the Trujillo Formation(Dockum),on the northern Young Ranch.

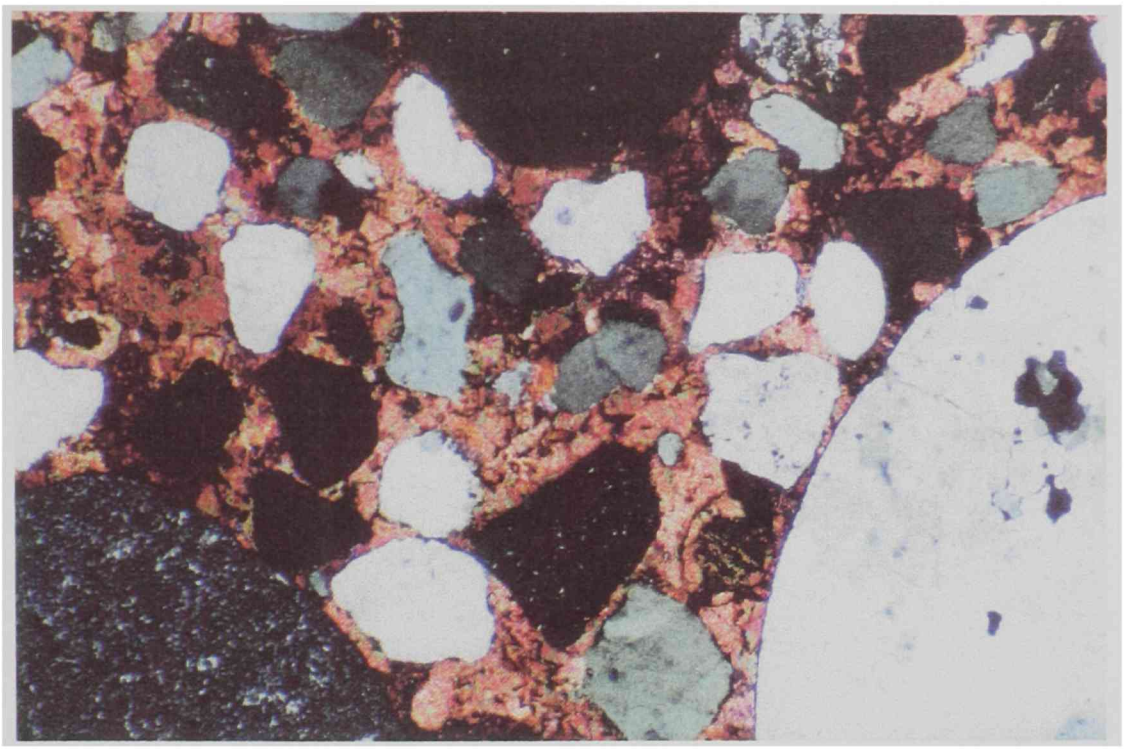

Figure 3.11. - Photomicrograph of a conglomerate from the Triassic Santa Rosa. This sample is representative of the gravel units in section 1A.

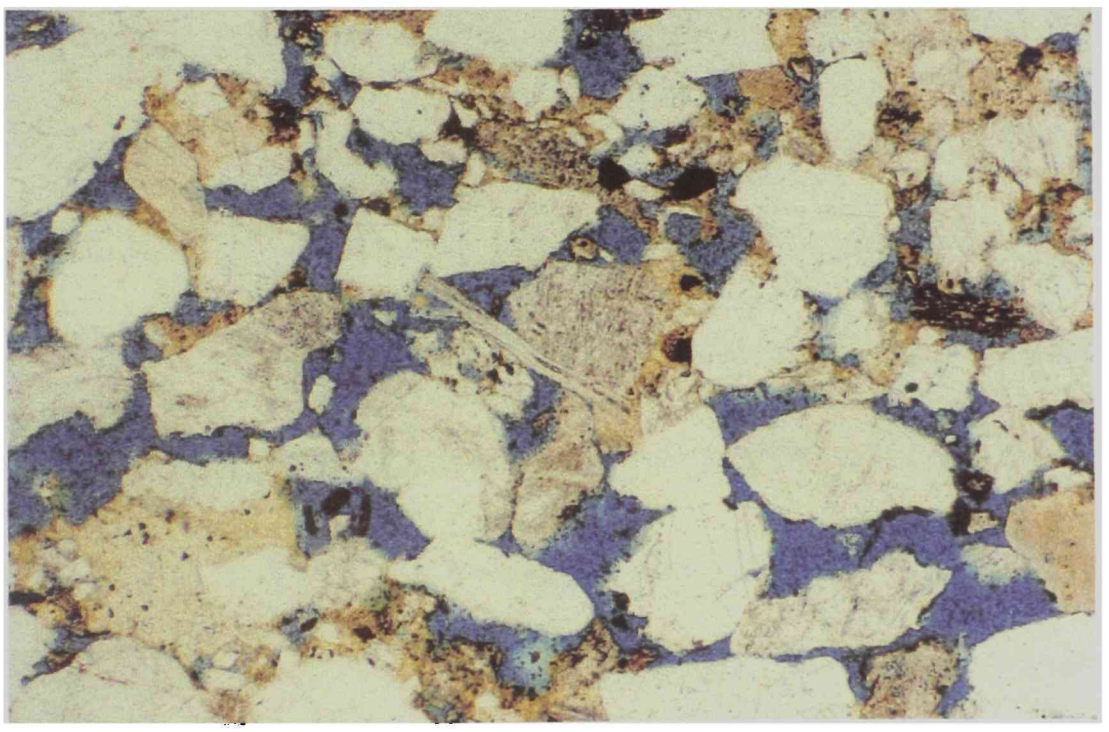

Figure 3.12. Photomicrograph of a miceous sandstone of Triassic Santa Rosa. Field of view is 2mm.

described in detail in the next section. The Antlers can be many colors in outcrop, varying from white to brown to red to purple. Its particles range in size from fine sands to gravels, and it is often well cemented into a quartzite (silcrete). In some cases, it may take several attempts to break with a rock hammer, giving off a distinct ping when struck.

Cretaceous Walnut Formation

The Walnut Formation on the Young Ranch represents the transgression of a sea over the continental deposits of the Antlers. It is a pelecypod algal wackestone/packstone (Figs. 3.13 and 3.14) and is most visible in the main quarry (Fig. 3.15). Three depositional cycles are visible on the west side of the quarry. Each of these cycles consists of three units: (1) a basal marly bioclastic wackestone, which is overlain by (2) bioturbated bioclastic wackestones, that grade upward into 3) bioclastic packstones (Fig. 3.16). Depositional cycles similar to those exposed in the quarry (Fig. 3.5 and 3.17) are present stratigraphically lower in the Walnut, but are poorly exposed. The best location is section 1D (Fig. 3.17) where the two wackestone units of one cycle are visible.

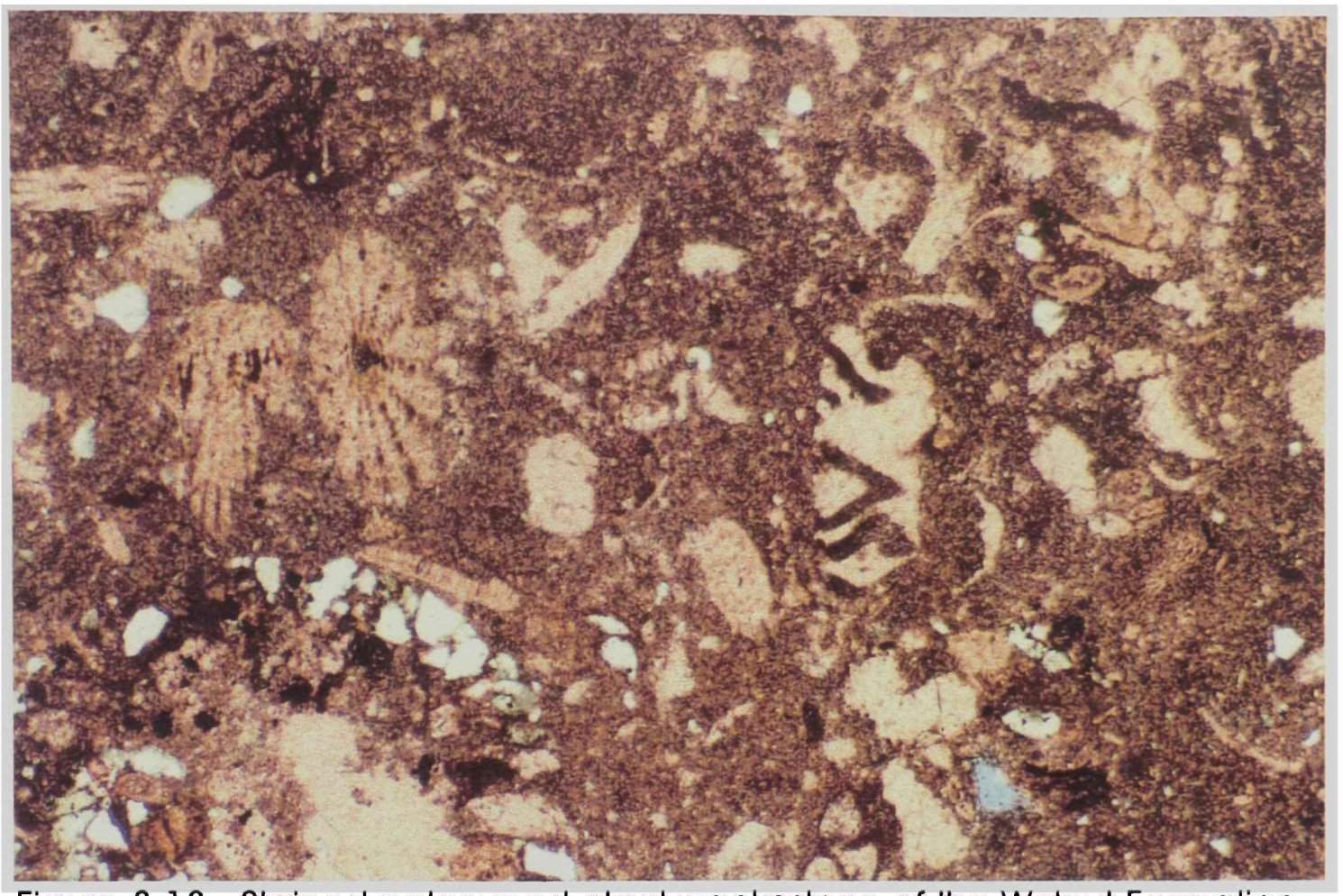

Figure 3.13. Stained pelecypod algal wackestone of the Walnut Formation. Field of view is 2mm.

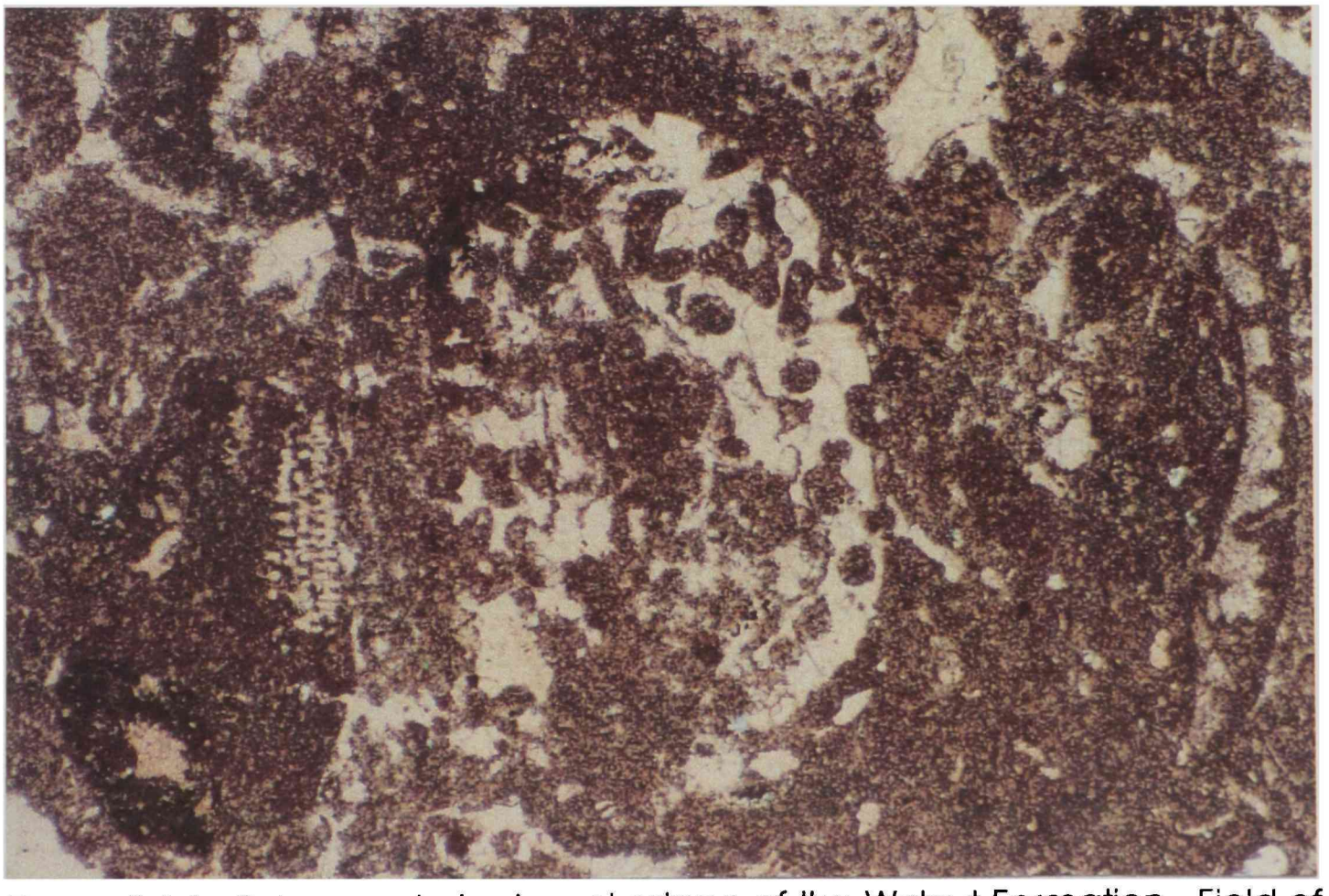

Figure 3.14. Pelecypod algal wackestone of the Walnut Formation. Field of view is 2mm.

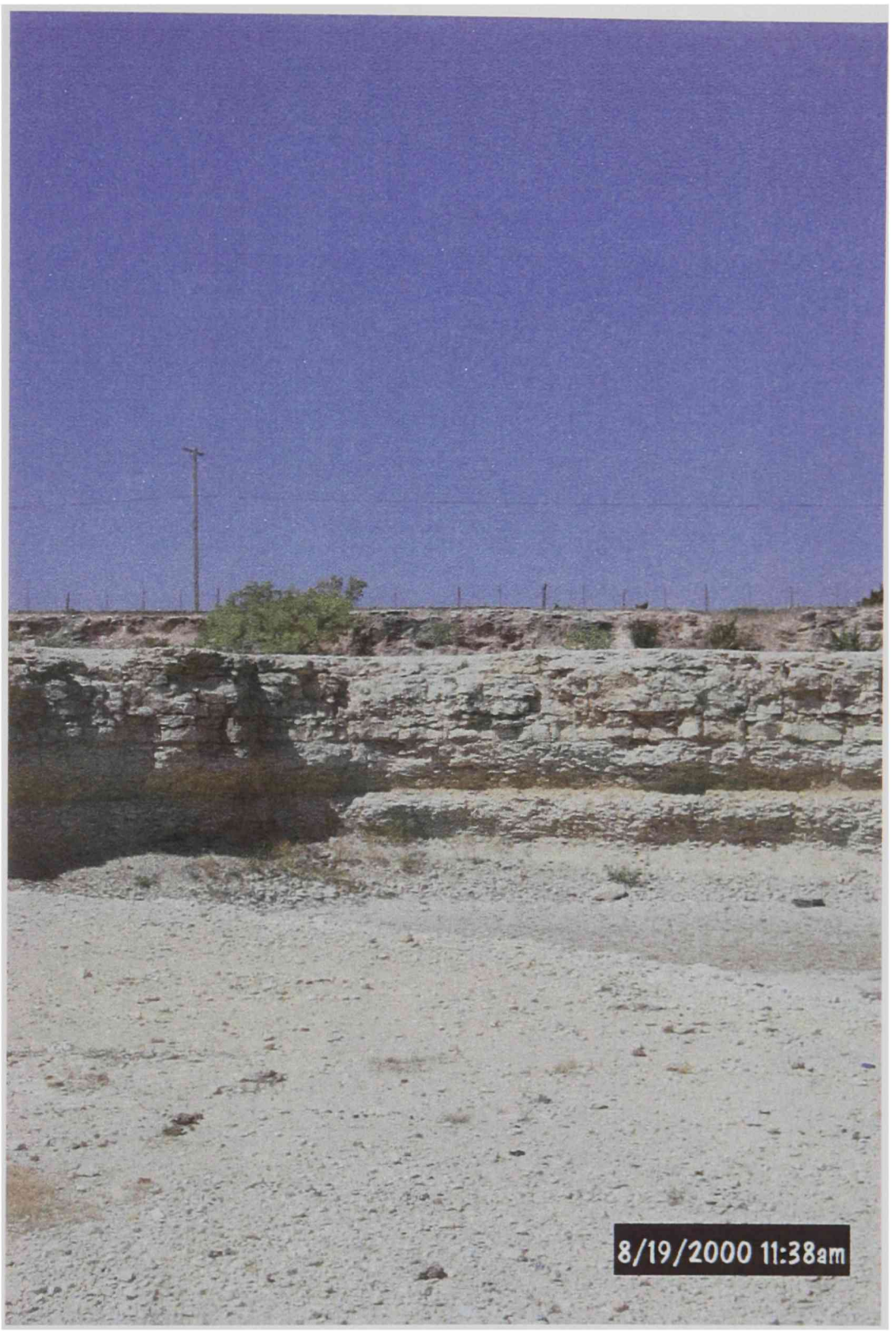

Figure 3.15. Overview of quarry on west side of Young Ranch. Three cycles of the Walnut are visible here.

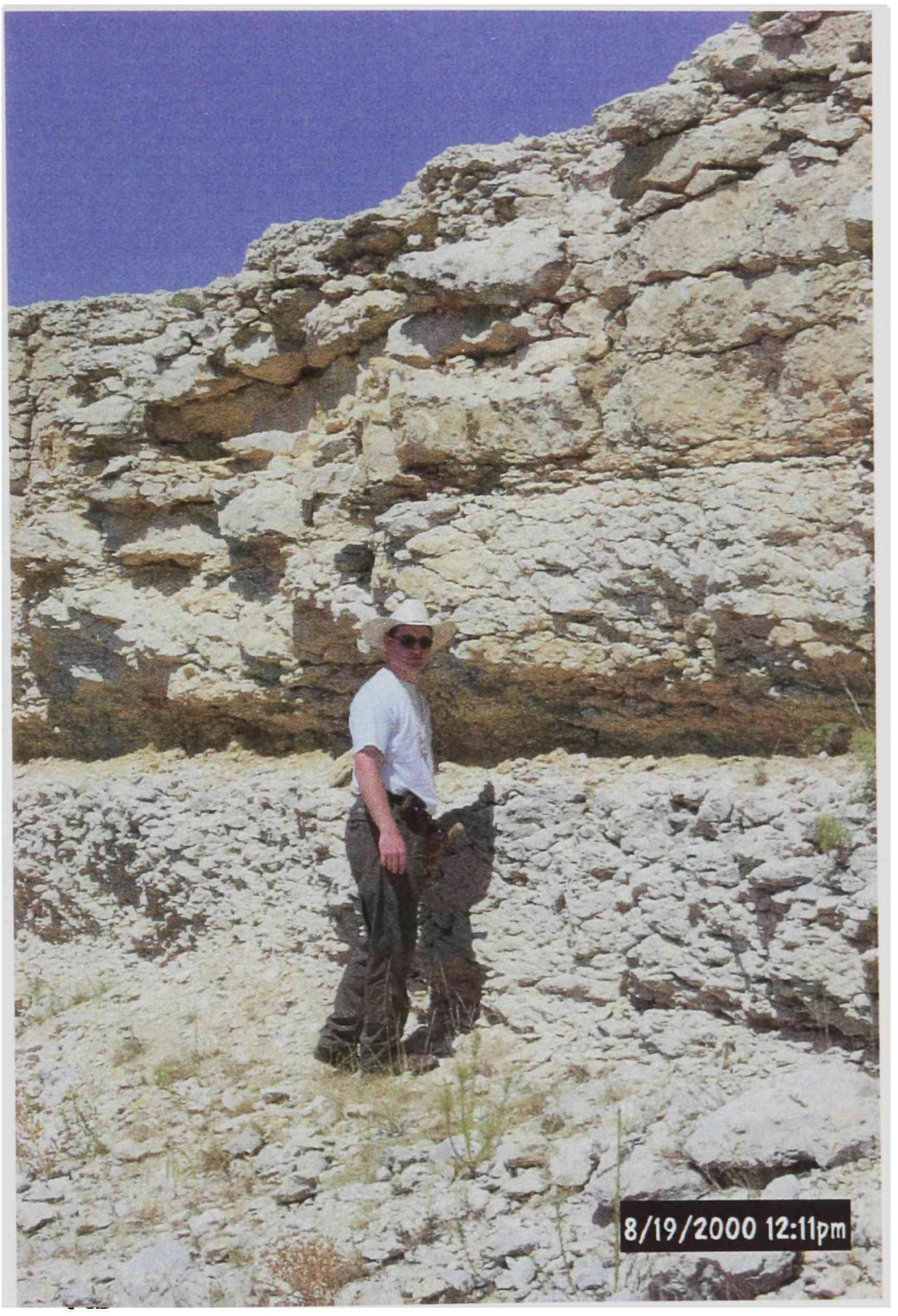

Figure 3.16. Lower two cycles of the Walnut limestone in quarry.

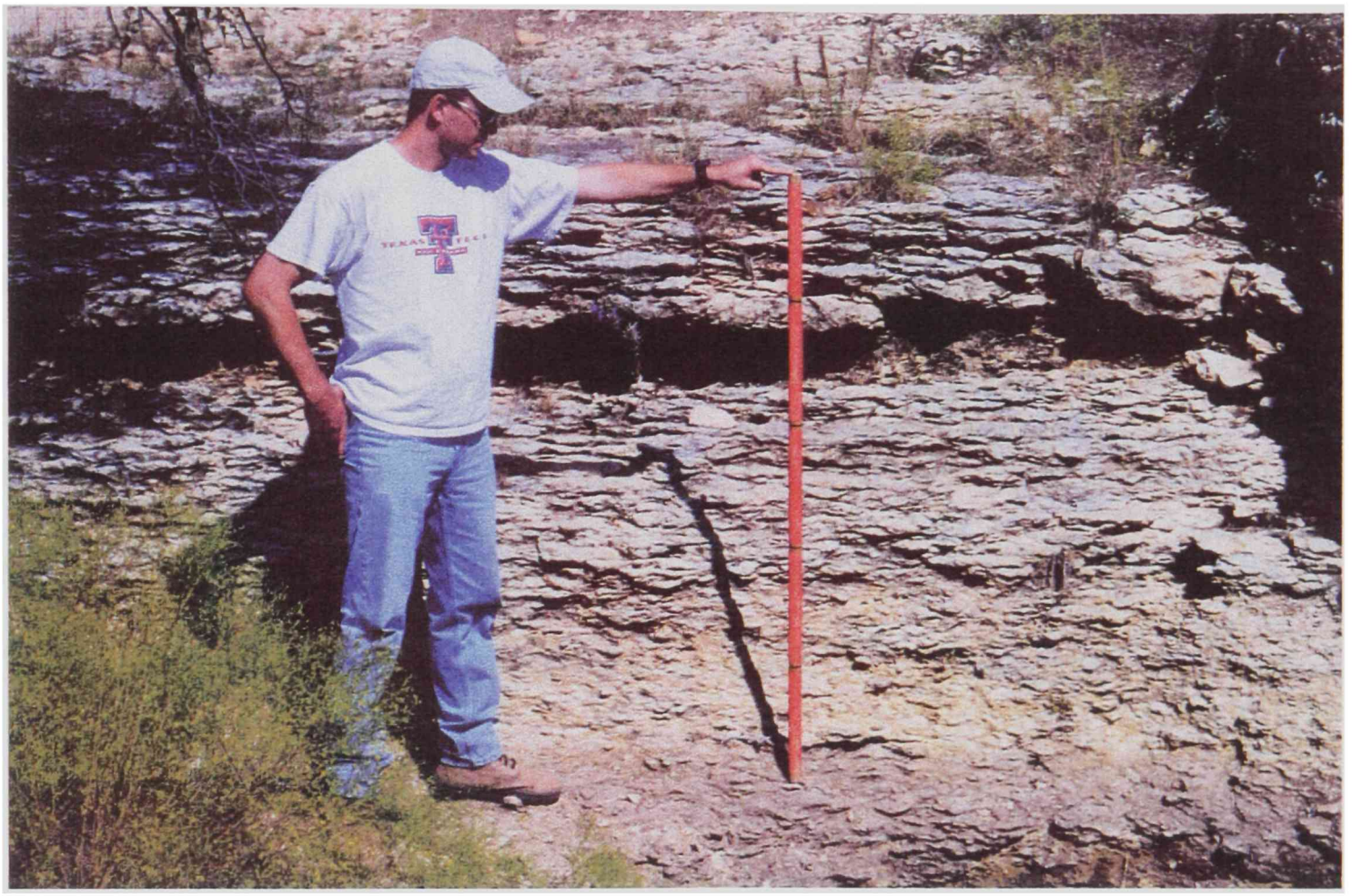

Figure 3.17 - Outcrop of lower cycles in the Walnut (Section 1D).

Depositional Environments of the Antlers Sand

General

The Antlers Sand represents the initial deposition of Cretaceous sediments onto the Wichita Paleoplain (Hobday et al., 1981). The Wichita Paleoplain was a Paleozoic erosional surface to the west of the Ouachita Structural Belt on the Texas Craton (Hobday et al., 1981). Antlers sediments deposited on the Wichita Paleoplain were mixed sand, silt, and gravel sequences characteristic of fluvial environments (Brothers, 1984). The numerous rivers that carried these mixed sediments generally flowed to the east into a transgressive sea (Hobday et al., 1981).

Initial field examination of the Antlers reveals predominately medium grain sandstone with some conglomeratic lens. The conglomerates consist primarily of sand mixed with chert and vein quartz gravels. The Antlers is very quartz rich, and locally well indurated with quartz cement. The Antlers also shows two types of sedimentary structures, trough cross beds (Fig. 3.18) and planar cross beds (Fig. 3.19), with trough cross beds being more dominant. Paleocurrents were measured at different localities throughout the ranch, and rose diagrams were constructed with measurements from 6 locations (Fig. 3.20; Appendix A). General flow direction was to the southeast, consistent with the previous work of

Figure 3.18. Trough cross beds in the channel facies of the Antlers sand.

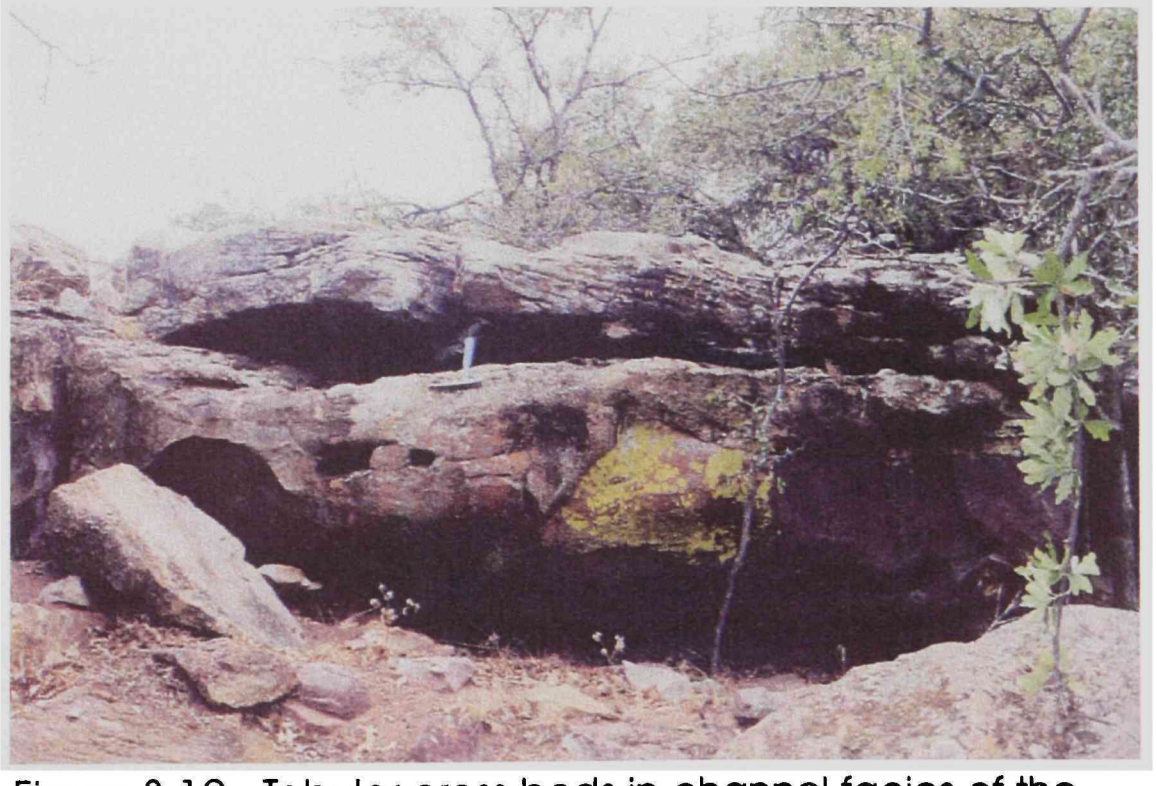

Figure 3.19. Tabular cross beds in channel facies of the Antlers sand.

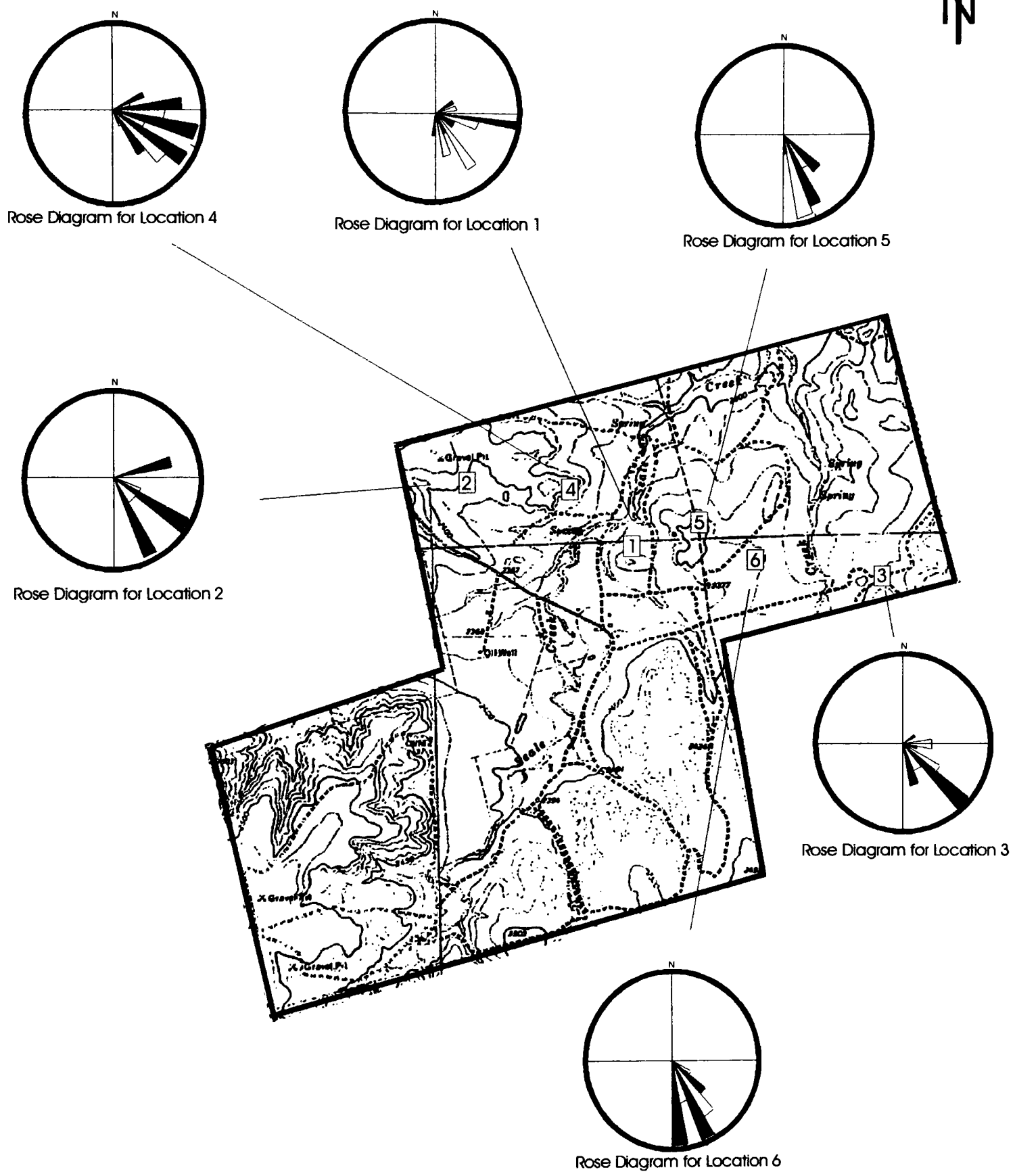

Figure 3.20. - Location of six paleocurrent measurement sites on the Young Ranch.

Hobday et al. (1981).

In the Callahan Divide region, Boone (1972) described eight facies of the Antlers that were deposited in seven depositional environments ranging from fluvial point bars to platform carbonates platforms. However, fieldwork on the Young Ranch only reveals 3 facies of the Antlers. The first facies is a fluvial channel fill facies that consists of trough and planar cross-bedded sandstones and conglomeratic sandstones. This facies is predominately well cemented with quartz cement (Fig. 3.21). The second facies consists of poorly exposed friable sandstones that appear structureless (Fig. 3.22). This facies contains almost no quartz cement. Some calcite cement is present in the lower part of this facies. The sands of this facies may represent floodplain deposits. The third facies is present only in the upper Antlers, and represents a marginal facies that is transitional into the overlying marine pelecypod algal wackestones/packstones of the Walnut Formation. This transitional facies consists of bioturbated sandstone (Fig. 3.23) that grades upward into a sandy oyster bearing wackestone (Fig. 3.24).

Channel Fill Deposits

Several authors (Boone, 1972; Brothers, 1984; Hobday et al., 1981) have noted that the Lower Antlers Formation represents fluvial deposition.

Figure 3.21. Common outcrop character of the well-indurated Antlers.

Figure 3.22. Outcrop of friable Antlers near ranch house.

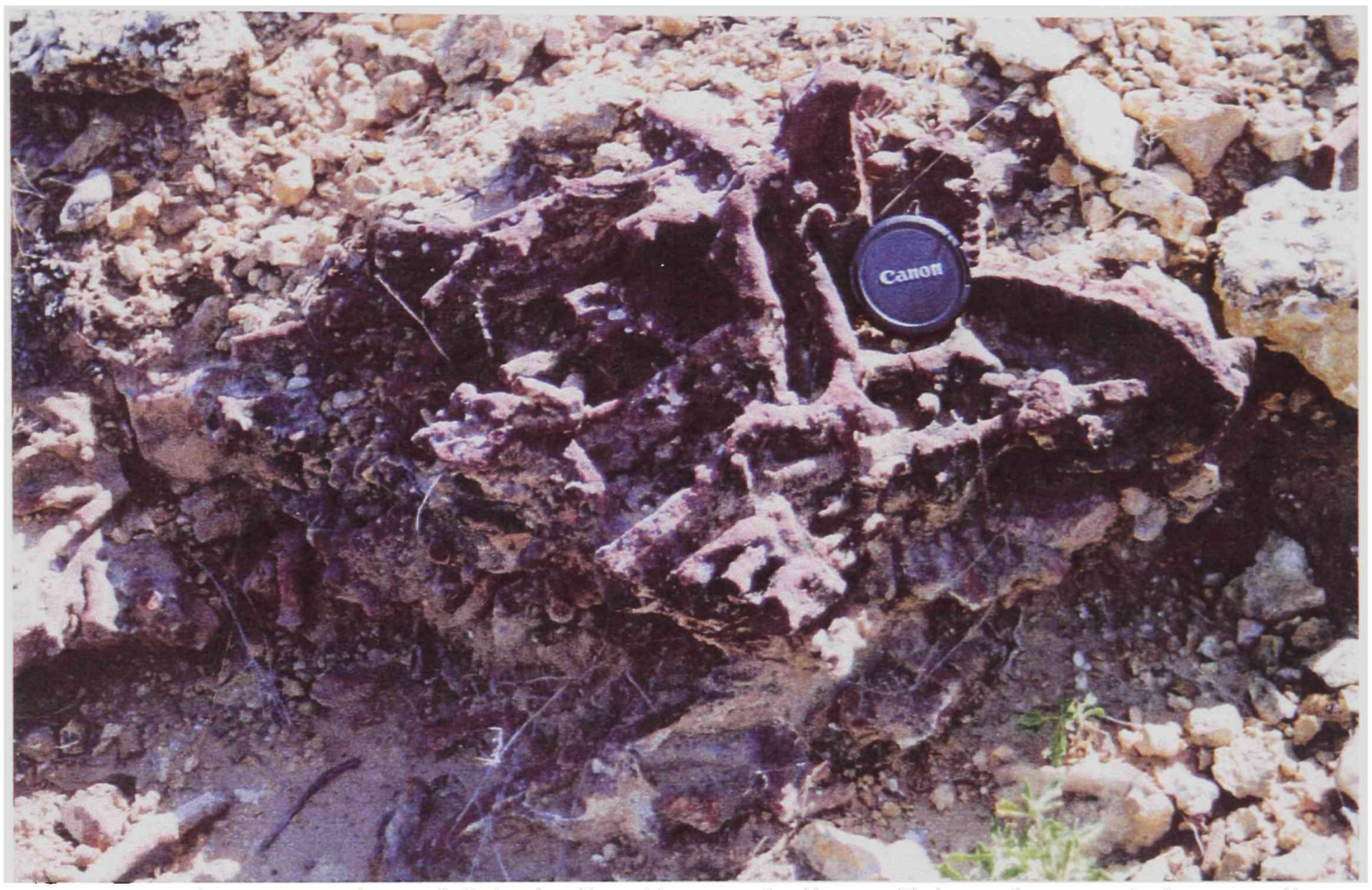

Figure 3.23. Burrowing visible in the Upper Antlers. This outcrops is beneath the sandy oyster wackestone unit.

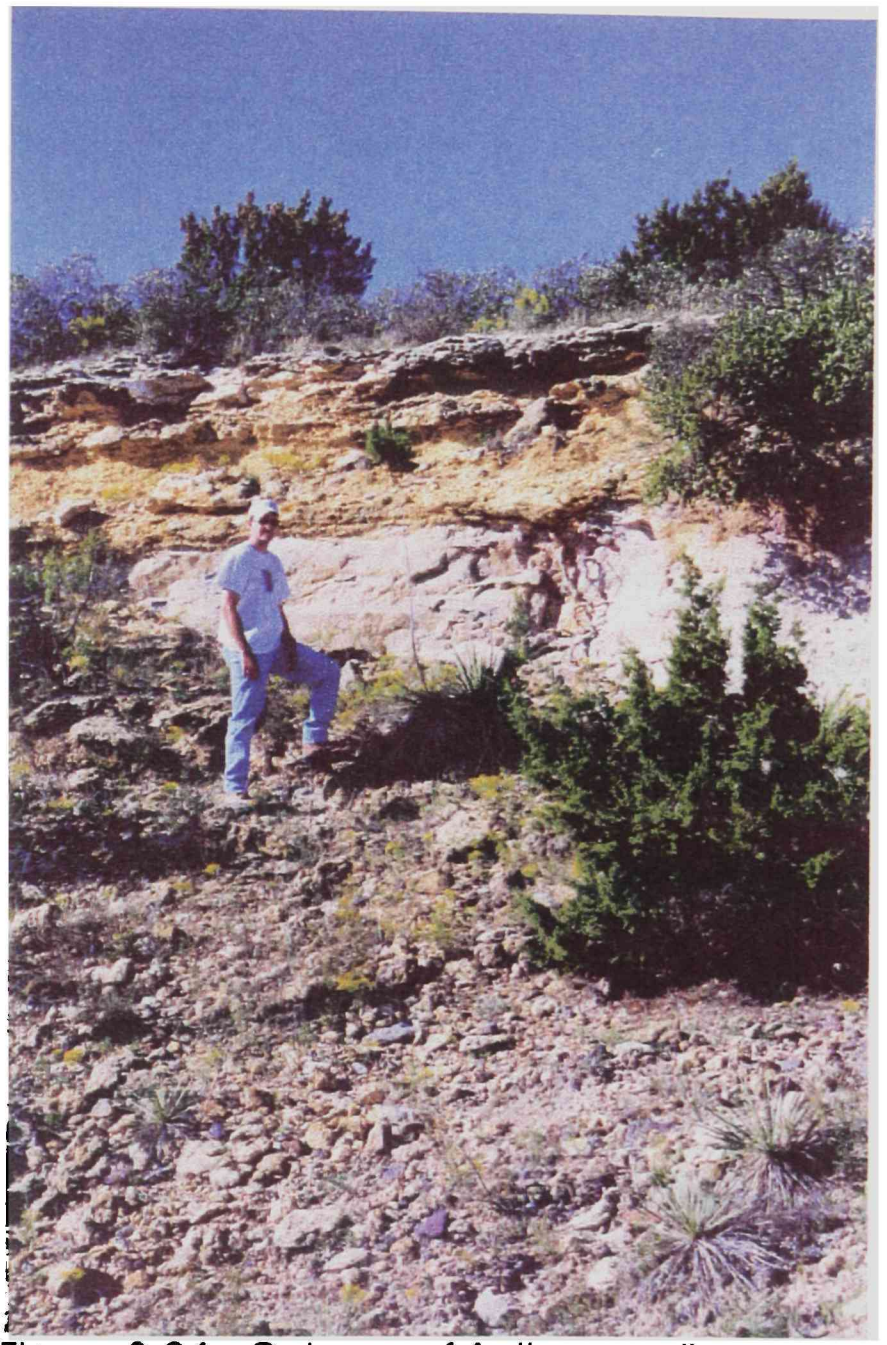

Figure 3.24. Outcrop of Antlers grading upwards into the overlying limestones of the Walnut Formation. Here the Antlers appears light purple in outcrop.

On the Young Ranch, the Antlers appears to have been deposited as a bed-load channel. The Antlers commonly has medium grain sands mixed with occasional gravels, which is consistent with bed-load channels that have been described by Galloway et al. (1996). The Antlers on the Young Ranch could be interpreted as both a braided or a course grained meandering stream deposit. Hobday et al. (1981) described the Antlers in North Texas as a coarse load braided stream. Boone (1972) described fluvial facies he saw in the Antlers as characteristic of meandering streams with gravelly point bar deposits. The finer sediments (silts and muds) that are usually associated with meandering streams (Pettijohn et al., 1987) are not present on the Young Ranch. Due the limited outcrop area and the inability to see the base of the Antlers on the Young Ranch, the best interpretation appears to be a bed-load channel deposit.

Flood Plain Deposits

Flood plain deposits do not appear to be abundant in the Antlers on the Young Ranch. This could be due to the Antlers being a bed-load dominated channel fill. Galloway et al (1996) notes that flood plain facies of bed-load channels are often sandy and occur less often when the channel fill is deposited in a narrow valley. This facies of the Antlers on the Young Ranch exhibits some characteristics of being an overbank or

flood plain deposit. First, the outcrop is very sandy with no mud and is located on the flank of the channel. Second, few if any sedimentary structures are preserved. Third, the upper portion of outcrop appears to be leached. This upper leached portion may have formed from subaerial exposure and is characteristic of many overbank deposits, such as levees and crevasse splays (Galloway et al., 1996).

Measured Sections

Thirteen stratigraphic sections (Fig. 3.25, Appendix B) were measured on the Young Ranch using a staff and Brunton compass. From these sections, variations in Antlers thickness can be seen, as well as the locations of different facies in the Antlers. Cross-section I (Fig. 3.26) is oriented along the interpreted channel trend which in some locations can outcrops for hundreds of meters (Fig. 3.27). Cross-section I shows variation of thickness in the Antlers silcrete on the ranch. Cross-section II (Fig. 3.28) is oriented perpendicular to the interpreted channel trend. All three facies of the Antlers are represented in this cross-section, showing the vertical relationship of the silcrete to the upper Antlers.

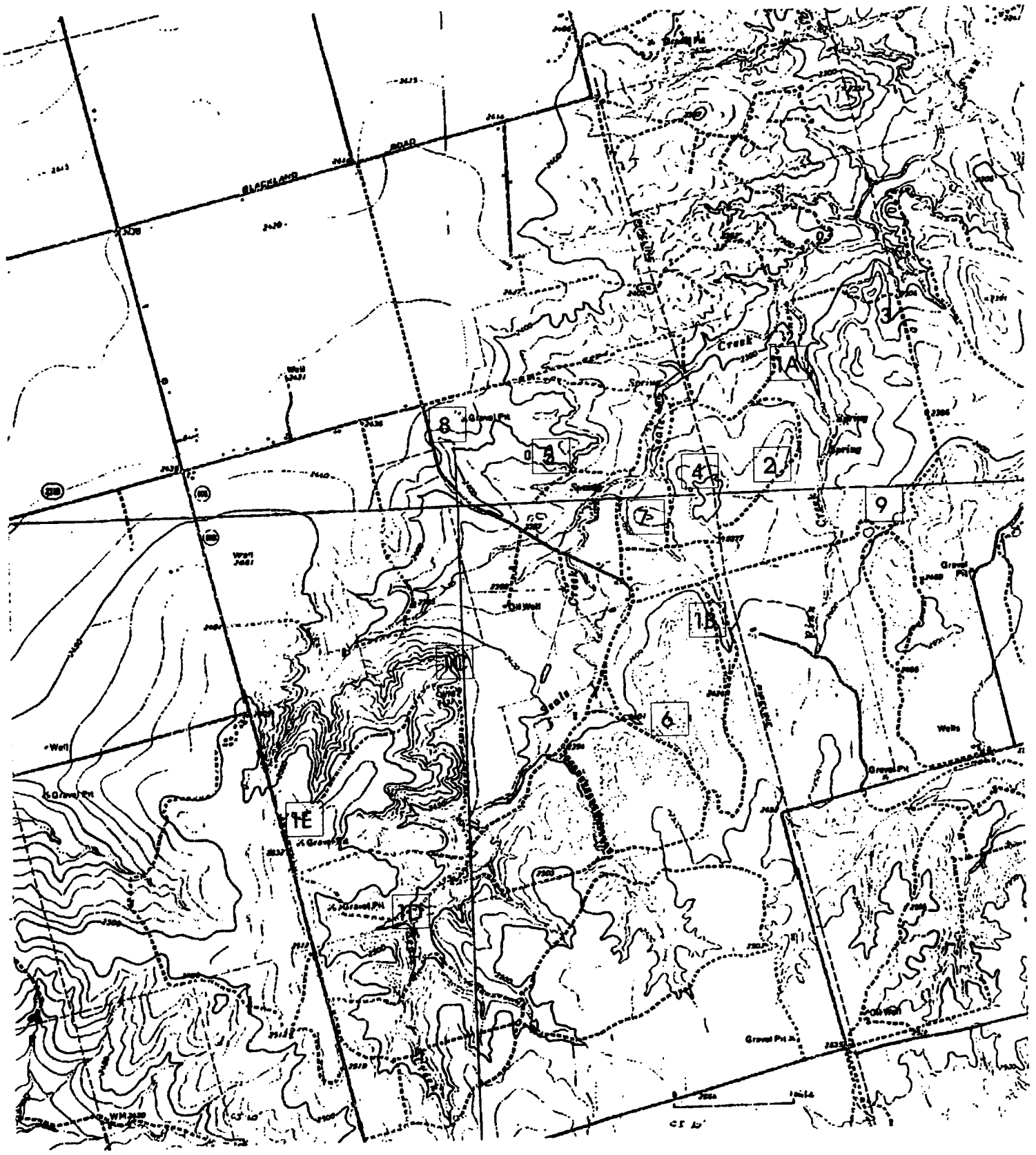

Figure 3.25. Topographic map showing locations of measured sections on the Young Ranch.

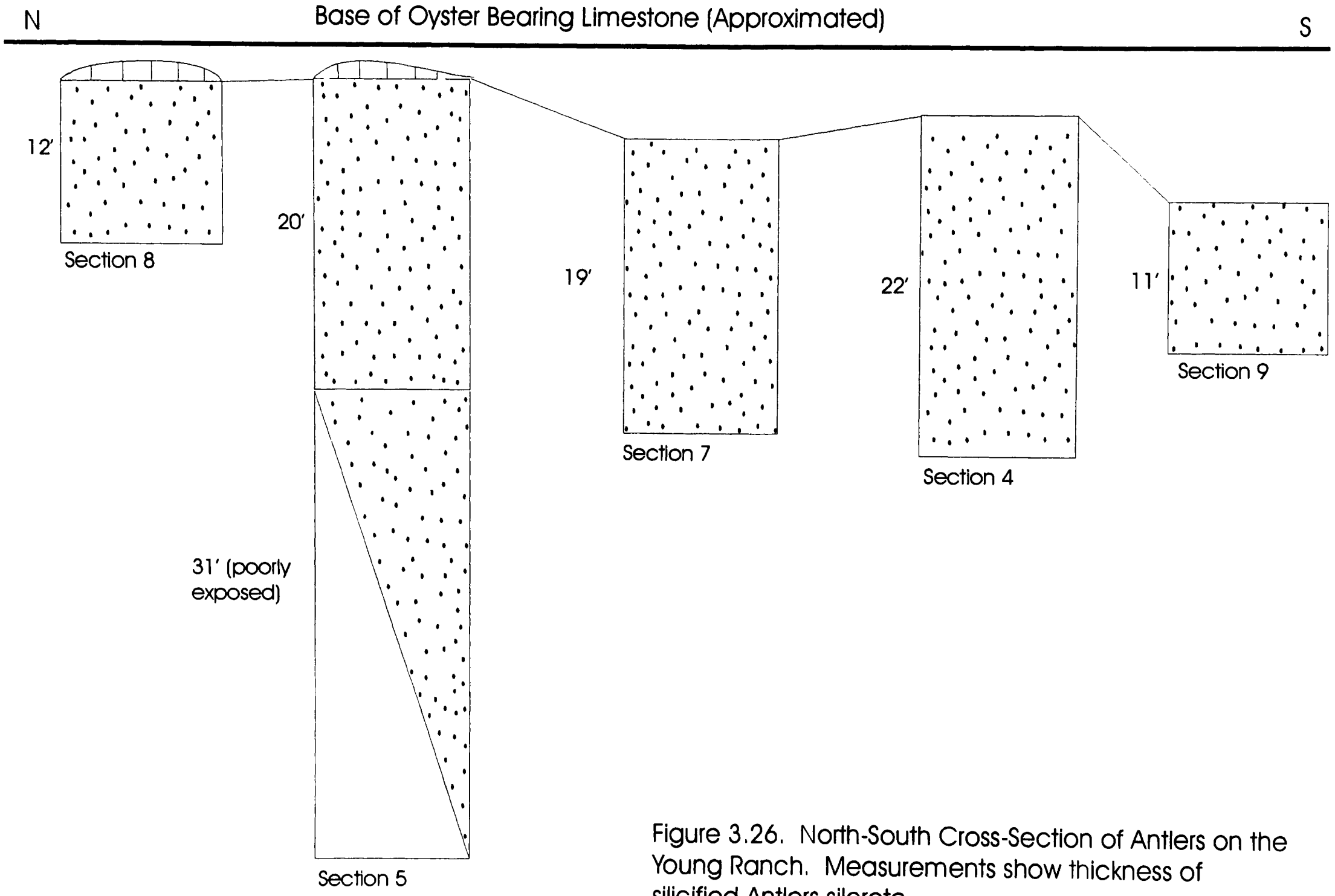

Figure 3.26. North-South Cross-Section of Antlers on the Young Ranch. Measurements show thickness of silicified Antlers silcrete.

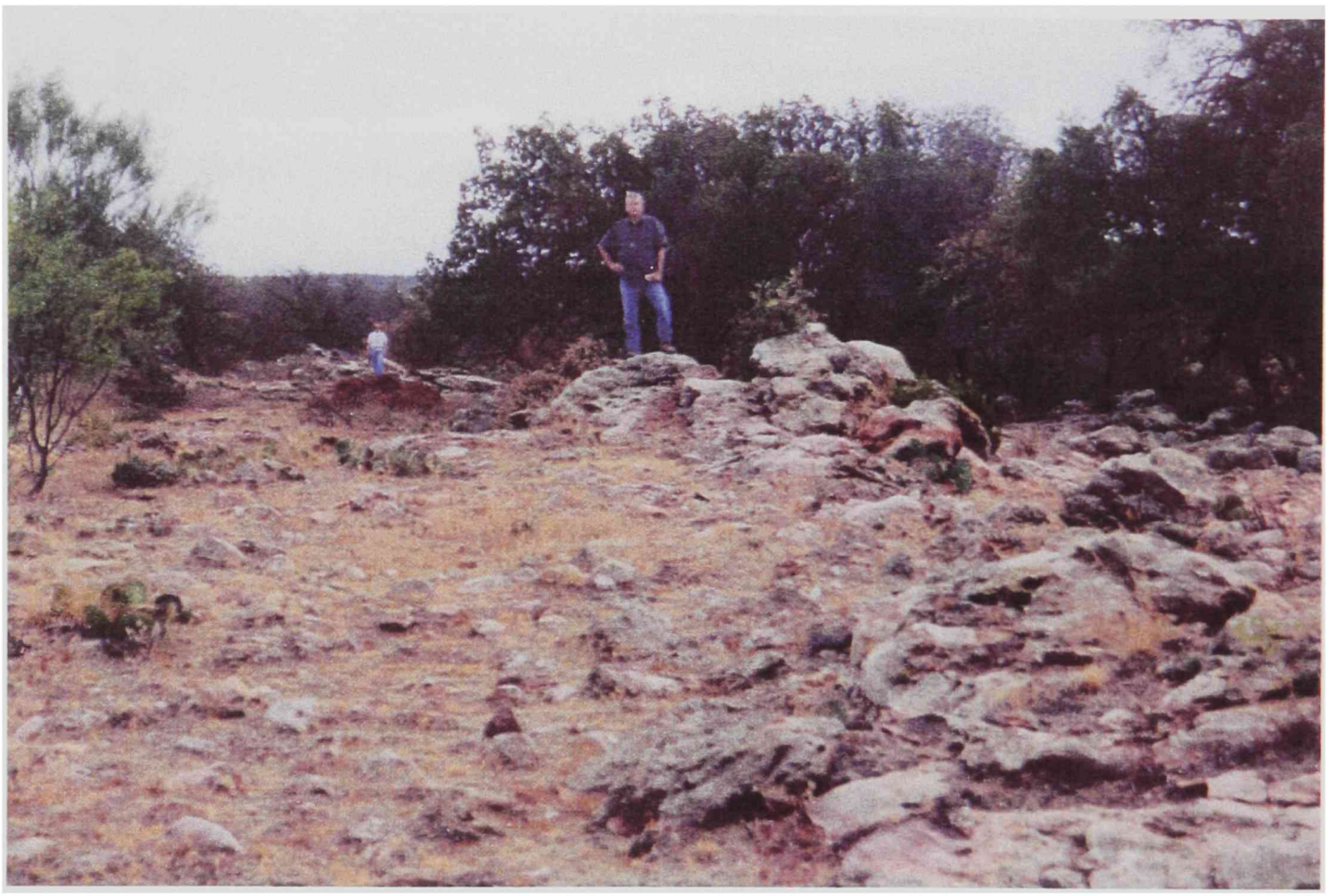

Figure 3.27. Photo showing distribution of Antlers channel deposits. Some outcrops on the ranch are exposed for several hundred yards.

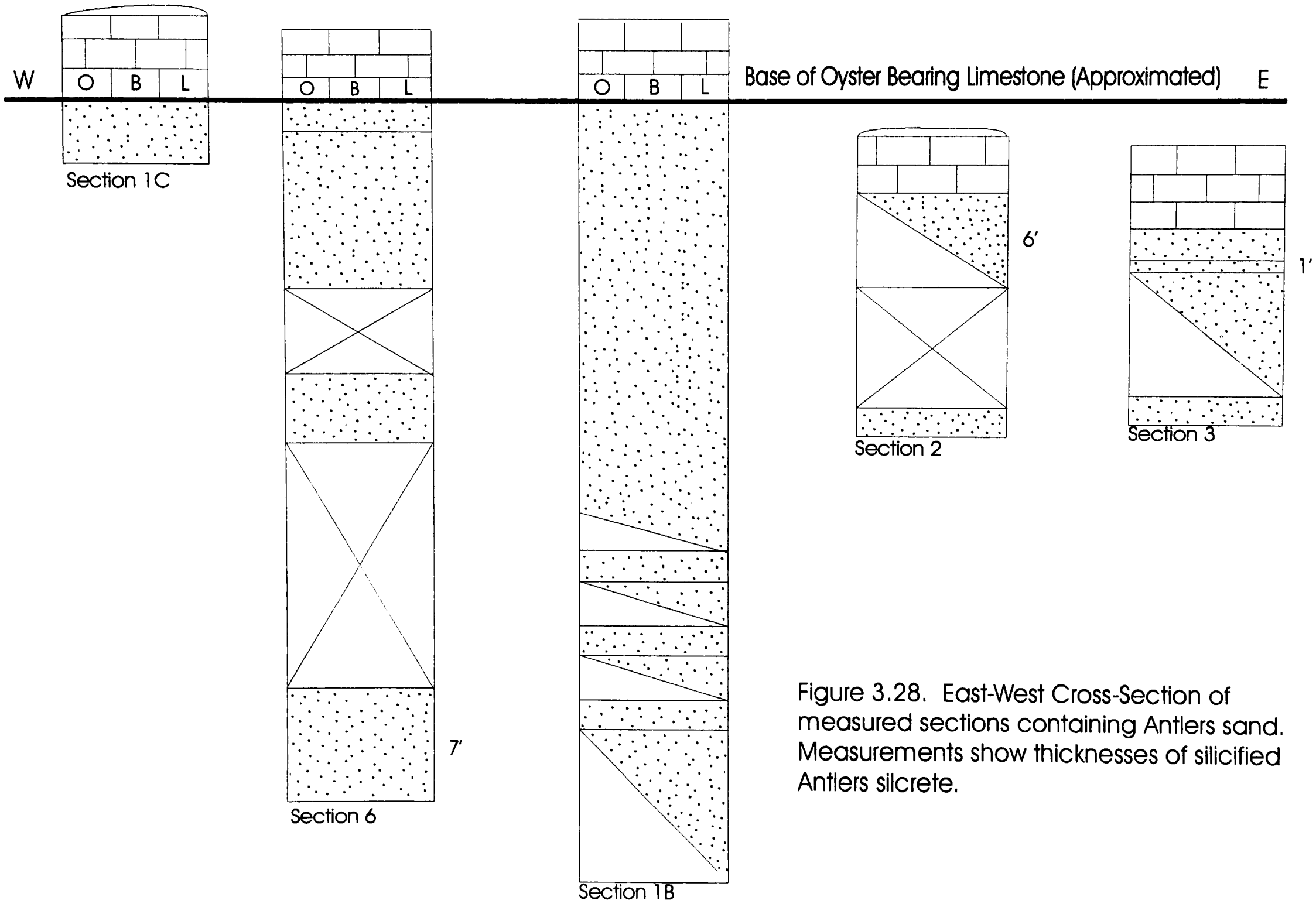

Figure 3.28. East-West Cross-Section of measured sections containing Antlers sand. Measurements show thicknesses of silicified Antlers silcrete.

CHAPTER IV

PETROGRAPHY

General

The Antlers Sandstone on the Young Ranch occurs throughout the ranch and varies in thickness from 1 to 2 feet in some locations to a maximum thickness of 56 feet in section 5. Samples of all stratigraphic units on the ranch were taken from thirteen localities (Fig. 4.1) and the Antlers was collected at ten localities. Thin sections were made from the Permian Quartermaster (Fig. 3.7), the Triassic Santa Rosa (Figs. 3.8 and 3.9), the Cretaceous Walnut (Figs. 3.13 and 3.14), and the Cretaceous Antlers, with the bulk of the thin sections focusing on the Cretaceous Antlers. Siliciclastic rock classification by Folk (1980) and carbonate rock classification by Dunham (1962) were used during both field and petrographic work.

Forty-seven slides of the Antlers Sandstone were systematically counted to 300 points (Appendix C), and error percentages were kept to approximately four percent based on work published by Van Der Plas et al. (1965). All of the Antlers except five were impregnated with blue epoxy, and half-stained with Alizarin Red-S for the presence of carbonate. The five slides not impregnated with blue epoxy were stained for potassium

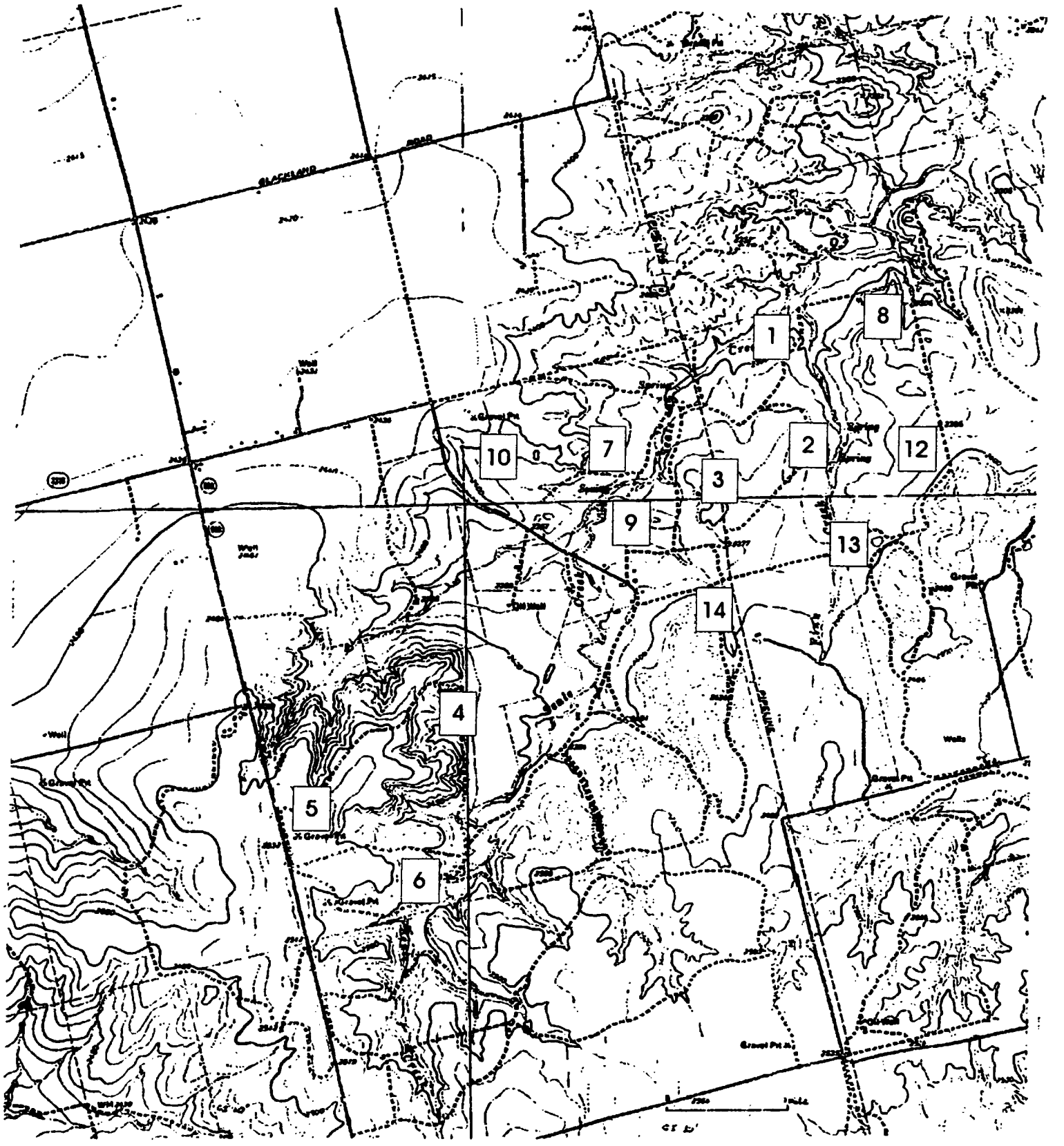

Figure 4.1. Topographic map showing sample collection locations.

feldspars. Detailed descriptions wiere made of the four different rock types found within the Antlers. They are: (1) a well-cemented quartzarenite with predominate quartz overgrowths, (2) a well-cemented quartzarenite with abundant microquartz cement, (3) a calcite cemented quartzarenite, and (4) a friable bleached quartzarenite. Associated with the friable bleached Antlers quartzarenite is an overlying transgressional marine unit that is a sandy oyster bearing wackestone/packstone (Fig. 4.2). This unit represents the end of Antlers deposition as a transition unit into the overlying marine limestones of the Walnut Formation.

Quartz is very abundant in the Antlers Sandstone, commonly comprising over 90% of the total rock composition. Compositionally, the Antlers Sandstone is a quartzarenite (Fig. 4.3). During point counting, quartz grains were distinguished based on crystalline type as well as extinction type. Monocrystalline quartz with straight extinction is the most abundant grain type in the Antlers, occurring twice as often as monocrystalline undulose grains (Appendix C). Polycrystalline quartz grains are also present, but usually make up less than 10% of quartz grains. With these three types of quartz grains plus the presence of chert grains, almost all of the framework grains in the Antlers are siliceous (Fig.

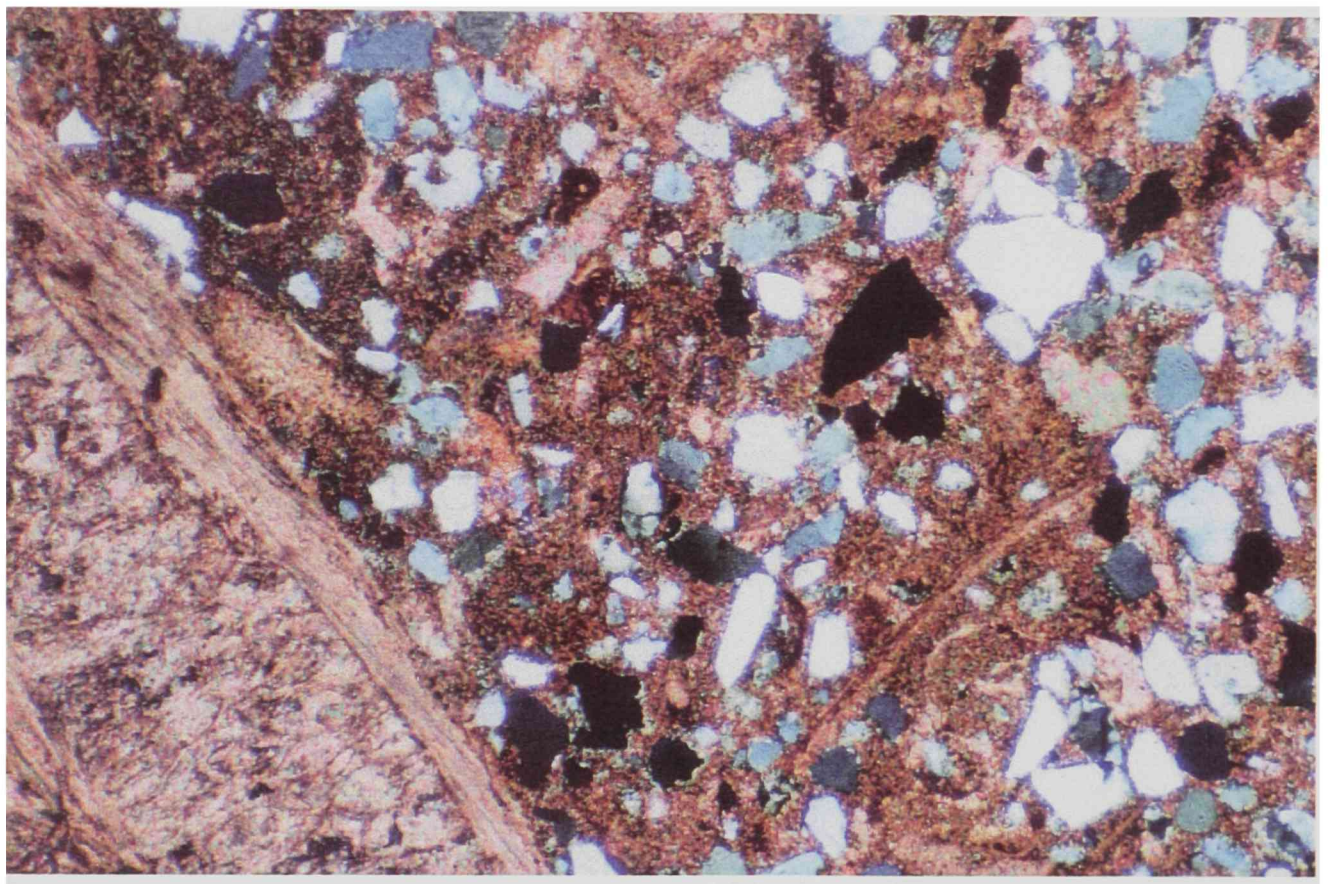

Figure 4.2. Photomicrograph of sandy oyster bearing wackestone. Field of view is 2mm.

4.4). Although chert is siliceous, using siliciclastic classification by Folk (1980), it is counted as lithic grain in clan name determination (Fig. 4.3).

Cement types were also distinguished between quartz overgrowths and microcrystalline quartz. Syntaxial overgrowths on the quartz grains are most common. Quartz overgrowths comprise about 70% (Table 4.1), whereas microcrystalline quartz comprises about 30% (Table 4.1). Red opaque cement (Fe oxide) is abundant in most slides (fig. 4.5) and comprises approximately 4% of total counts (Appendix C). Calcite cement was only observed in the friable Antlers and point counted in four slides. Where present, calcite cement locally comprises over 25% of total rock volume.

Detailed Descriptions

Sample LW-13-2: Antlers sandstone with quartz overgrowth cement

LW-13-2 (Fig. 4.6) is a medium grained sandstone with well-developed quartz overgrowths. Grains in this sample range in size from 177 to 350μm. This sample is moderate to well sorted, with most grains appearing subround to round in shape. Most framework grains in this sample are monocrystalline, with 40% having straight and extinction and 30% having undulose extinction. Polycrystalline grains (%7) and chert

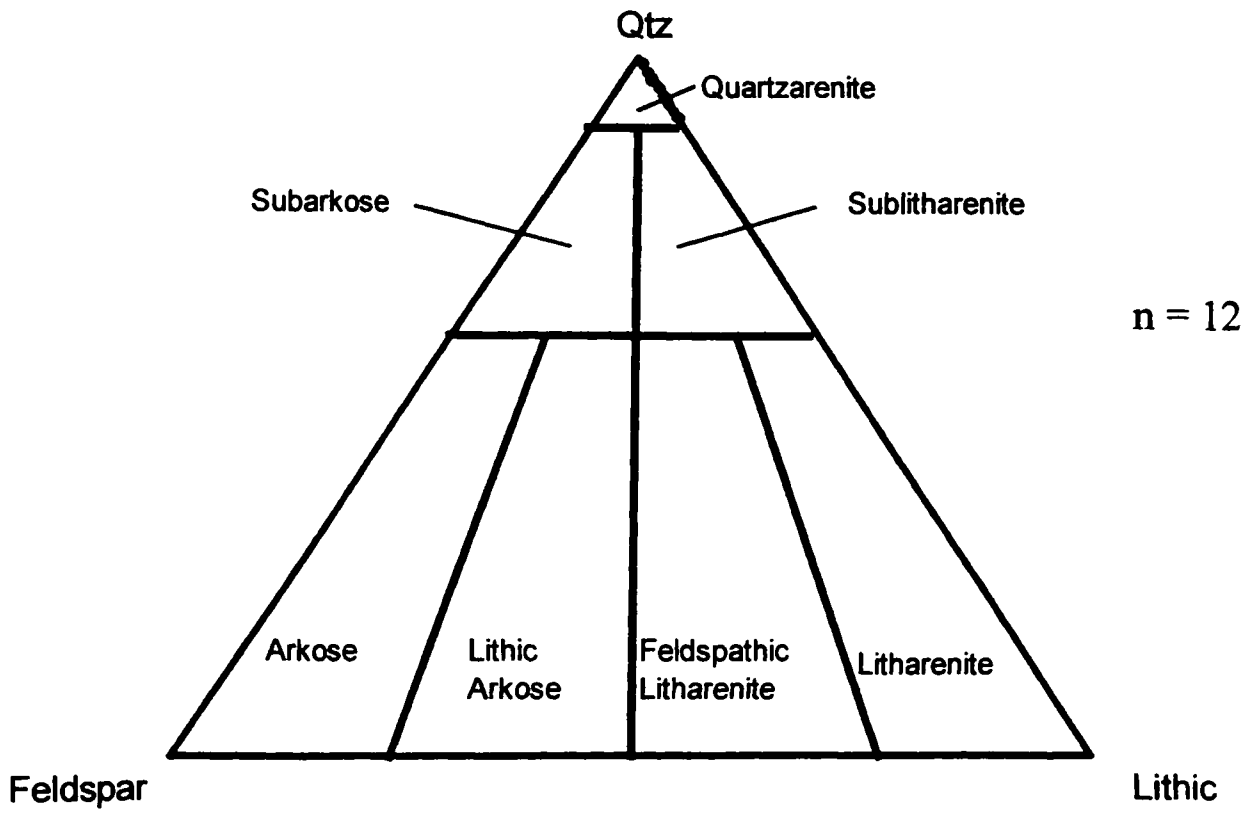

Figure 4.3. Ternary diagram showing composition of Antlers sandstone. All lithic grains were chert.

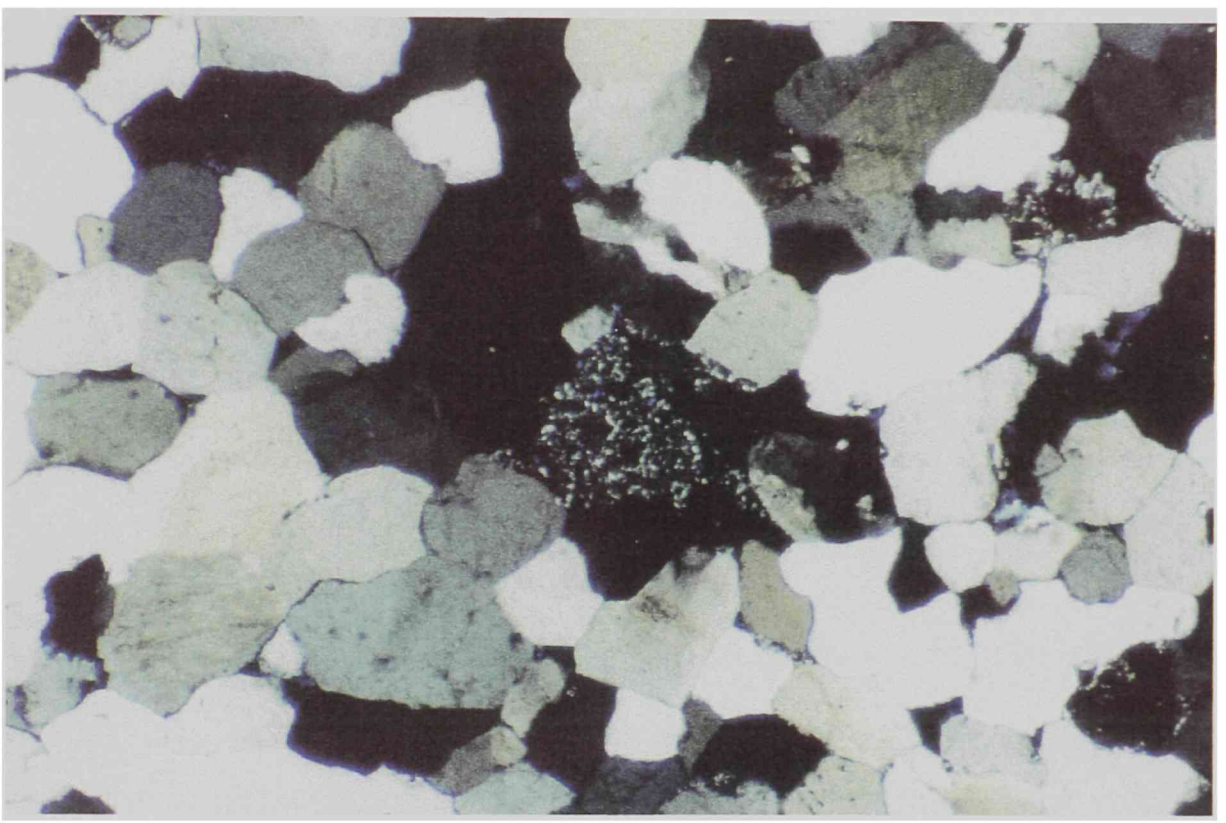

Figure 4.4. Photomicrograph taken under cross-polars showing almost all detrital quartz grains with a chert grain in the center of field of view. Field of view is 2mm.

Table 4.1. - Percentages of silica cement from Antlers point count data.

Collected from	% Overgrowths	% Microquartz	Number of slides
Locality 2	70	30	1
Locality 3	76	24	13
Locality 4*	0	0	1
Locality 7	89	11	4
Locality 8	29	71	1
Locality 9	100	0	1
Locality 10	65	35	11
Locality 12	100	0	1
Locality 13	91	9	6
Locality 14	9	91	8
TOTAL**	**67.4**	**32.6**	**47**

* = All cement in this sample was Iron oxide (red opaque)
** = Percentages taken from Appendix C

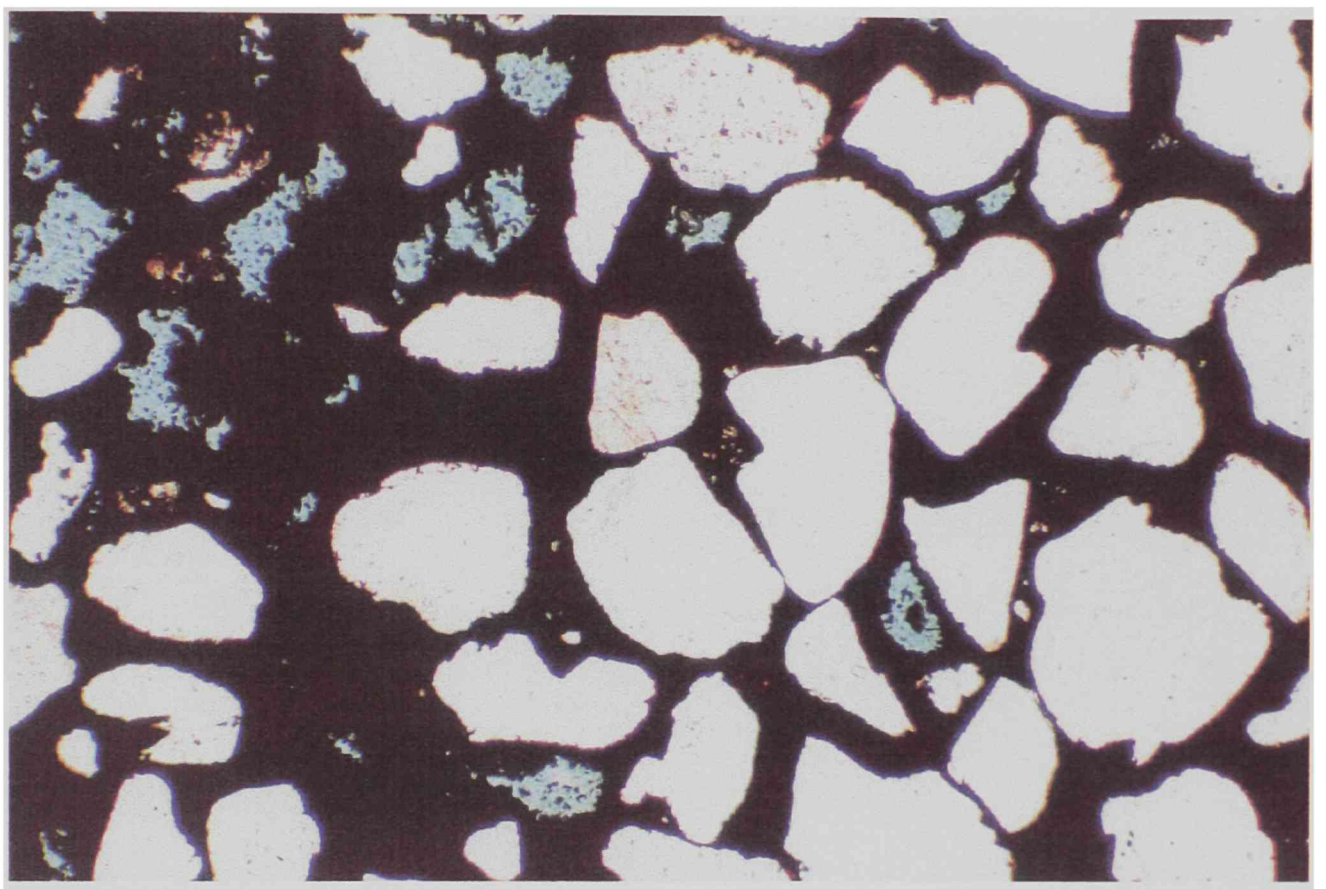

Figure 4.5. Photomicrograph of red opaque cement, possibly iron oxide(?), In the Antlers. Field of view is 1mm and photo was taken with uncrossed nicols.

Figure 4.6. Photomicrograph of Antlers sandstone with abundant and well-developed quartz overgrowths. Field of view is 1mm.

grains (3%) are also present. Syntaxial quartz overgrowths (15%) are the most abundant cement type, with microcrystalline quartz (2%) also being present. This sample has well-developed dust lines, making the overgrowths very visible.

Sample LW-3-11: Antlers sandstone with microcrystalline (mircoquartz cement)

LW-3-11 (Fig. 4.7) is a medium grained sandstone with abundant microcrystalline quartz cement (mircoquartz). This sample shows some maturity, with subrounded to rounded grains and appears well sorted. The majority of the framework grains in this sample are monocrystalline (66%), with straight extinction (38%) being more prominent than undulose extinction (28%). Polycrystalline quartz (2%) and chert grains (1%) are but in low abundance. Microquartz cement (21%) is present on almost all grains, with larger mircoquartz crystals filling the intergranular porosity.

Sample 14-9: Calcite cemented Antlers sandstone

LW-14-9 (Fig. 4.8) is a fine to medium grained sandstone with grain sizes ranging from 125-500μm. It is moderately sorted with most grains being subangular to subround. In outcrop, the sand is friable, but can be

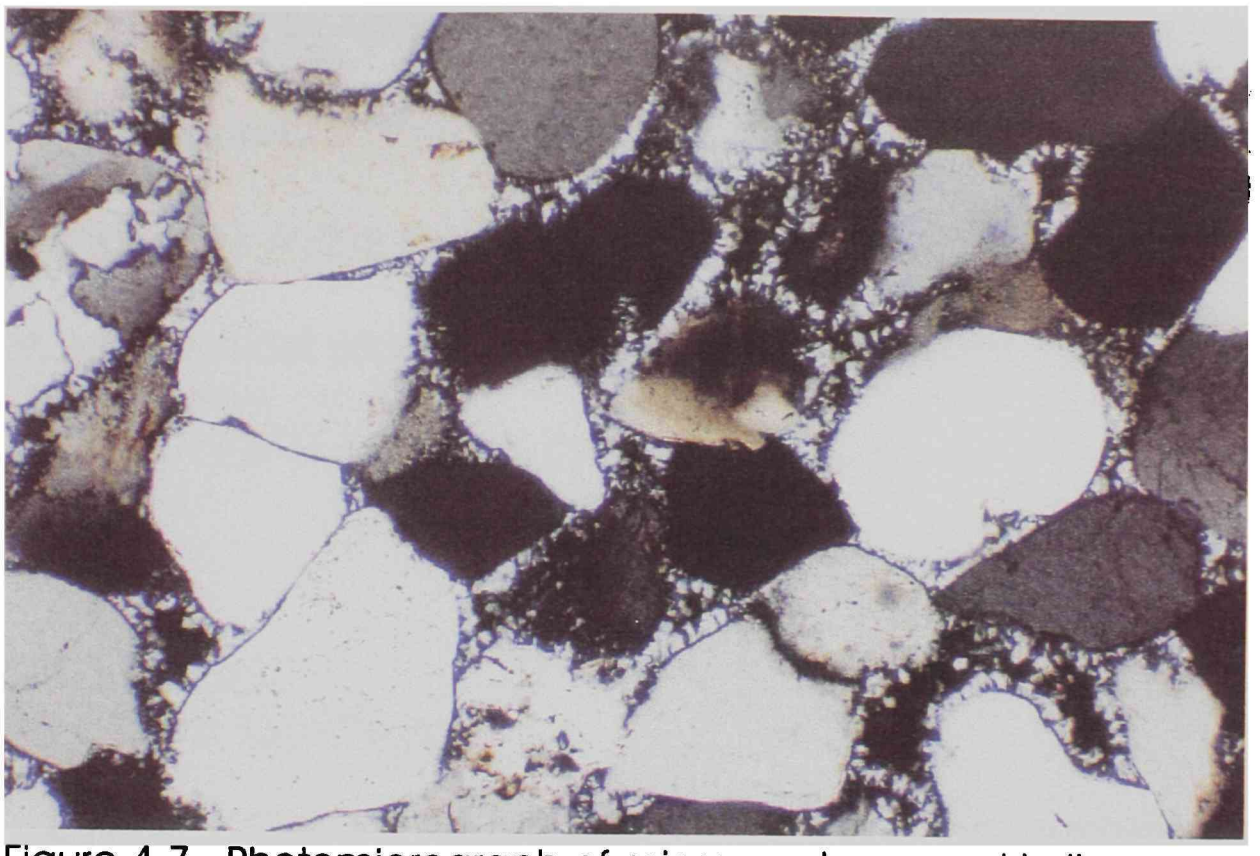

Figure 4.7. Photomicrograph of microquartz cement in the Antlers sandstone. Field of view is 1mm.

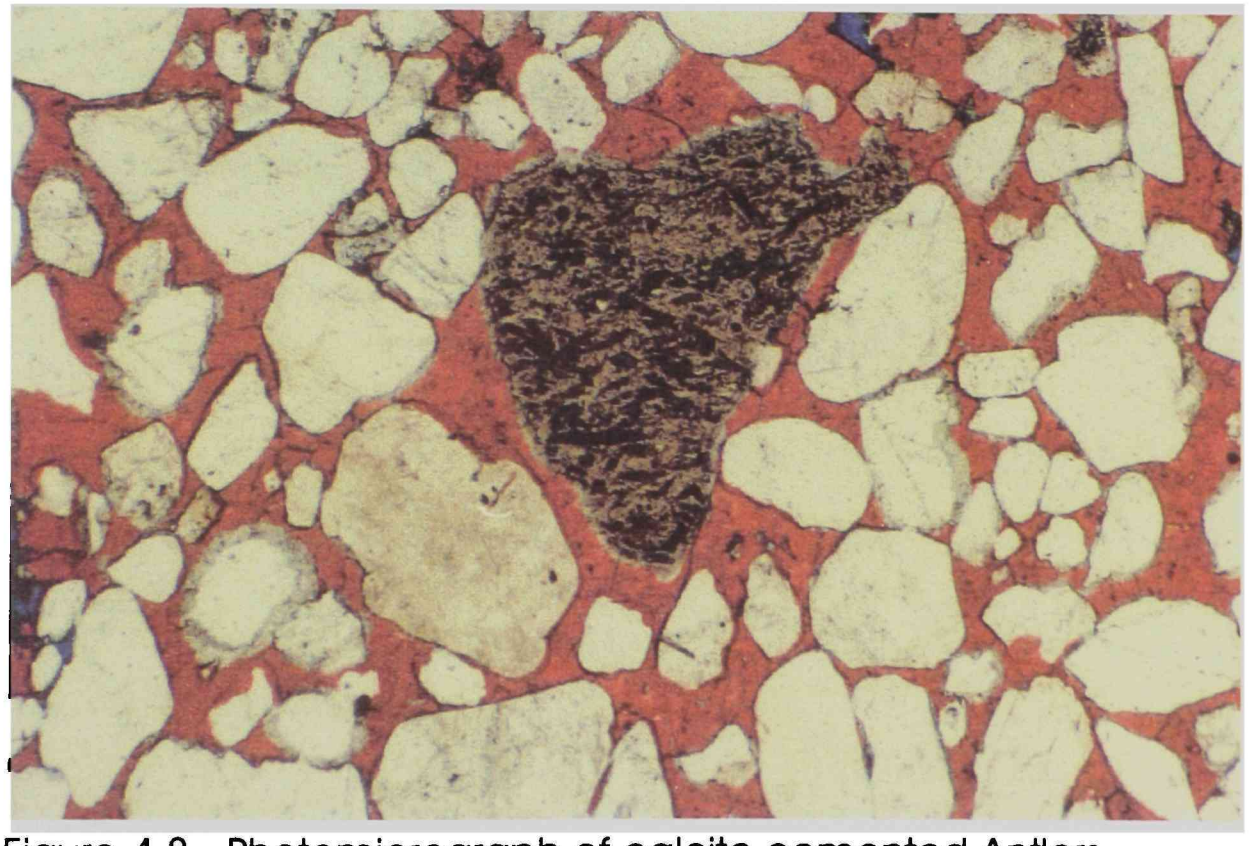

Figure 4.8. Photomicrograph of calcite cemented Antlers sandstone. Sample has been stained for calcite. Field of view is 1mm.

locally cemented by calcite. This sample was stained with Alizarin R-S to confirm the presence of calcite cement. By volume, calcite cement is very abundant (27%) and is the only cement type present. Monocrystalline grains are the most prominent framework grains (58%), with polycrystalline quartz (11%) and chert grains (3%) also present.

Sample LW-14-1:
Friable Antlers sandstone

LW-14-1 (Fig. 4.9) is a fine to medium grained sandstone with grain sizes ranging from 177-350μm. This sample shows almost no cement and is very porous (23%). Blue epoxy (visible porosity) was used to help hold grains together for thin sectioning. Sample LW-14-1 is 67% monocrystalline, with some polycrystalline quartz (6%) and chert grains (2%) present.

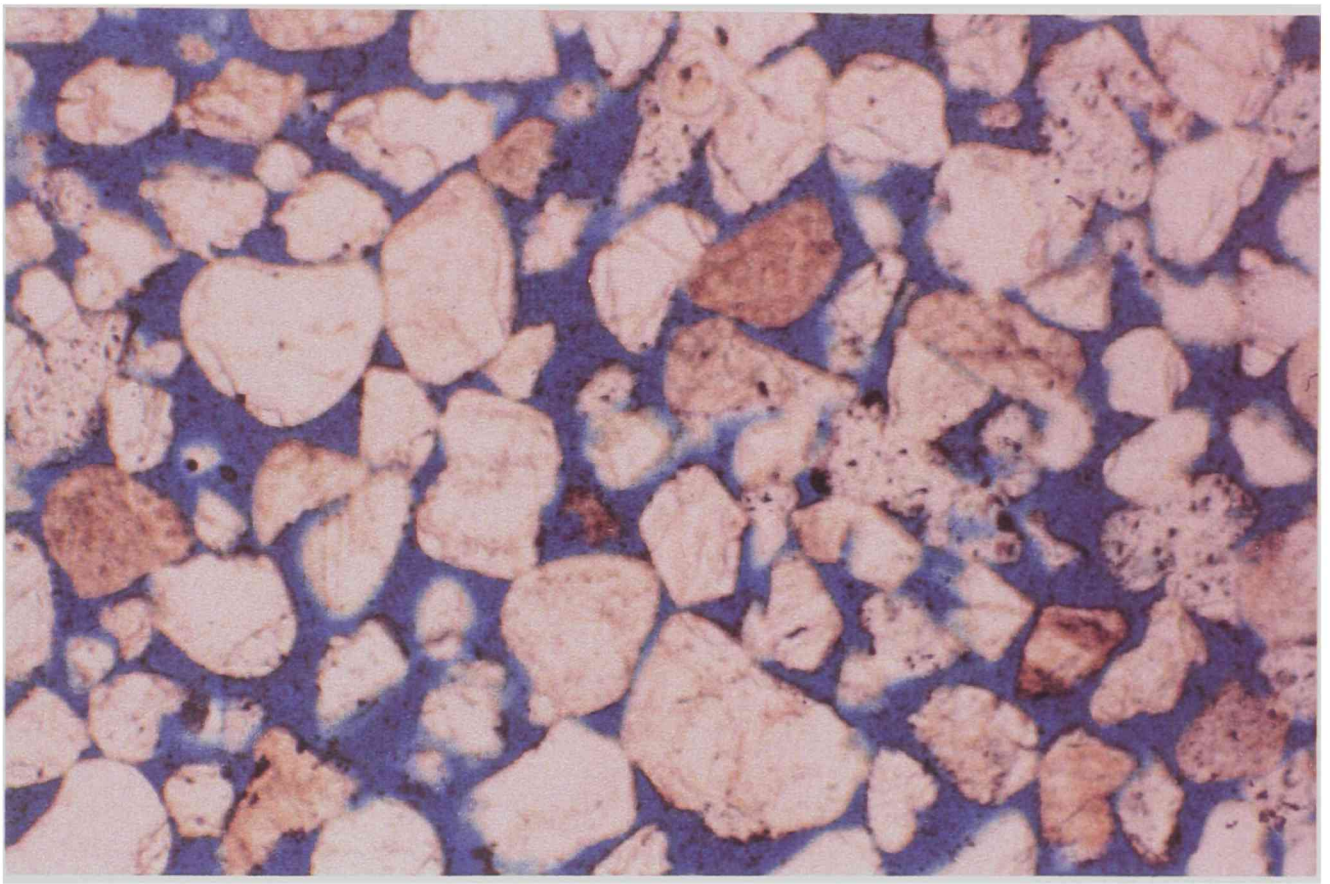

Figure 4.9. Photomicrograph of friable uncemented Antlers sandstone. Blue epoxy shows porosity. Field of view is 2mm.

CHAPTER V

SCANNING ELECTRON MICROSCOPY

Methods

Samples of the Antlers Sandstone were selected for scanning electron microscopy (SEM) analysis based on the type of cement the rock showed in thin section when viewed with a petrographic microscope. Each of the selected samples were mounted on aluminum stubs with carbon tape. The samples were then sputter coated with palladium to prevent charging due to build up of electrons on the sample surface. The aluminum stubs were then placed individually into the SEM microscope for analysis. Electron microscope analysis was performed in the Department of Biology (TTU) using a Hitachi S-570 scanning electron microscope. Samples were photographed under varied parameters, but photos were always taken using T-MAX black and white film and developed with D-76 developer.

Descriptions of SEM Photomicrographs

Sample: LW-10-5

Initial thin section analysis of this sample revealed syntaxial quartz overgrowths. Under the petrographic microscope, the overgrowths are

distinctly visible (Fig. 5.1) due to the presence of a dust ring. This sample was selected for SEM analysis to attempt to photograph crystalline quartz overgrowths. These overgrowths have nucleated on the quartz grain, and have grown into pore space. When viewed with a petrographic scope, the grains appear rounded to well-rounded. The SEM photomicrographs (Fig. 5.2) show grains with an angular appearance from overgrowths which have nucleated and grown together.

Sample: LW-10-3

This sample was selected to determine if the SEM analysis would show structures that were characteristics of amorphous silica (opal) or fibrous microquartz (chalcedony). The microquartz viewed in the petrographic microscope (Fig. 5.3) does not show fibrous bundles characteristic of chalcedony or the opaque banded structures characteristic of opal. These structures are also not present when viewed with the SEM. However, the microquartz that is visible in thin section is very distinct when viewed under the SEM. Figure 5.4 shows mircocrystalline quartz between two detrital quartz grains. The crystals are approximately 10μm in width. These quartz microcrystals are more distinct when viewed at higher magnifications (Fig. 5.5.). This microquartz (crystal

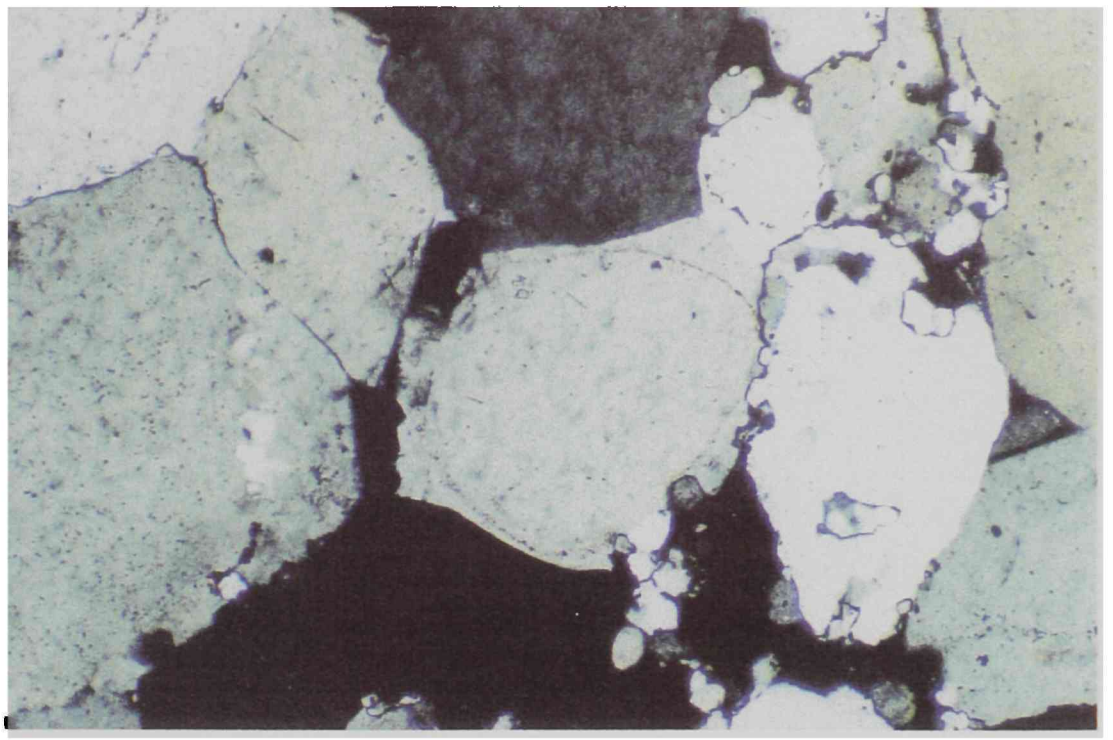

Figure 5.1. Photomicrograph of sample LW-10-5, which shows good syntaxial overgrowths.

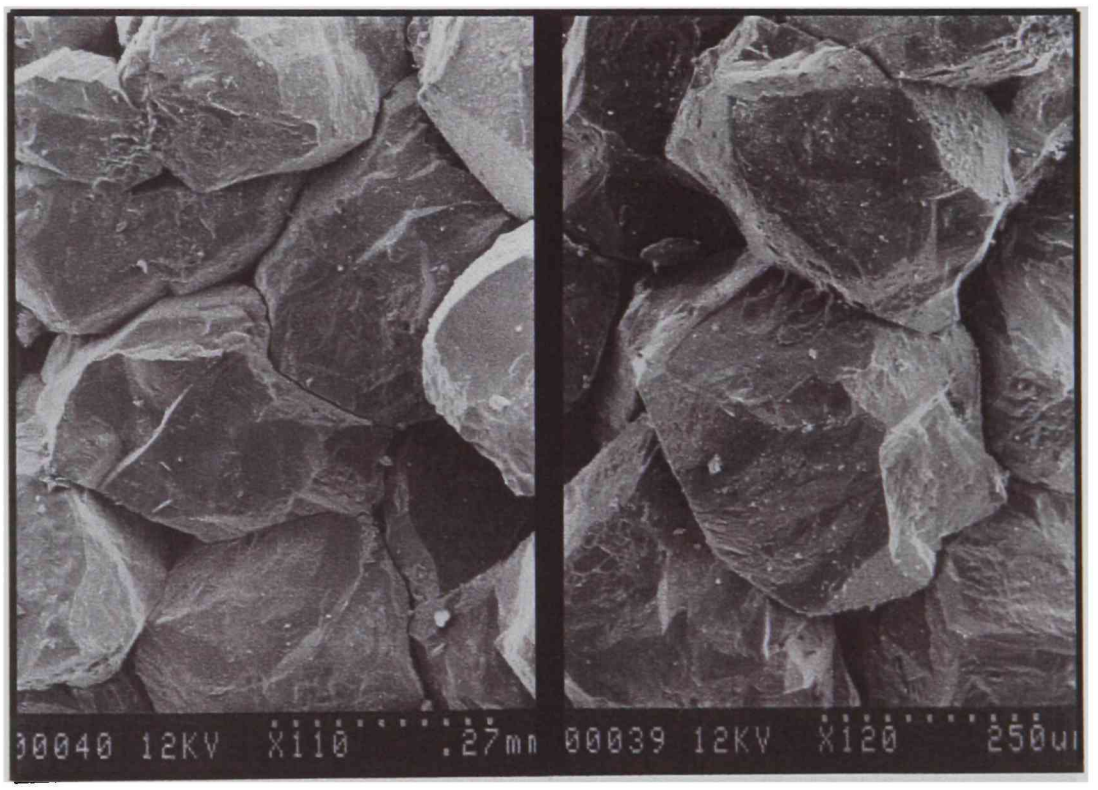

Figure 5.2. Two SEM photo-micrographs showing angular grains. In Fig. 5.1. The grains appear round. The angular appearance is from the overgrowtrhs.

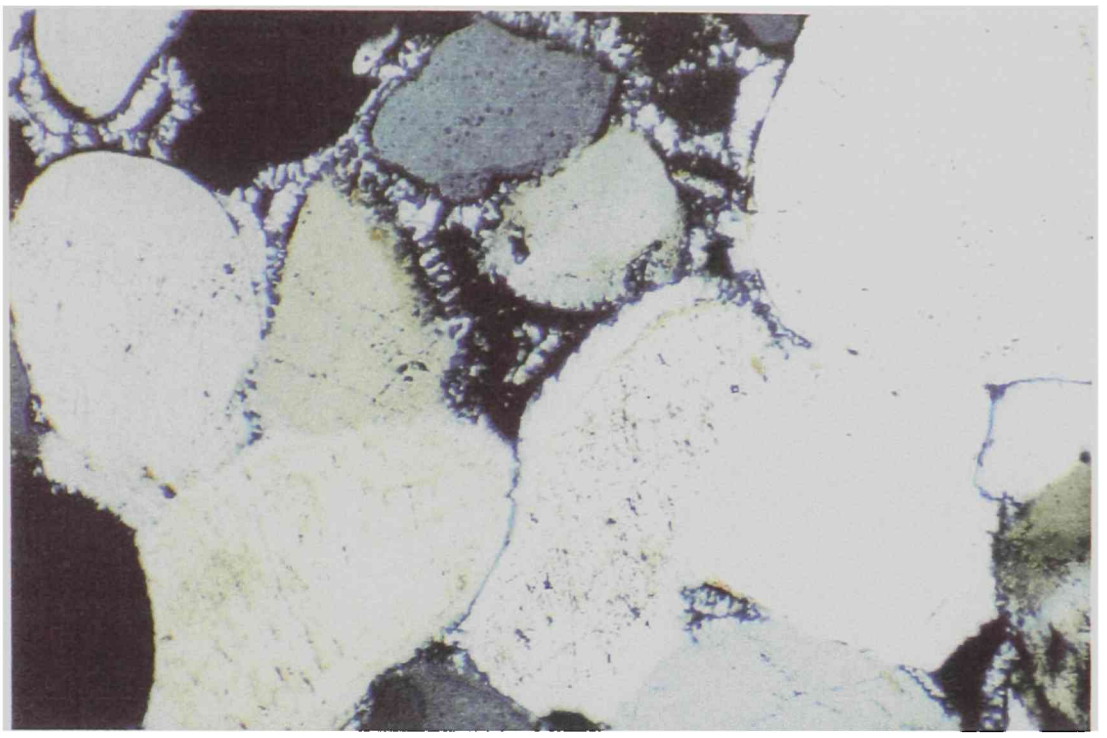

Figure 5.3. Photomicrograph showing abundant "microquartz" cement on grains and filling pore space.

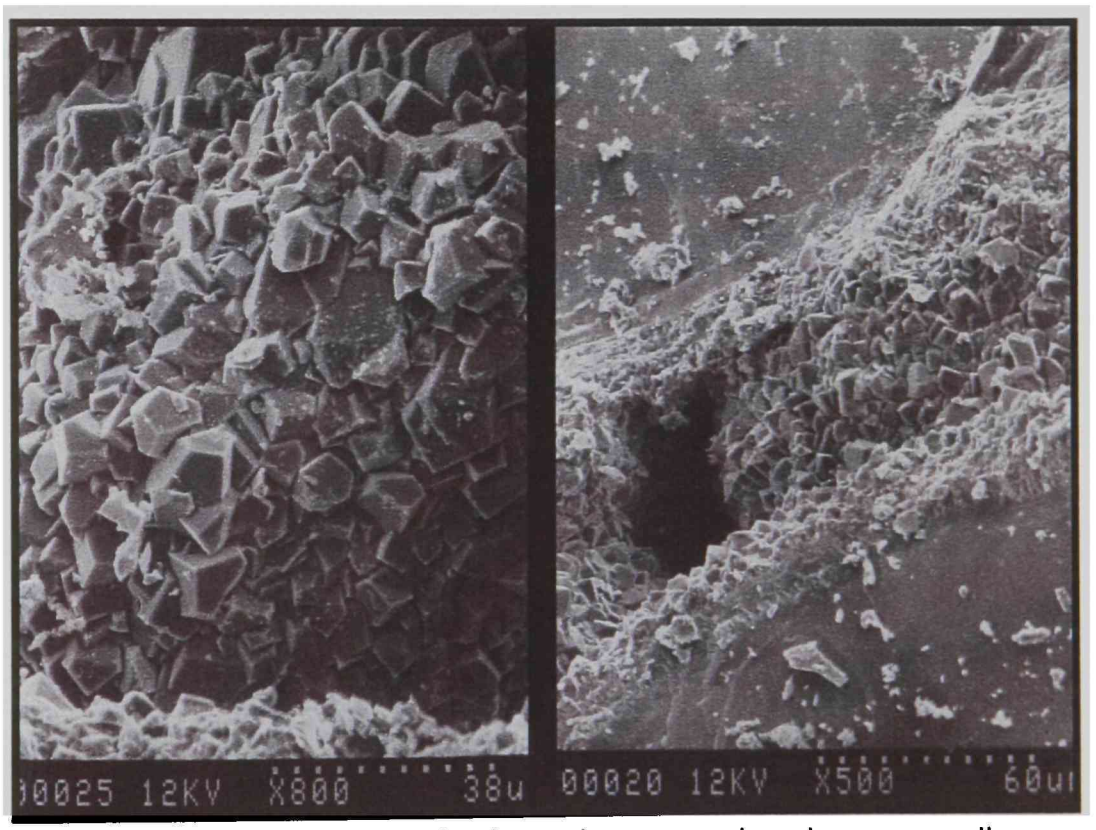

Figure 5.4. Two SEM photo-micrographs show smaller crystals that are characteristic of microcrystalline quartz.

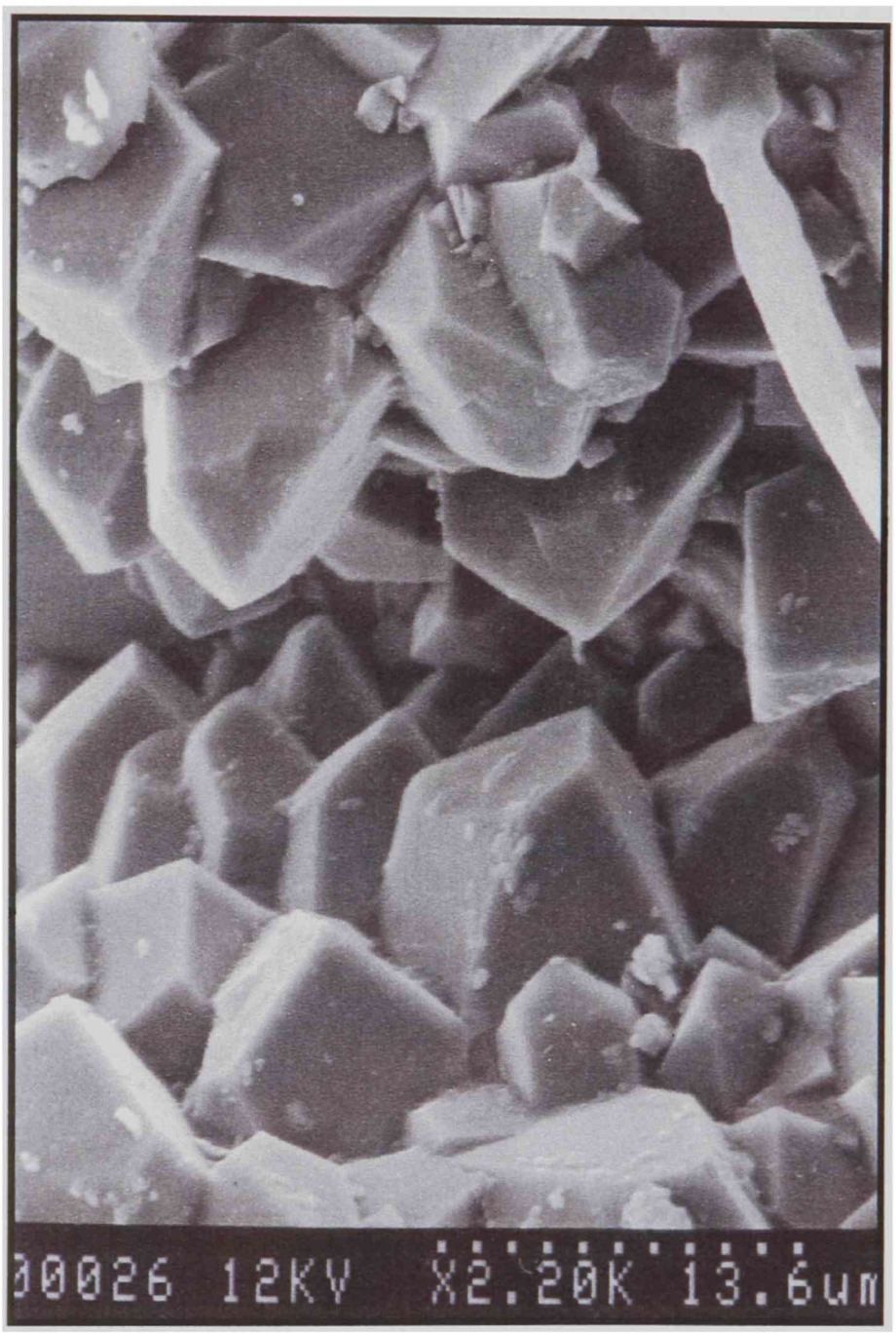

Figure 5.5. Photomicrograph showing micro-crystalline quartz crystals. Field of view is 35um.

size < 20um) was probably precipitated as opal, then converted to microquartz, probably through an quartz mineral with intermediate stability, such as chalcedony.

Sample: LW-3-6

When viewed under the petrographic microscope, this sample contains large quantities of red opaque cement (Fig. 5.6). Without x-ray analysis, it is sometimes difficult to identify small minerals such as clays by use of the petrographic microscope alone. However, the use of a scanning electron microscope is often usefully in identifying fibrous and small crystalline minerals. SEM analysis (Fig. 5.7) of this sample shows a thin coating on the quartz grains, but the coating does not have any crystalline structure that would identify it as a clay mineral. With its chemical composition unknown, this cement will be described as a red opaque (possible Fe oxide) cement in this study.

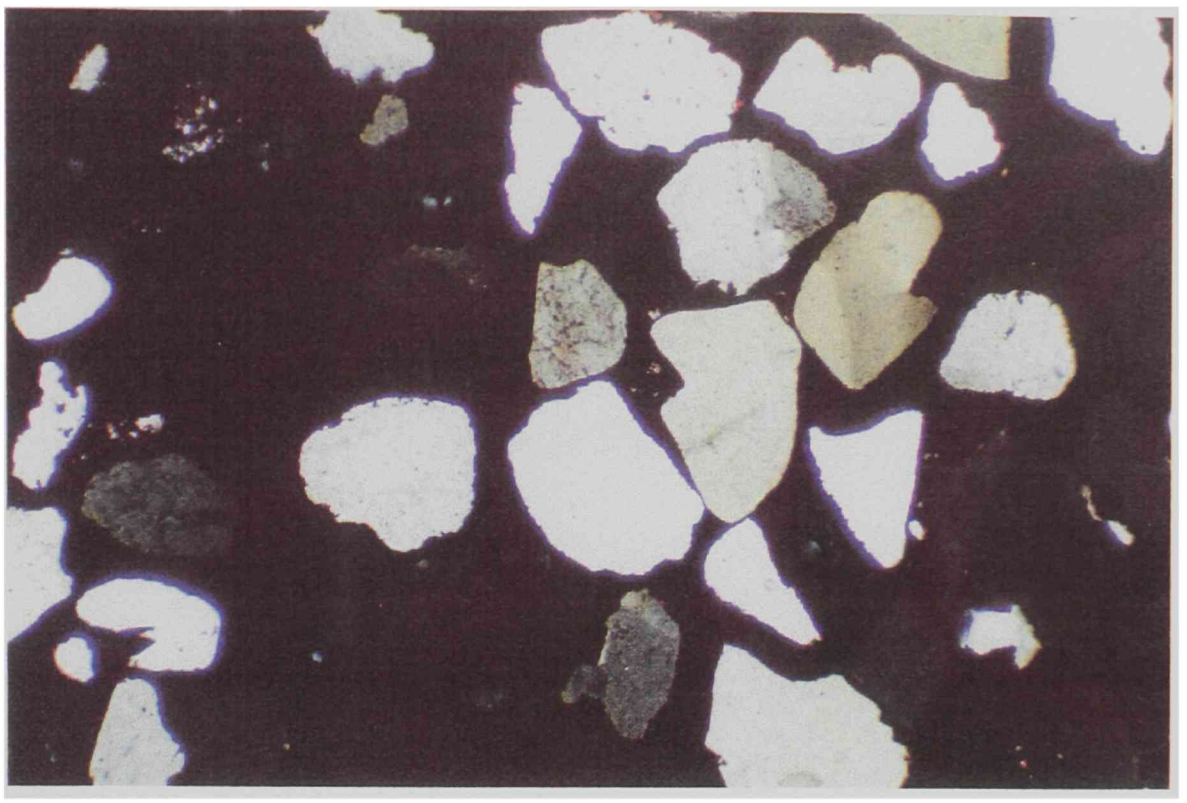

Figure 5.6. - Photomicrograph of Antlers sandstone with red opaque cement. Field of view is 1mm.

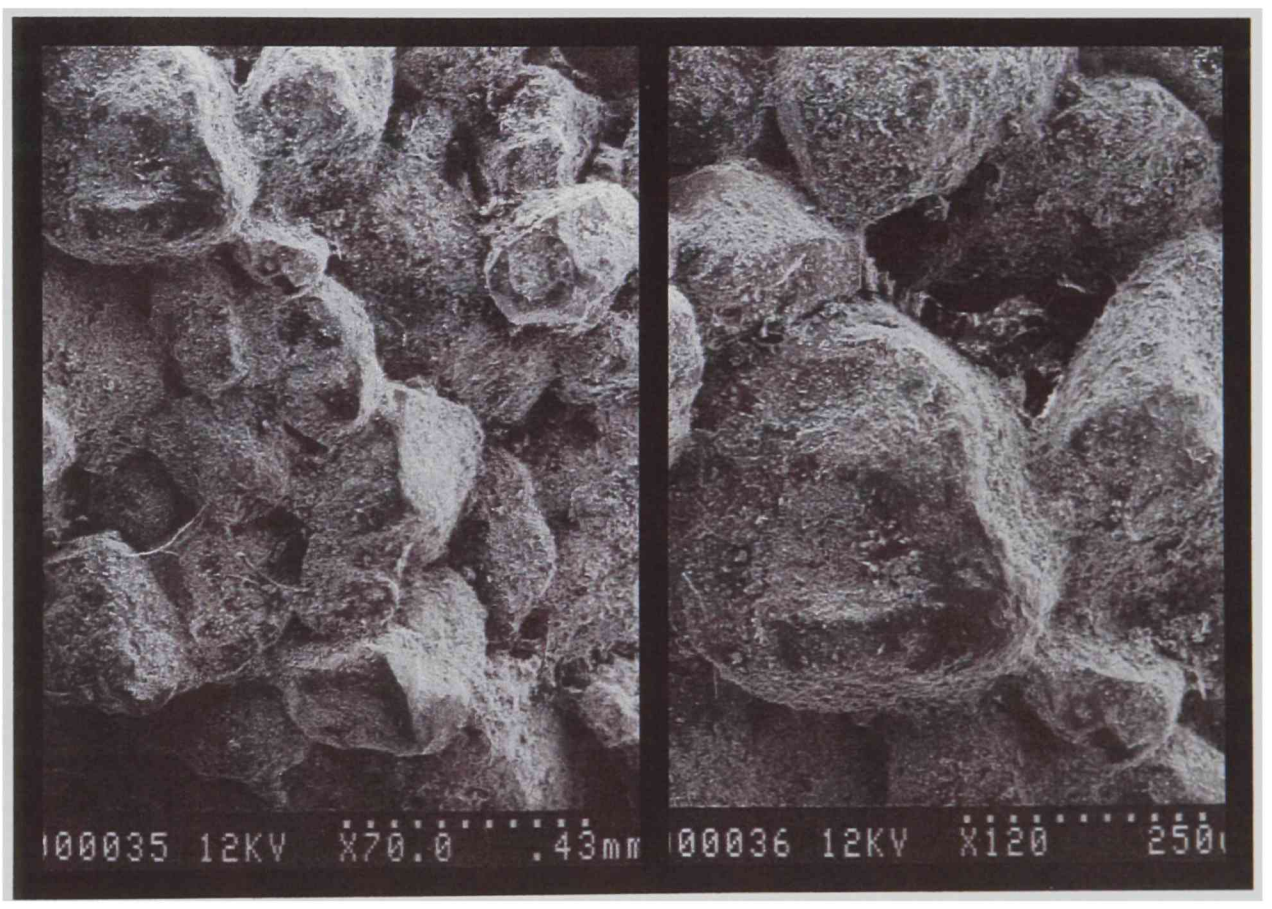

Figure 5.7. - Two SEM photomicrographs showing unidentied mineral coating on grains. Scale bar is shown on photos.

CHAPTER VI

DIAGENETIC HISTORY

General

The Antlers Sandstone on the Young Ranch is a discontinuous bed-load channel deposit only present where post-depositional silicification has occurred or where an overlying marine limestone caps it. The limestone capped Antlers shows no signs of cementation by quartz and is very friable. The diagenetic conditions that the well-indurated channel sands and gravel where exposed to were the main interest of this study. The Antlers on the Young Ranch appears similar to a quartzarenite that was cemented at depth (burial quartzite) based on quartz overgrowths abundance (Table 6.1). However, other evidence (Table 6.1) supports shallow burial cementation (diagenetic quartzarenite or silcrete). This quartz cementation was probably due to silica-rich meteoric water that moved through the Antlers, forming a silcrete horizon similar to those described by Thiry et al. (1988).

Distribution of Silica Cemented Sandstone

Numerous outcrops of the quartz cemented Antlers Sandstone can be found throughout the Young Ranch (Fig. 6.1). These outcrops seem to

Table 6.1 - Characteristics of Burial Quartzarenites, and Shallow Diagenetic Quartzarenites (Silcretes).

CHARACTERISTICS	Burial Quartzarenite	Silcretes		ANTLERS
		Groundwater	Pedogenic	
All quartz overgrowths, no micro-crystalline quartz cement	YES	NO	NO	NO
Abundant quartz overgrowths, some micro-crystalline quartz cement	NO	YES	NO	YES
Abundant micro-crystalline quartz cement, minor quartz overgrowths	NO	NO	YES	NO
Multicolored	NO	YES	YES	YES
Burial Depth > 3km	YES	NO	NO	NO
Burial Depth << 3km	NO	YES	YES	YES
Weathering profile	NO	NO	YES	NO

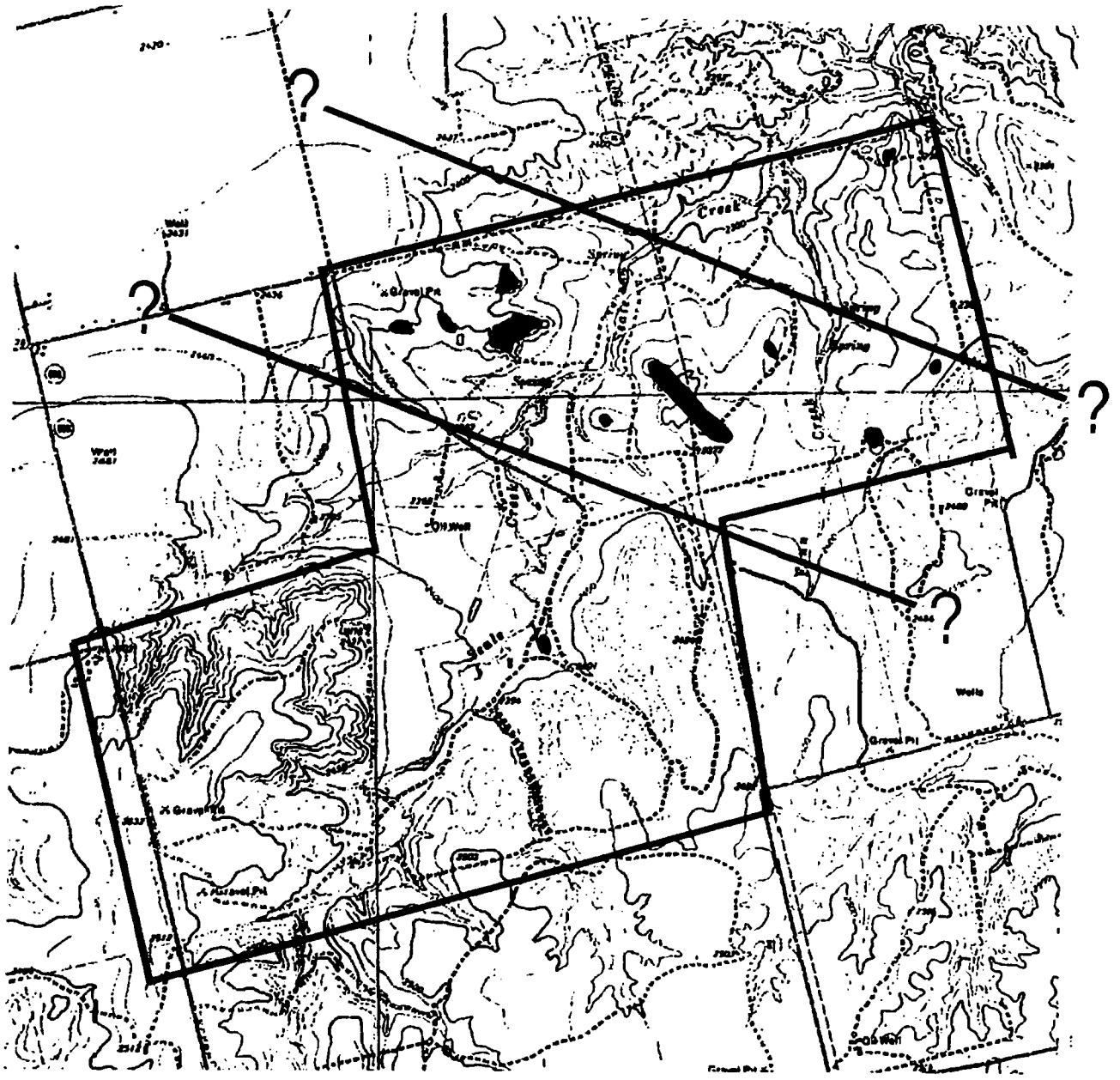

Figure 6.1. Antlers silcrete distribution on the Young Ranch. The silcretes to the north are all roughly at the same stratgraphic level (Fig. 3.26) and follow an exhumed channel trend. The small exposure of quartzite to the south is stratigraphically much lower (Fig. 3.28).

be restricted to the bed-load channel deposit facies. Antlers facies interpreted to be overbank and transitional marine contain almost no quartz cement. The well-cemented Antlers within the channel facies is multicolored (Fig.6.2a-d) and ranges in color from white to tan to red to purple. Hutton et al. (1979) described variation in colors in silcretes in Australia. These variations are usually due to variations in oxide mineral content, because silcretes often contain a variety of oxide minerals (Taylor, 1979). X-ray analysis was not preformed on any of the samples; therefore precise oxide minerals cannot be determined. Figures 6.2a – 6.2d show variations in color in the Antlers. Color variation is one line of evidence to support silcrete formation versus deep burial silicification (Table 6.1).

Cement Types

The well-indurated Antlers shows several types of quartz cement. The most dominant cement type on the Young Ranch is syntaxial overgrowths (Fig. 4.9) These overgrowths in thin section appear representative of deeper burial quartzarenites, and make up approximately 70% of silica cement. Microquartz (Fig. 4.10) represents almost all of the remaining silica cement (30%). This abundance of overgrowths is

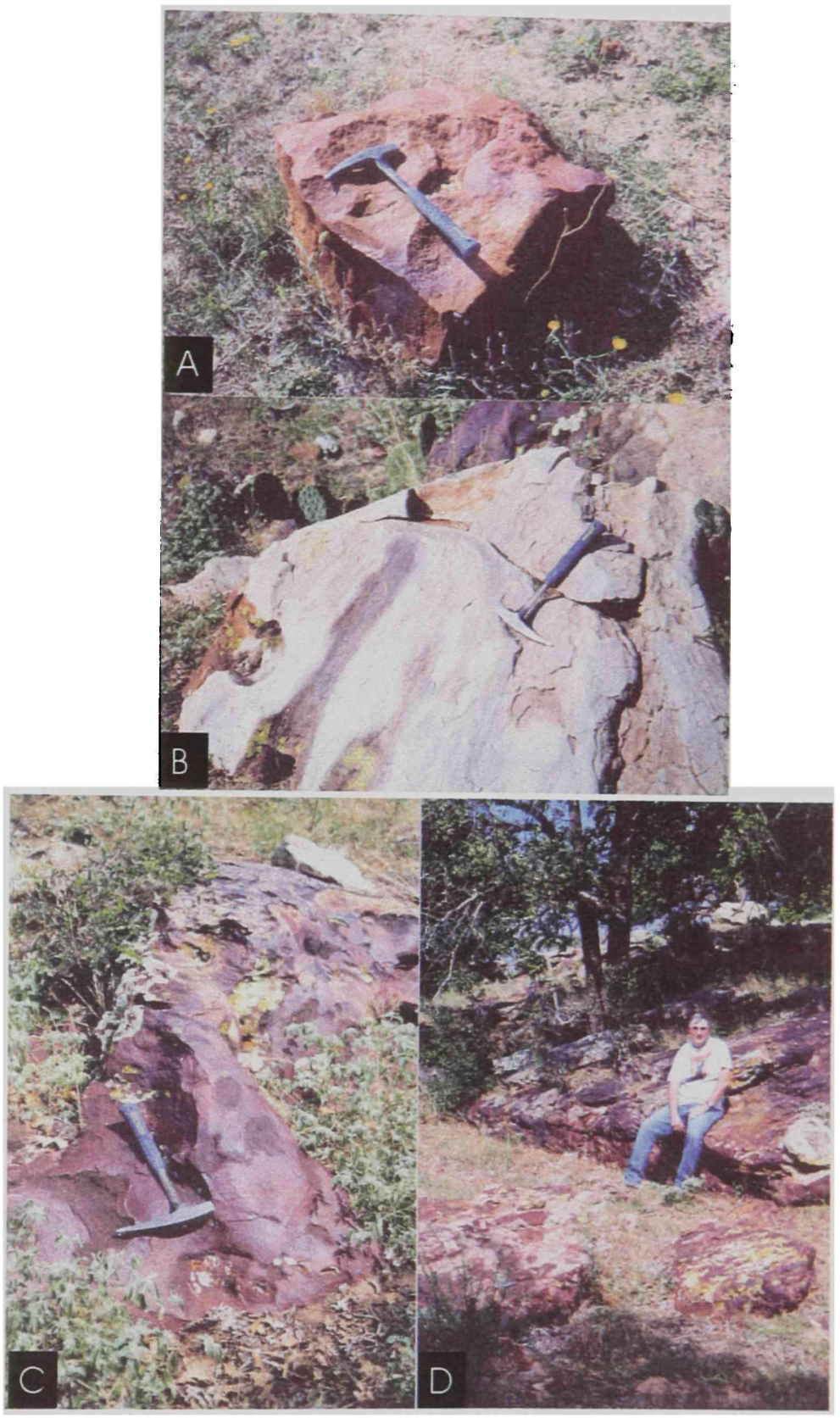

Figures 6.2A-D. Variations in color of Antlers silcrete on the Young Ranch.

representative of groundwater silcretes; however, the quantity of microquartz cement in some samples might be indicative of a pedogenic silcrete (Table 6.1). The microquartz cement was probably originally opal or chalcedony, but has recrystallized to a more stable crystalline form. Murray (1985) interpreted the microcrystalline cement in the Antlers further to the east to have been precipitated directly as chalcedony. Opal may have been present originally in the Antlers before recrystallization to microquartz (Fig. 6.3).

Depth and Timing of Silicification

The depth at which silicification of the Antlers occurred can be estimated by considering several variables. First, based on the reconstruction of burial depth, the Antlers was not exposed to deep-burial conditions thought to be required to produce abundant quartz overgrowths (Table 6.1). Second, the presence of (or interpreted presence of) other polymorphs and crystal habits of quartz indicate shallow burial. If silicification occurred during post Edwards exposure, depth of burial could have been as shallow as 160 feet (Table 6.1). This burial depth was

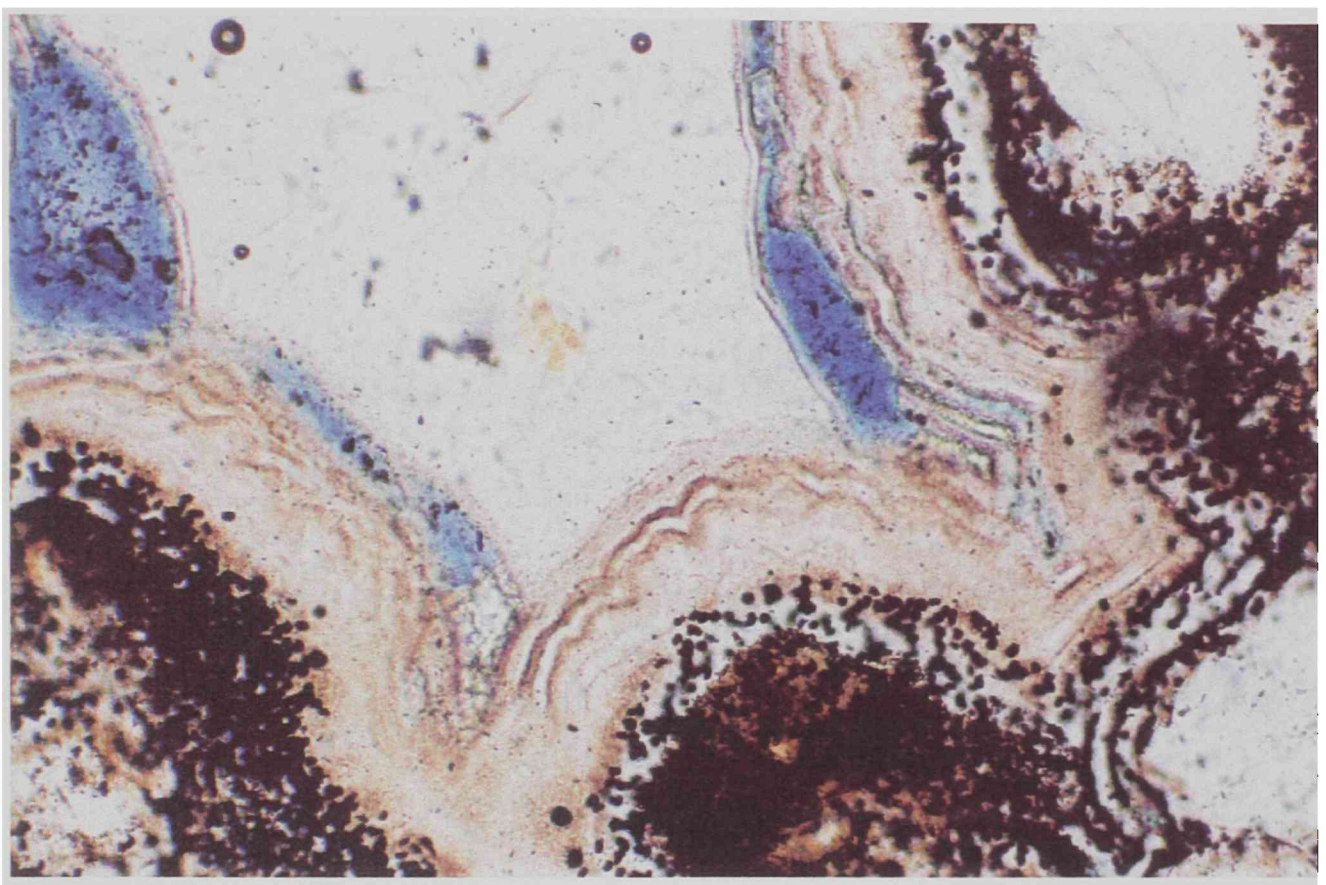

Figure 6.3. Photomicrograph showing banding in microquartz cement. Banding is often typical in opal and chalcedony cements. Field of view is .5mm.

based on the stratigraphic work by Meade et al. (1974). Silicification after Edwards exposure appears possible, if cementation did not occur penecontemporaneous with Antlers deposition, due to the quantity of microcrystalline quartz present. If the microquartz was originally precipitated as opal, then silicification occurred with in tens of meters of the surface (Blatt, 1992).

The presence of chert in the Walnut-Comanche Peak (Fig. 6.4) is also indicative of shallow silicification during the post-Edwards exposure. The silicification in the Edwards occurred after aragonitic shells were selectively dissolved, because only original calcitic shell material has been replaced by granular microquartz (chert), chalcedony, and megaquartz (Jacka, 1977). Silicification of the underlying Antlers may have also occurred during post-Edwards exposure. The maximum burial depth for the Antlers would have been 160ft., much less than the 3km required for the formation of well-cemented burial quartzarenites.

The variation in vertical distribution of the silicified Antlers (see cross sections, Figs. 3.26 and 3.28) would indicate more than one stage of silicification. This vertical variation is probably due to water table fluctuations as been described in the Fontainebleau Sandstone in France (Thiry et al., 1988). The vertical distribution of the amount of microquartz

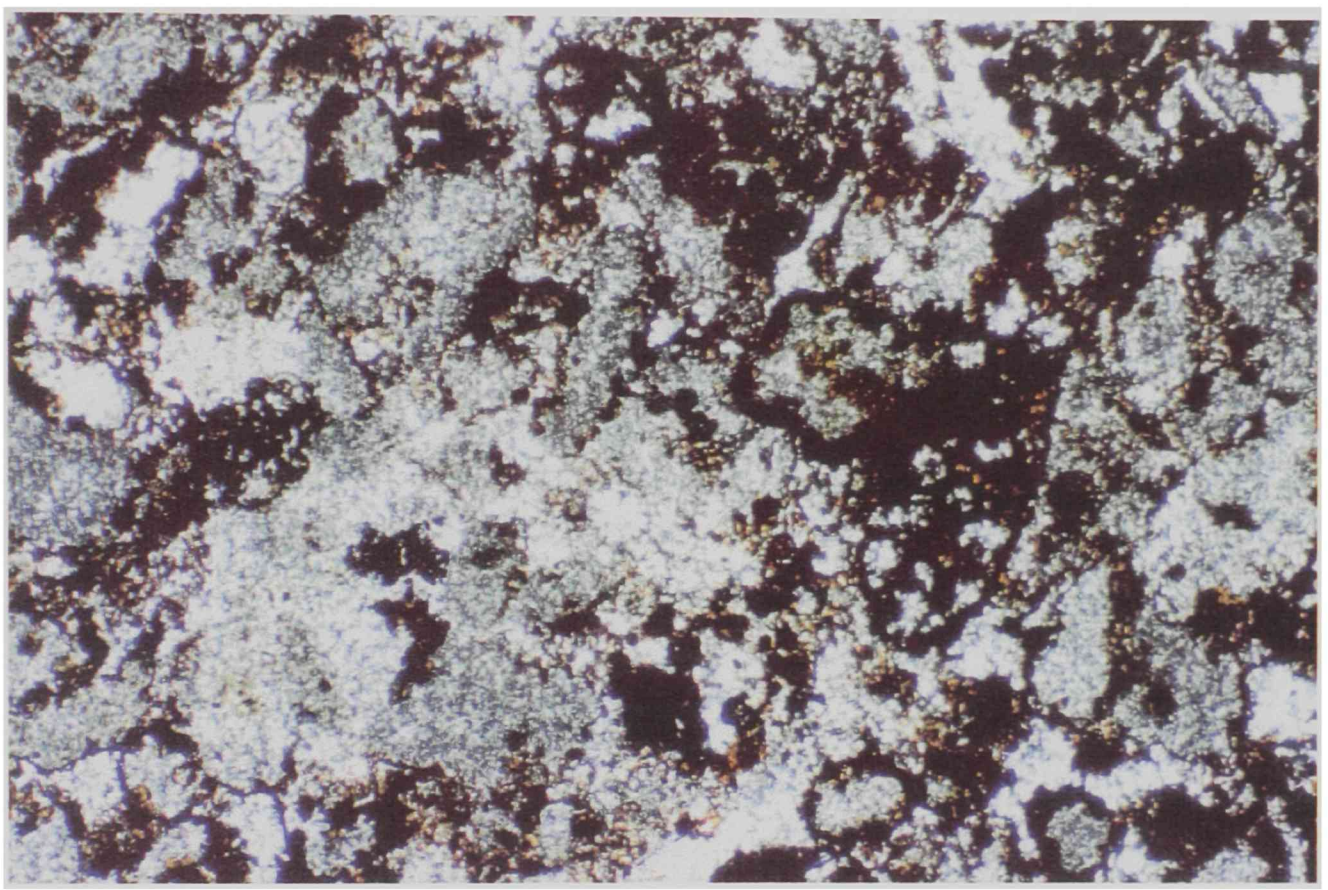

Figure 6.4. Photomicrograph of silicified Walnut Limestone, which was probably silicified after post-Edwards exposure.

versus quartz overgrowths exhibited no systematic variation. The only exception was in Location 3 where the highest sample contained only microquartz cement, and all the lower samples contained both microquartz and quartz overgrowths. This division between only microquartz and microquartz and quartz overgrowths may define a paleo water table. It should also be noted that microquartz was precipitated after the quartz overgrowths (Fig. 6.5), which suggests that the Antlers was originally cemented with quartz overgrowths in the phreatic zone (i.e. groundwater silcrete). As the water table lowered, the Antlers was further cemented with microquartz in the vadose zone (i.e. pedogenic silcrete). This silicification in the Antlers may have occurred prior to the post-Edwards exposure, and probably represents subaerial diagenesis.

Diagenetic Quartzarenites

The conditions under which the Antlers on the Young Ranch appears to have been silicified are consistent with two types of diagenetic quartzarenites or silcretes (Table 6.1). These two silcrete types form under shallow burial conditions and contain large volumes of silica cement. Silcretes cemented by groundwater (groundwater silcretes) are cemented

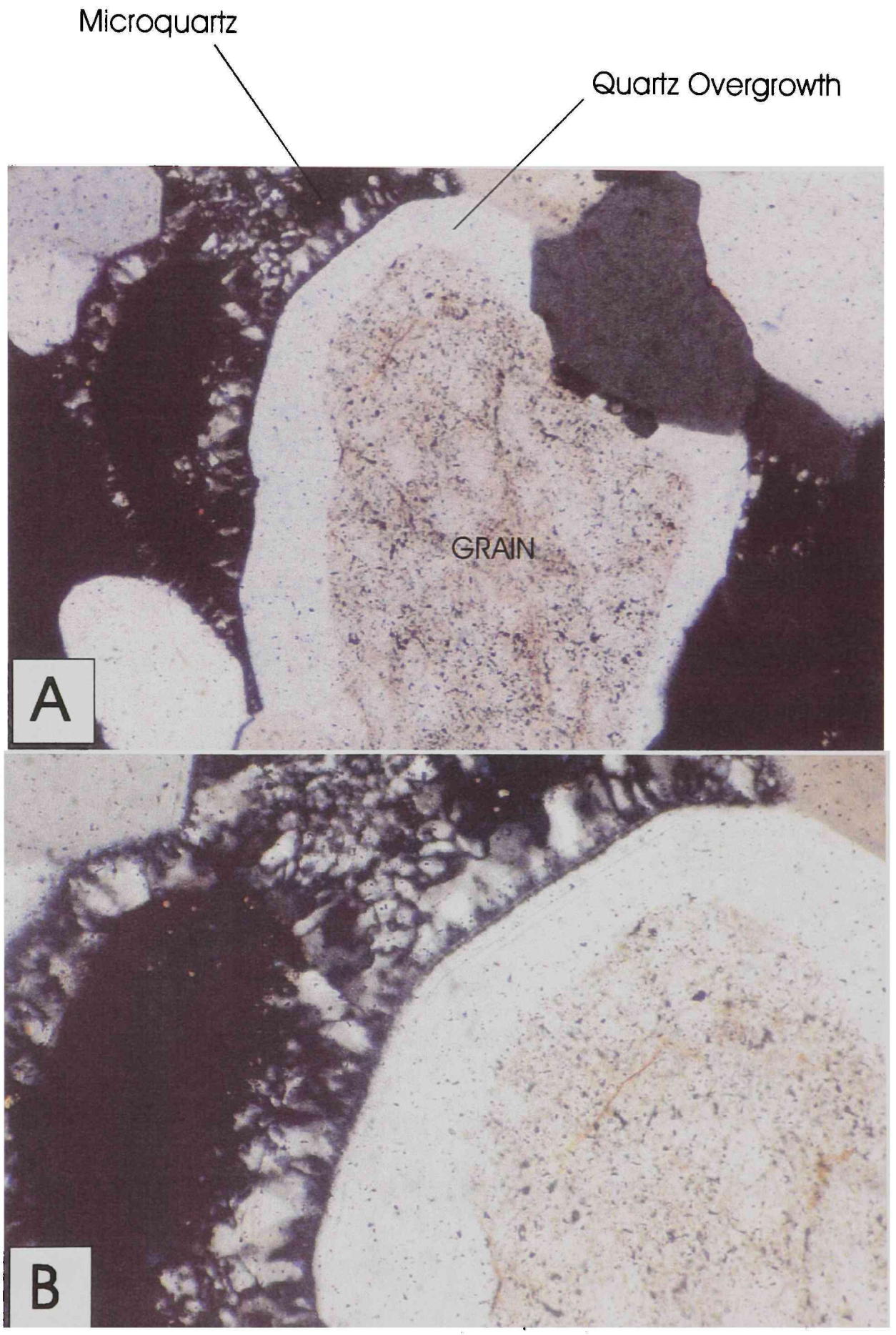

Figure 6.5. Photomicrographs showing ordering of cement. The quartz grain was first cemented by an overgrowth, then by microquartz. Field of view is 1mm for photo A, .5 mm for photo B.

with large amounts of quartz overgrowths and contain little microquartz (Thiry et al., 1991). Silcretes that represent silicified soil horizons (pedogenic silcretes) contain large amounts of opal, chalcedony, and microquartz cement with abundant soil features such as root marks and weathering profiles (Thiry et al., 1988). In the Antlers Sandstone, the greater abundance of quartz overgrowths versus microquartz (Table 6.1) and the lack of numerous soil features such as root marks and weathering profiles (Table 6.1) would indicate that the Antlers was cemented primarily in the phreatic zone as a groundwater silcrete. However, the abundance of microquartz cement and the multi-coloration seen in the Antlers is more representative of a pedogenic silcrete.

Source of Silica

The source of silica needed to completely cement the Antlers on the Young Ranch would be quite large. However, the Antlers outcrops have varying degrees of cementation. The Antlers is well-indurated with cement on the outer portions of each outcrop. The depth of cementation into the formation varies between outcrops and in most outcrops the Antlers in not indurated completely with silica cement.

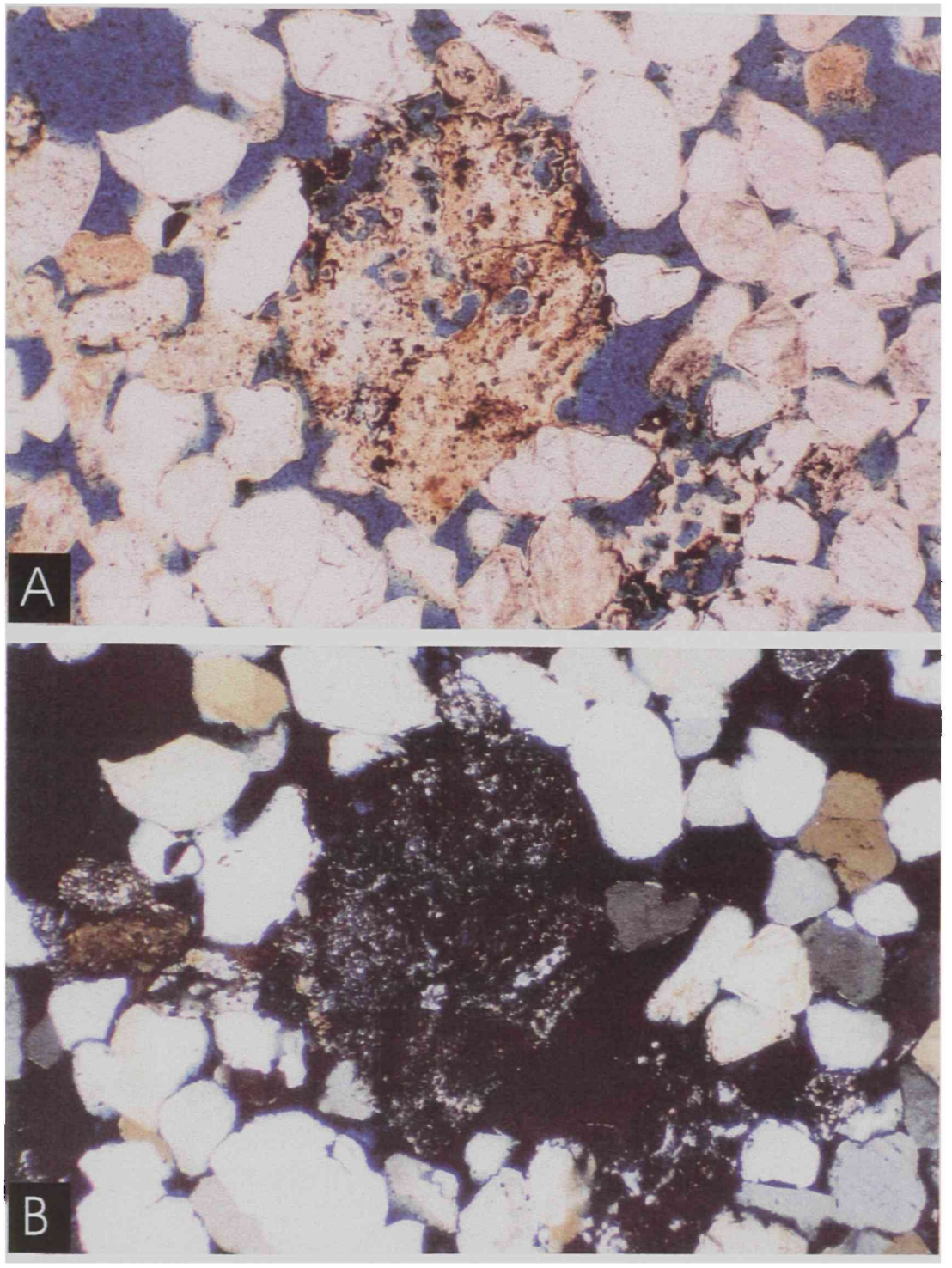

Figure 6.6. - Photomicrographs showing the dissolution of a chert grain. Photo A was taken with uncrossed nicols and photo B was taken with crossed nicols. Field of view is 2mm.

At first, an internal source of silica does not seem obvious. The absence of feldspars and clays suggest that they were probably not the source since there is no evidence of them ever being present. Other possible sources of silica include the dissolution of chert and polycrystalline quartz grains. Some chert grains in the Antlers have been partially or almost completely dissolved (Fig. 6.6), but are not present in large volumes. However, the volume of silica derived from polycrystalline quartz and chert grain dissolution may not be as significant as the lack of complete cementation in the Antlers. Intraformational transfer of silica between cemented and uncemented portions of the Antlers could have account for the silica for quartz cementation. This silica transfer could have occurred both laterally and vertical with the assistance of meteoric fluids (Blatt, 1979).

If the source of the silica for quartz cementation was not internal, then an unknown source of silica outside of the Antlers could have contributed the silica for cementation. Silica released into laterally and vertically moving fluids outside the Antlers could have moved through the formation. Evidence for this type of cementation has been described in the Fontainebleau Sandstone by Thiry et al., (2001) in France. Thiry et al. (2001) concluded that the silica that cemented the Fontainebleau

Sandstone was released from cherts that were exposed near the sandstone. Cementation of the Antlers by meteoric water does not reveal whether the source was internal or external; however, it is assumed do to the lack of complete cementation and the siliceous composition of the Antlers that the source of silica was intraformational.

CHAPTER VII

SUMMARY

1. The lower Cretaceous Antlers on the Young Ranch was deposited by a bed-load channel or channels characteristic of braided and meandering streams. These deposits are sands and sandy gravels with little silt or clay. Paleocurrent direction of the bed-load channel facies was the southeast, towards the transgressing ancestral Gulf of Mexico.

2. These channel sediments are discontinuous and are present only where they have been silicified or capped by more resistant limestones. The majority of the Antlers is not capped by limestone and appears on the ranch as an exhumed channel sand.

3. Upper Antlers deposits show evidence of changing environment: continental to marine. In several localities, the bleached friable Antlers grades upward into a sandy oyster bearing wackestone which is overlain by the marine algal fossiliferous wackestones and packstones of the Walnut Formation.

4. The silicified Antlers contains both quartz overgrowths and microcrystalline quartz cement. Syntaxial quartz overgrowths are well developed in most samples of the bed-load channel facies. These overgrowths are more abundant than microcrystalline quartz cement also found in the bed-load channel facies. These cement types represent approximately 70% and 30% respectively.

5. Depth of burial of the Antlers on the Young Ranch was shallow, less than 160 feet at the time of silicification. This shallow depth would account for the amount of microcrystalline quartz seen in the Antlers.

6. The Antlers on the Young Ranch is distinct paleosilcrete horizon, showing features of both groundwater and pedogenic silcretes. The abundance of syntaxial overgrowth is typical of a groundwater silcrete, but in some samples the dominant cement is microcrystalline quartz. An abundance of microquartz as well as multicoloration seen in the field is more typical of a pedogenic silcrete.

7. Although the exact source of silica is for cementation is not known, the Antlers does show signs of having internal silica dissolution (chert and polycrystalline quartz). However, these grains do not appear abundant enough to be the sole contributor of silica to solution needed to precipitate quartz overgrowths. Additional silica may have been distributed intraformationally, due to the fact that the Antlers is highly siliceous and not indurated completely by quartz cement. Whether the source of silica was internal or external, the Antlers Formation on the Young Ranch was silicified by the accumulation of large amounts of silica. This accumulation of silica is what defines a true silcrete.

REFERENCES CITED

Atlee, William A., 1962, The Lower Cretaceous Paluxy Sand in Central Texas: Baylor Geological Studies Bulletin 2, 26p.

Bjorkum, P.A., 1996. How important is pressure in causing dissolution of quartz in sandstones? J. Sediment. Research, v.66, no. 6, 147-154.

Bjorlykke, K., and Egeberg, P.K., 1993. Quartz Cementation in Sedimentary Basins. AAPG Bulletin, v.77, no. 9, 1538-1548.

Blatt, Harvey., 1992. Sedimentary Petrology. W.H. Freeman and Co., New York, pp. 125-135.

Blatt, H., 1979. Diagenetic processes in sandstones. In: P.A. Scholle, and P.R. Schluger (Editors), Aspects of Diagenesis. SEPM Spec. Publ., 26: 141-157.

Boone, Peter A., 1972, Facies Patterns during Transgressive Sedimentation, Antlers Formation, Lower Cretaceous, West-Central Texas: Ph.D. Dissertation, Texas A&M University, 166p.

Brothers, James C., 1985, The Antlers Sand in North Texas: Master's Thesis, Baylor University, 130p.

Dunham, R.J., 1962. Classification of carbonate rocks according to depositional texture. In: Classification of carbonate rocks (ed. W.E. Ham), pp. 108-121, AAPG Mem. No. 1.

Faure, G., 1997. Principles and Applications of GeoChemistry, Prentice Hall, 600p.

Fisher, Q., Knipe,R., and Worden, R.H., 2000. The relationship between faulting, fractures, transport of silica and quartz cementation in North Sea oil fields. In: *Quartz Cementation in Sandstones.* (eds. Worden, R.H. and Morad, S.) pp 1-20. Special Publication of International Association of Sedimentologists, no. 29, 129-146.

Fisher, W.L., and Rodda, P.U., 1966, Nomenclature Revision of Basal Cretaceous Rocks Between the Colorado and Red Rivers, Texas: Bureau of Economic Geology, Rept. of Investigation 58.

Folk, R.L., 1950. Petrology of authegenic silica in the Beekmantown group of central Pennsylvania. M.S. thesis, Penn State College, 114p.

Folk, R.L., 1980. Petrology of Sedimentary Rocks. Hemphill Publishing Co., Austin, Texas, 185 pp.

Forgotson, J.M. Jr., 1957, Stratigraphy of Comanchean Cretaceous Trinity Group: AAPG Bulletin v. 41, no. 10, p.2333-2335.

Frederickson, E.A., Redman, R.H., and Westheimer, J.M., 1965, Geology and Petroleum of Love County, Oklahoma: Oklahoma Geol. Survey Circ. 63, 91p.

Gluyas, J., Grant, S.M., and Robinson, A., 1993. Geochemical evidence for temporal link control on sandstone cementation. In: Diagenesis and Basin Development. (eds Horbury, A.D. and Robinson A.G.) pp. 23-33. AAPG Studies in Geology 36.

Graetsch, Heribert, 1994. Structure of opaline and microcrystalline silica. In: Silica: Physical Behavior, Geochemistry, and Materials Applications, MSA Reviews in Mineralogy 29, 209-232.

Hill, R.T., 1891, The Comanche Series of the Texas-Arkansas region, Geol. Soc. Of Amer. Bull., v.2, p.503-524.

Hill, R.T., 1901, Geography and Geology of the Black and Grand Prairies, Texas: United States Geol. Surv. 21st Ann. Rept., part 7, 666p.

Hobday, D.K, Woodward, C.M., and McBride, M.W., 1981, Paleotopographic and Structural Controls on Non-Marine Sedimentation of the Lower Cretaceous Antlers Formation and Correlatives, North Texas and Southeastern Oklahoma: SEPM Special Publicaiton 31, p.71-87.

Hutton, J.T., Twidale, C.R., and Milnes, A.R., 1979. Characteristics and origin of some Australian silcretes. In: Silcrete in Australia (ed. Smith, T.L.), University of New England Press, pp. 19-39.

Jacka, A.D., 1977. Deposition and Diagenesis of the Fort Terrett Formation (Edwards Group) in the Vicinity of Junction, Texas. In: Cretaceous Carbonates of Texas and Mexico, Applications to Subsurface Exploration (eds. Bebout,D.G. and Loucks, R.G.), Bureau of Economic Geology, Report of Investigation no. 89, pp. 182-200.

James, W.C., Wilmar, G.C. and Davidson, B.G., 1986. Role of quartz type and grain size in silica diagenesis, Nugget Sandstone, south-central Wyoming, Jour. Sediment. Petrol., 56: 657-662.

Khalaf, F.I., 1988. Petrography and Diagenesis of Silcrete from Kuwait, Arabian Gulf, J. Sediment. Petrol., v.58, no.6, p. 1014-1022.

Knauth, L.Paul, 1994. Petrogenesis of chert. In: Silica: Physical Behavior, Geochemistry, and Materials Applications, MSA Reviews in Mineralogy 29, 233-258.

Kraishan, G.M., Rezaee, M.R., and Worden, R.H., 2000. Trace element composition of quartz cement: a key to reveal the origin of quartz cement. In: *Quartz Cementation in Sandstones* (eds. Worden, R.H. and Morad, S.) pp 1-20. Special Publication of International Association of Sedimentologists, no. 29, 317-331.

Krauskopf, K.B.,1955. Dissolution and precipitation of silica at low temperatures. Geochim et Cosmochim. Acta., v. 10, 1-26.

McBride, E.F., 1989. Quartz cement in sanstones- a review. Earth Science Reviews, v. 26, 69-112.

Meade, G.E., Evans, G.L., and Brande, J.P., 1974. Mesozoic and Cenozoic Geology of the Southern Llano Estacado: Lubbock, TX: Lubbock Geological Society, Texas Tech Department of Geosciences and ICASALS, p. 45.

Moore, Clyde H. Jr., 1969. Stratigraphic Framework, Lower Cretaceous, West-Central Texas. In: A Guidebook to the Depositional Environments and Depositional History Lower Cretaceous Shallow Shelf Carbonate Sequence West-Central Texas (ed. C.H. Moore), Dallas Geological Society, p.1-16.

Morad, S., Ben Ismail, H., Al-Aasm, I.S., and De Ros, L.F., 1994. Diagenesis and formation-water chemistry of Triassic reservoir sandstones from southern Tunisia. Sedimentology, v. 41, 1253-1272.

Murray, Robert C., 1985, Checkerboard Chalcedony in a Paleosilcrete, North Texas: Masters Thesis, University of Texas at Austin, 82p.

Oelkers, E.H., Bjorkum, P.A., and Murphy, W.M., 1996. A petrographic and computational investigation of quartz cementation and porosity reduction from North Sea sandstones, Amer. Jour. Science, v.296, 420-452.

Passchier, C.W. and Trouw, R.A.J., 1996. Microtectonics. Springer, Berlin, 289pp.

Pettijohn, F.J., Potter, P.E., and Siever, R., 1987. Sand and Sandstone. Springer-Verlag, New York, pp. 447-474.

Porter, E.W., and James E.C., 1986. Influence of pressure, salinity, temperature and grain size on silica diagenesis in quartzose sandstones. Chem. Geol., 52: 259-369.

Salem, A.M.K., Abdel-Wahab, A., McBride, E.F., 1998. Diagenesis of shallowly buried cratonic sandstones, southwest Sinai, Egypt. Sedimentary Geology, vol. 119, p.311-335.

Scott, G., and Armstrong, J.M., 1932, The Geology of Wise County, Texas: Bureau of Economic Geology Bull. 3224, 77p.

Sippel, R.F., 1968. Sandstone petrology: evidence from luminescence petrology. J. Sediment. Petrol., 38: 530-554.

Smale, D., 1973. Silcretes and associated silica diagenesis in southern Africa and Australia. J. Sediment. Petrol., 43: 1077-1089.

Summerfield, M.A., 1983. Petrology and diagenesis of silcrete from the Kalahari Basin and Cape Coastal Zone, southern Africa. J. Sediment. Petrol., 895-909.

Summerfield, M.A., 1986. Silcrete in the sedimentary record: identification, occurrence and paleoenvironmental significance. 12th Int. Sediment. Congr., Canberra, Abstr., p.290.

Taylor, G., 1979. Silcretes in the Walgett-Cumborah Region of New South Wales. In: Silcrete in Australia (ed. Smith, T.L.), University of New England Press, pp. 187-194.

Thiry, M., Ayrault, M.B., Grisoni, J., 1988. Ground-water silicification and leaching in sands: Example of the Fountainebleu Sand (Oligocene) in the Paris Basin. GSA Bull., v.100, p.1283-1290.

Thiry, M., and Marechal, B., 2001. Development of tightly cemented sandstone lenses in uncemented sand: Example of the Fountainebleu Sand (Oligocene) in the Paris Basin. J. Sediment. Research, v.71, no.3, p.473-483.

Thiry, M., and Millot, G., 1987. Mineralogical forms of silica and their sequence of formation in silcretes. J. Sediment. Petrol., vol. 57, no.2, p.343-352.

Thiry, M., and Milnes, A.R., 1991. Pedogenic and groundwater silcretes at Stuart Creek Opal Field, South Australia. J. Sediment. Petrol., vol. 61, no. 1, p. 111-127.

Trewin, N.H. and Fallick, A.E., 2000. Quartz cement origins and budget in the Tumblagooda Sandstone, Western Australia. In: *Quartz Cementation in Sandstones* (eds. Worden, R.H. and Morad, S.) pp 1-20. Special Publication of International Association of Sedimentologists, no. 29, 219-229.

Worden, R.H., and Morad, S., 2000. Quartz cementation in oil field sandstones: a review of key controversies. In: *Quartz Cementation in Sandstones* (eds. Worden, R.H. and Morad, S.) pp 1-20. Special Publication of International Association of Sedimentologists, no. 29, 1-20.

APPENDIX A

PALEOCURRENT DATA

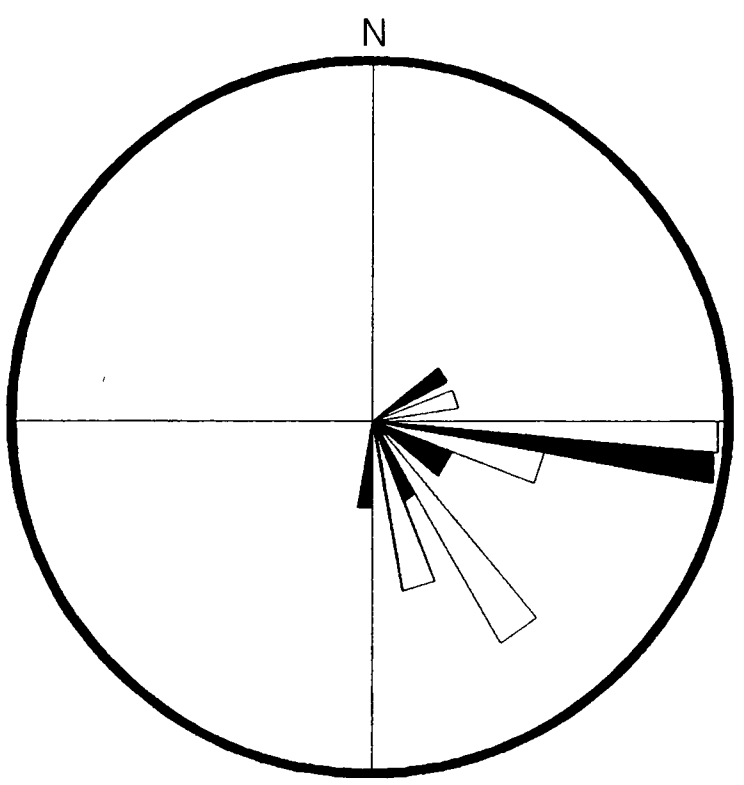

Figure A.1. Rose Diagram for Location 1

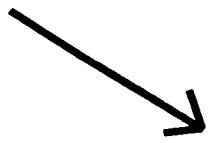

Vector Mean = 122

Table A.1. Paleocurrent calculations from location 1

PALEOCURRENT ANALYSIS

Degrees = paleocurrent reading

Radians = Paleocurrent reading in radians (degrees/57.3)

Vmean = Vector Mean Vmean = {ATAN[SUM(SIN)/SUM(COS)]}*57.3

R = Vector Magnitude R = {SUM(SIN)^2+SUM(COS)^2]^0.5

L = Consistency Ratio L = (R/ No. of readings)*100

Location 1 - Stop 9

Degrees	Radians	SIN	COS	Vmean	R	L
100	1.745	0.985	-0.174	-57.637	14.072	0.828
105	1.832	0.966	-0.259			
95	1.658	0.996	-0.087			
125	2.182	0.819	-0.573			
148	2.583	0.530	-0.848			
115	2.007	0.906	-0.422			
100	1.745	0.985	-0.174			
80	1.396	0.985	0.174			
145	2.531	0.574	-0.819			
165	2.880	0.259	-0.966			
105	1.832	0.966	-0.259			
165	2.880	0.259	-0.966			
155	2.705	0.423	-0.906			
92	1.606	0.999	-0.035			
144	2.513	0.588	-0.809			
190	3.316	-0.173	-0.985			
55	0.960	0.819	0.574			
	SUM	11.886	-7.533			

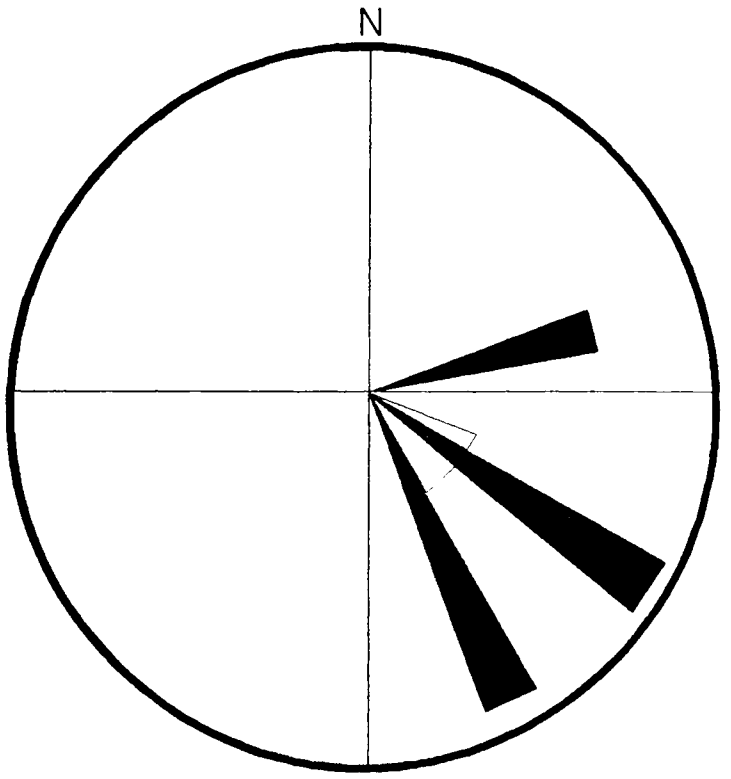

Figure A.2. Rose Diagram for Location 2

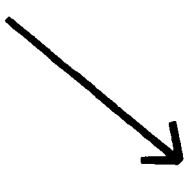

Vector Mean = 130

Table A.2. Paleocurrent calculations from location 2

PALEOCURRENT ANALYSIS
Degrees = paleocurrent reading
Radians = Paleocurrent reading in radians (degrees/57.3)
Vmean = Vector Mean Vmean = {ATAN[SUM(SIN)/SUM(COS)]}*57.3
R = Vector Magnitude R = {SUM(SIN)^2+SUM(COS)^2]^0.5
L = Consistency Ratio L = (R/ No. of readings)*100

Location 2 - Stop 10

Degrees	Radians	SIN	COS	Vmean	R	L
72	1.257	0.951	0.309	-49.64	9.717	0.883
80	1.396	0.985	0.174			
155	2.705	0.423	-0.906			
140	2.443	0.643	-0.766			
160	2.792	0.342	-0.940			
130	2.269	0.766	-0.643			
150	2.618	0.500	-0.866			
160	2.792	0.342	-0.940			
130	2.269	0.766	-0.643			
125	2.182	0.819	-0.573			
120	2.094	0.866	-0.500			
	SUM	7.404	-6.293			

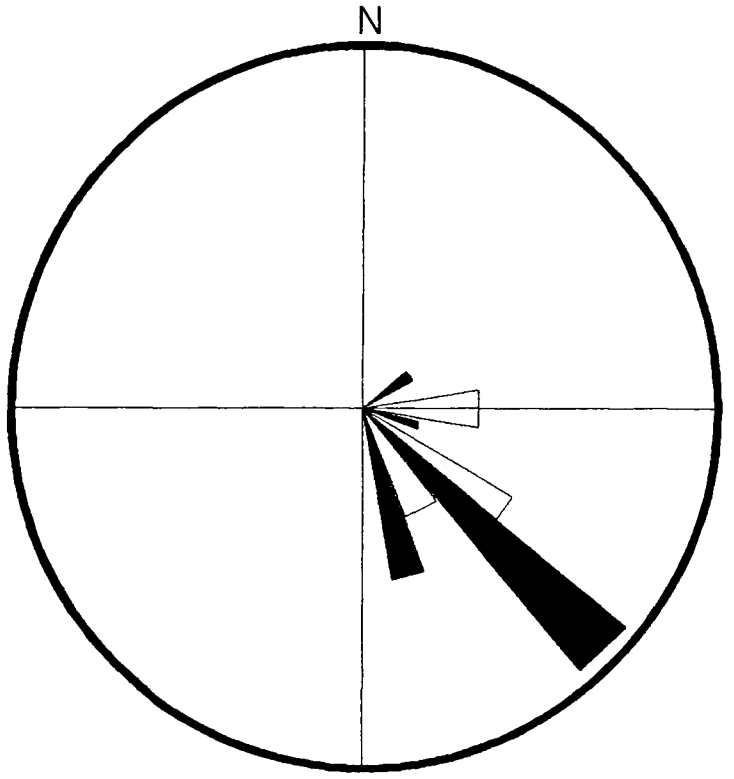

Figure A.3. Rose Diagram for Location 3

Vector Mean = 131

Table A.3. Paleocurrent calculations from location 3

PALEOCURRENT ANALYSIS
Degrees = paleocurrent reading
Radians = Paleocurrent reading in radians (degrees/57.3)
Vmean = Vector Mean Vmean = {ATAN[SUM(SIN)/SUM(COS)]}*57.3
R = Vector Magnitude R = {SUM(SIN)^2+SUM(COS)^2]^0.5
L = Consistency Ratio L = (R/ No. of readings)*100

Location 3 - Stop 13

Degrees	Radians	SIN	COS	Vmean	R	L
130	2.269	0.766	-0.643	-49.324	19.606	0.891
140	2.443	0.643	-0.766			
125	2.182	0.819	-0.573			
100	1.745	0.985	-0.174			
135	2.356	0.707	-0.707			
140	2.443	0.643	-0.766			
165	2.880	0.259	-0.966			
168	2.932	0.208	-0.978			
170	2.967	0.174	-0.985			
146	2.548	0.559	-0.829			
140	2.443	0.643	-0.766			
152	2.653	0.470	-0.883			
145	2.531	0.574	-0.819			
157	2.740	0.391	-0.920			
127	2.216	0.799	-0.602			
133	2.321	0.731	-0.682			
135	2.356	0.707	-0.707			
110	1.920	0.940	-0.342			
90	1.570681	1.000	0.000			
60	1.047	0.866	0.500			
90	1.571	1.000	0.000			
100	1.745	0.985	-0.174			
	SUM	14.869	-12.780			

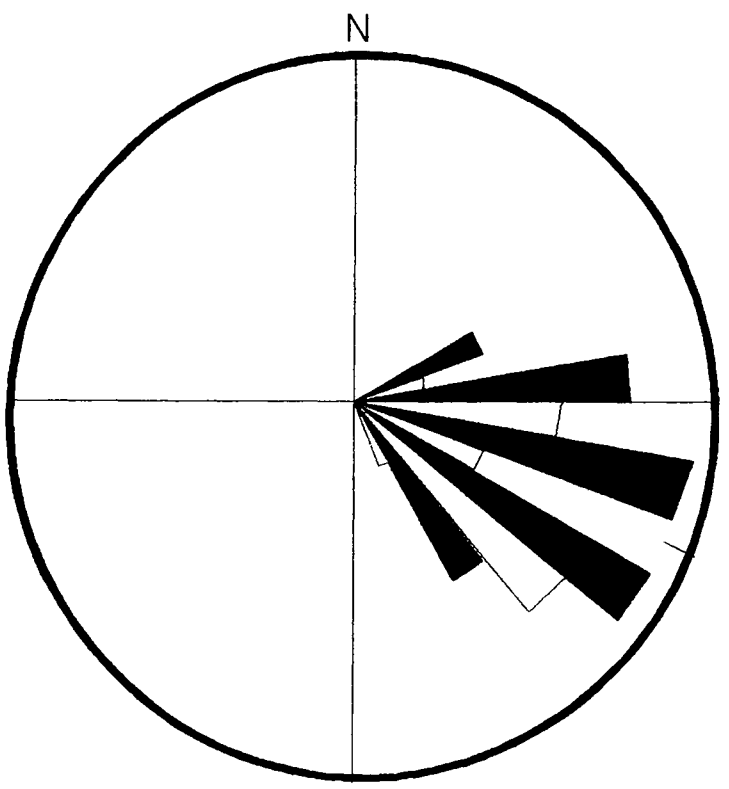

Figure A.4. Rose Diagram for Location 4

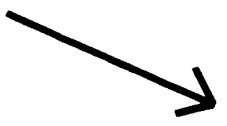

Vector Mean = 114

Table A.4. Paleocurrent calculations from location 4

PALEOCURRENT ANALYSIS

Degrees = paleocurrent reading

Radians = Paleocurrent reading in radians (degrees/57.3)

Vmean = Vector Mean Vmean = {ATAN[SUM(SIN)/SUM(COS)]}*57.3

R = Vector Magnitude R = {SUM(SIN)^2+SUM(COS)^2]^0.5

L = Consistency Ratio L = (R/ No. of readings)*100

Location 4 - Ranch House Road

Degrees	Radians	SIN	COS	Vmean	R	L
75	1.309	0.966	0.259	-65.76	27.397	0.913
110	1.920	0.940	-0.342			
110	1.920	0.940	-0.342			
85	1.483	0.996	0.087			
100	1.745	0.985	-0.174			
130	2.269	0.766	-0.643			
120	2.094	0.866	-0.500			
110	1.920	0.940	-0.342			
145	2.531	0.574	-0.819			
90	1.571	1.000	0.000			
70	1.222	0.940	0.342			
85	1.483	0.996	0.087			
70	1.222	0.940	0.342			
105	1.832	0.966	-0.259			
100	1.745	0.985	-0.174			
125	2.182	0.819	-0.573			
138	2.408	0.669	-0.743			
150	2.618	0.500	-0.866			
124	2.164	0.829	-0.559			
115	2.007	0.906	-0.422			
100	1.745	0.985	-0.174			
130	2.269	0.766	-0.643			
135	2.356	0.707	-0.707			
144	2.513	0.588	-0.809			
160	2.792	0.342	-0.940			
126	2.199	0.809	-0.588			
137	2.391	0.682	-0.731			
140	2.443	0.643	-0.766			
110	1.920	0.940	-0.342			
85	1.483	0.996	0.087			
	SUM	24.981	-11.250			

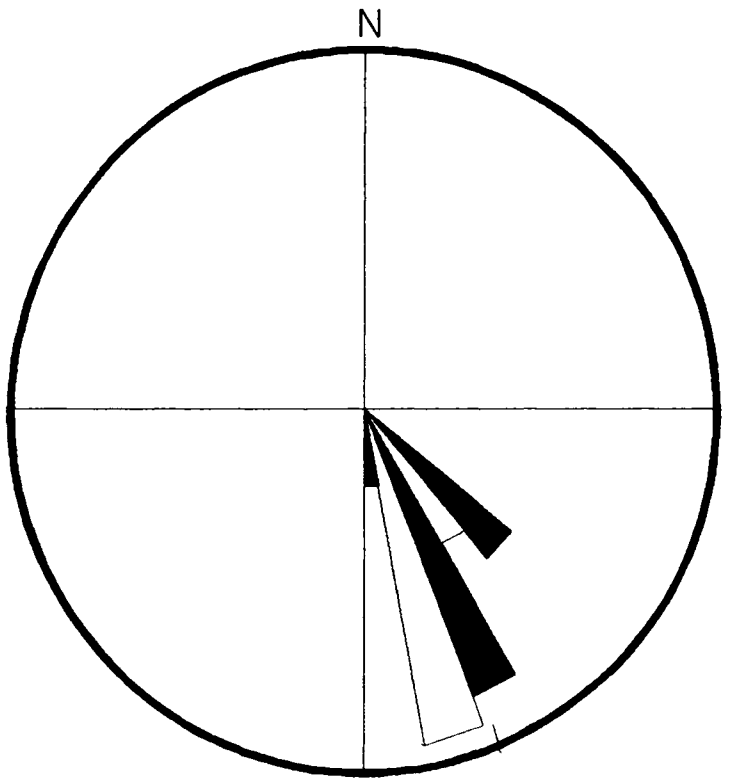

Figure A.5. Rose Diagram for Location 5

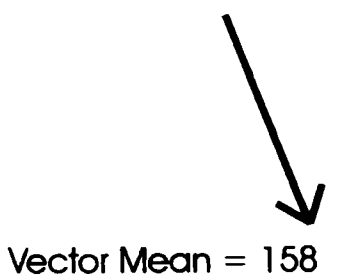

Table A.5. Paleocurrent calculations from location 5

PALEOCURRENT ANALYSIS
Degrees = paleocurrent reading
Radians = Paleocurrent reading in radians (degrees/57.3)
Vmean = Vector Mean Vmean = {ATAN[SUM(SIN)/SUM(COS)]}*57.3
R = Vector Magnitude R = {SUM(SIN)^2+SUM(COS)^2]^0.5
L = Consistency Ratio L = (R/ No. of readings)*100

Location 5 - Main Channel

Degrees	Radians	SIN	COS	Vmean	R	L
165	2.880	0.259	-0.966	-21.674	29.322	0.977
159	2.775	0.359	-0.934			
140	2.443	0.643	-0.766			
180	3.141	0.000	-1.000			
170	2.967	0.174	-0.985			
140	2.443	0.643	-0.766			
150	2.618	0.500	-0.866			
140	2.443	0.643	-0.766			
147	2.565	0.545	-0.839			
155	2.705	0.423	-0.906			
155	2.705	0.423	-0.906			
165	2.880	0.259	-0.966			
168	2.932	0.208	-0.978			
150	2.618	0.500	-0.866			
158	2.757	0.375	-0.927			
180	3.141	0.000	-1.000			
140	2.443	0.643	-0.766			
155	2.705	0.423	-0.906			
161	2.810	0.326	-0.945			
146	2.548	0.559	-0.829			
172	3.002	0.139	-0.990			
170	2.967	0.174	-0.985			
155	2.705	0.423	-0.906			
169	2.949	0.191	-0.982			
158	2.757	0.375	-0.927			
137	2.391	0.682	-0.731			
170	2.967	0.174	-0.985			
156	2.723	0.407	-0.913			
175	3.054	0.087	-0.996			
152	2.653	0.470	-0.883			
167	2.914	0.225	-0.974			
	SUM	10.828	-27.181			

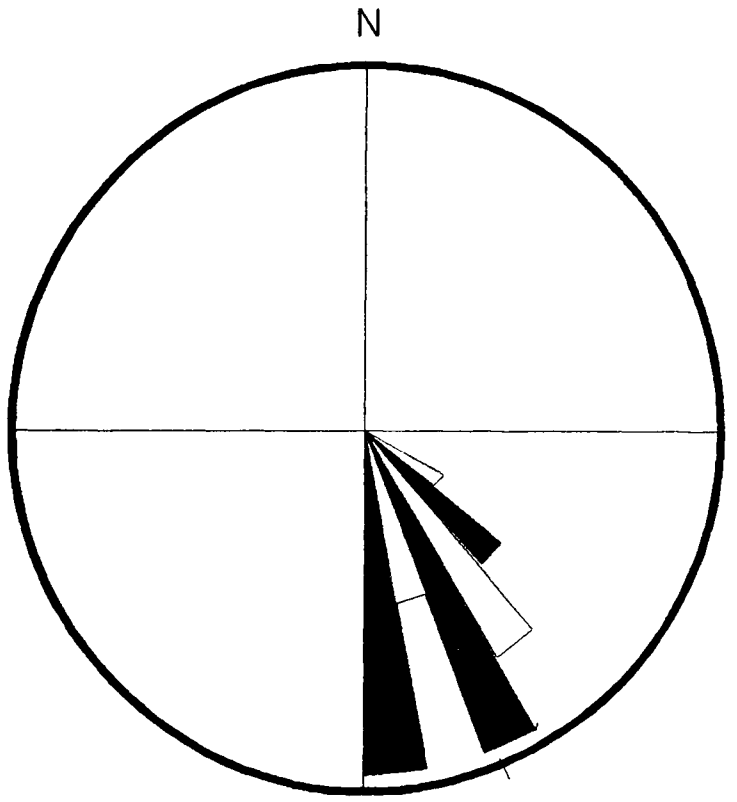

Figure A.6. Rose Diagram for Location 6

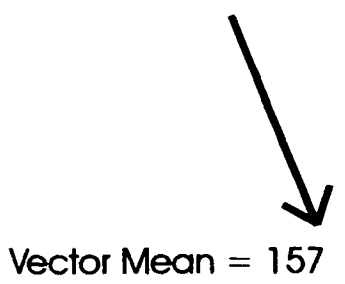

Table A.6. Paleocurrent calculations for location 6

PALEOCURRENT ANALYSIS

Degrees = paleocurrent reading

Radians = Paleocurrent reading in radians (degrees/57.3)

Vmean = Vector Mean — Vmean = {ATAN[SUM(SIN)/SUM(COS)]}*57.3

R = Vector Magnitude — R = {SUM(SIN)^2+SUM(COS)^2]^0.5

L = Consistency Ratio — L = (R/ No. of readings)*100

Location 6 - Main Channel across road

Degrees	Radians	SIN	COS	Vmean	R	L
150	2.618	0.500	-0.866	-22.474	16.412	0.965
144	2.513	0.588	-0.809			
142	2.478	0.616	-0.788			
160	2.792	0.342	-0.940			
140	2.443	0.643	-0.766			
175	3.054	0.087	-0.996			
160	2.792	0.342	-0.940			
172	3.002	0.139	-0.990			
165	2.880	0.259	-0.966			
180	3.141	0.000	-1.000			
171	2.984	0.157	-0.988			
175	3.054	0.087	-0.996			
155	2.705	0.423	-0.906			
169	2.949	0.191	-0.982			
139	2.426	0.656	-0.755			
155	2.705	0.423	-0.906			
125	2.182	0.819	-0.573			
	SUM	6.273	-15.166			

APPENDIX B

MEASURED SECTIONS

Total thickness = 31'
Antlers thickness = 0'
Silcrete thickness = 0'

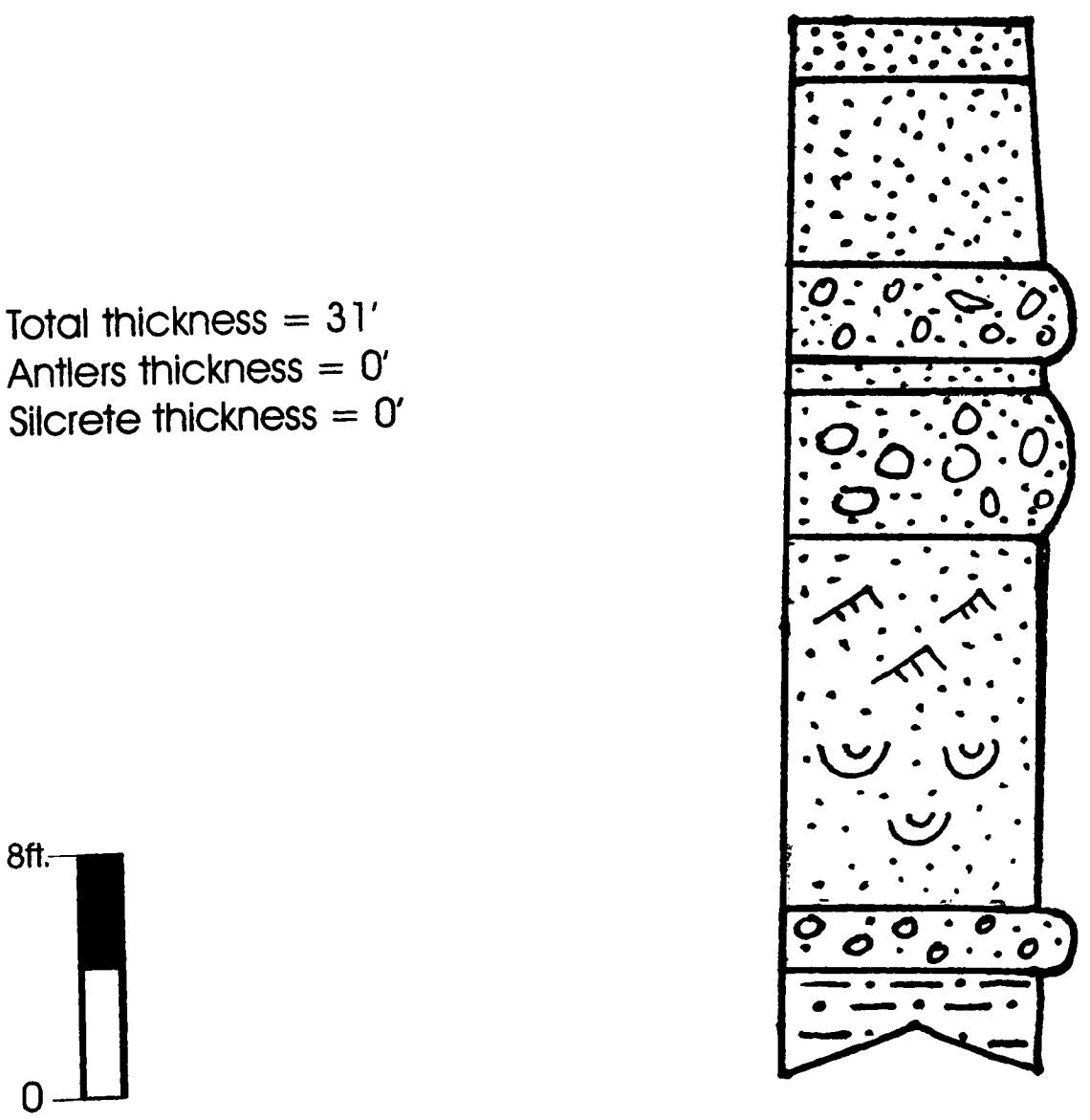

Figure B.1. Young Ranch Section 1A.

Total thickness = 57'
Antlers thickness = 49'
Silcrete thickness = 0'

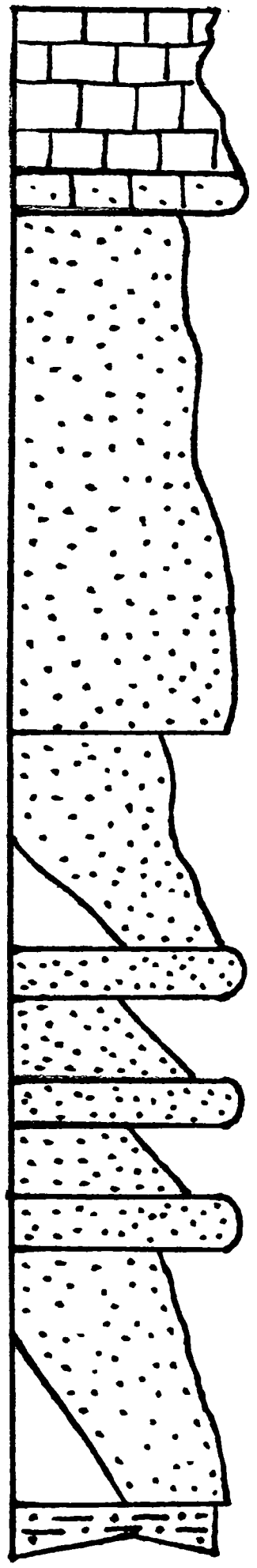

Figure B.2. Young Ranch Section 1B.

Total thickness = 11'
Antlers thickness = 4'
Silcrete thickness = 0'

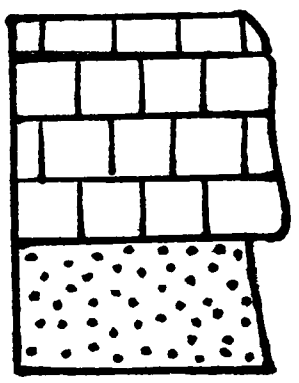

Figure B.3. Young Ranch Section 1C.

Total thickness = 37'
Antlers thickness = 0'
Silcrete thickness = 0'

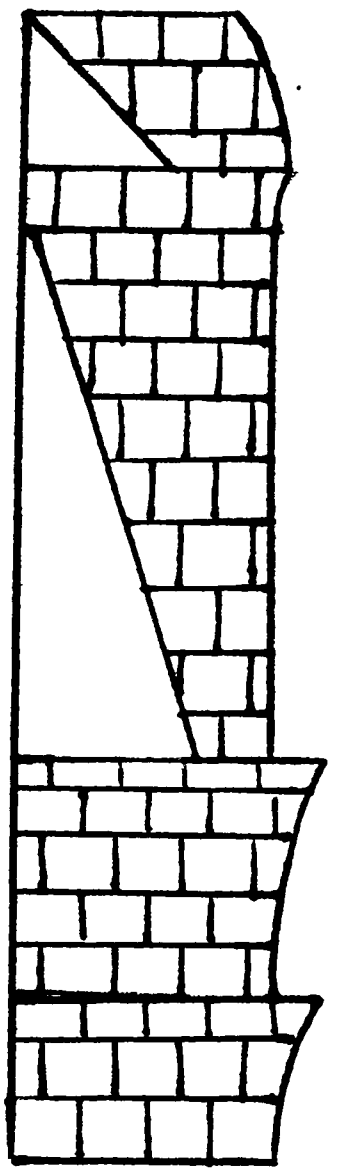

Figure B.4. Young Ranch Section 1D.

Total thickness = 30'
Antlers thickness = 0'
Silcrete thickness = 0'

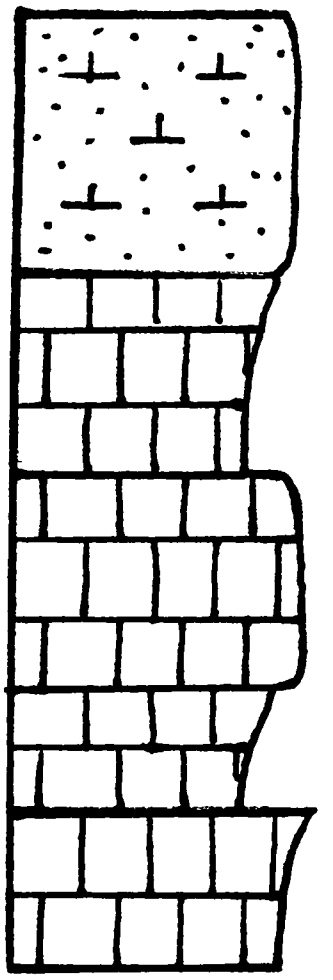

Figure B.5. Young Ranch Section 1E.

Total thickness = 19'
Antlers thickness = 6'
Silcrete thickness = 6'

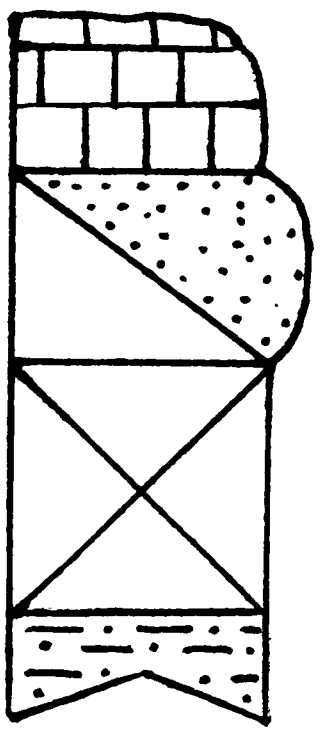

Figure B.6. Young Ranch Section 2.

Total thickness = 18'
Antlers thickness = 4'
Silcrete thickness = 1'

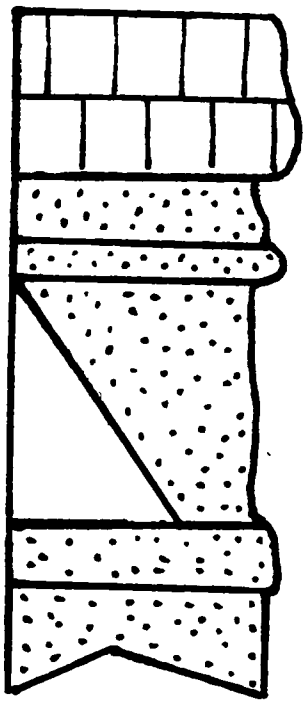

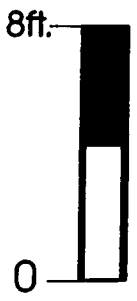

Figure B.7. Young Ranch Section 3.

Total thickness = 22'
Antlers thickness = 22'
Silcrete thickness = 22'

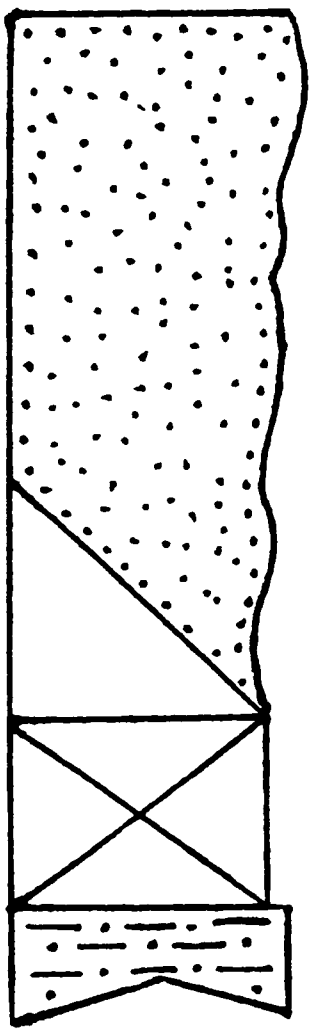

Figure B.8. Young Ranch Section 4.

Total thickness = 54'
Antlers thickness =54'
Silcrete thickness = 54'

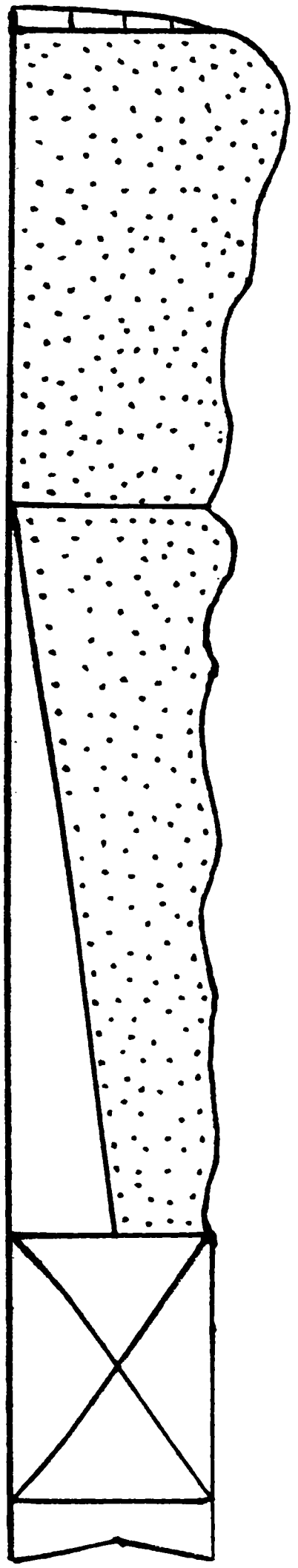

Figure B.9. Young Ranch Section 5.

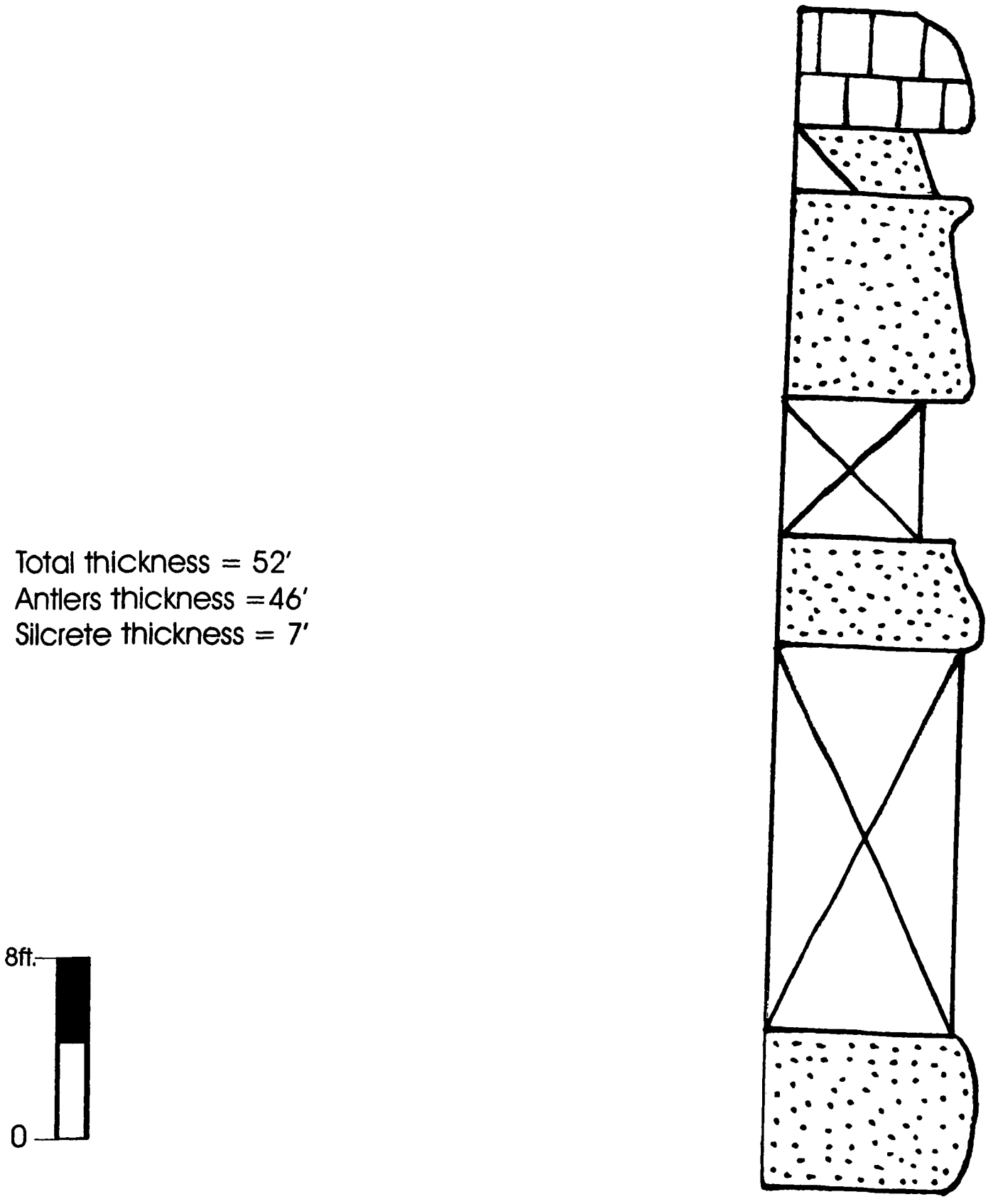

Figure B.10. Young Ranch Section 6.

Total thickness = 19'
Antlers thickness = 19'
Silcrete thickness = 19'

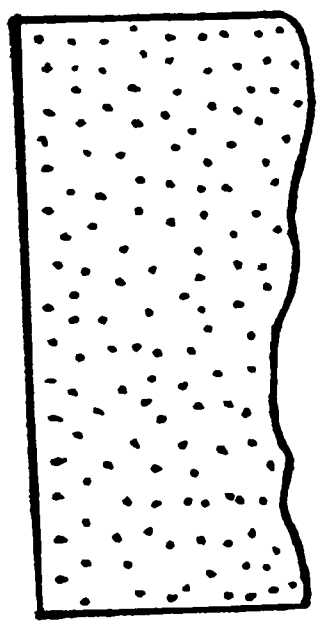

Figure B.11. Young Ranch Section 7.

Total thickness = 14'
Antlers thickness = 12'
Silcrete thickness = 12'

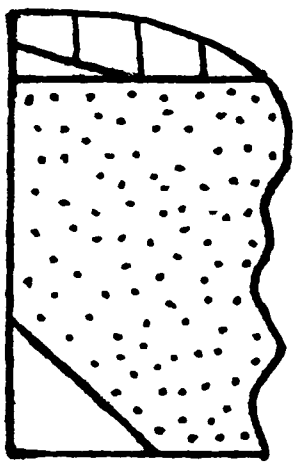

Figure B.12. Young Ranch Section 8.

Total thickness = 11'
Antlers thickness = 11'
Silcrete thickness = 11'

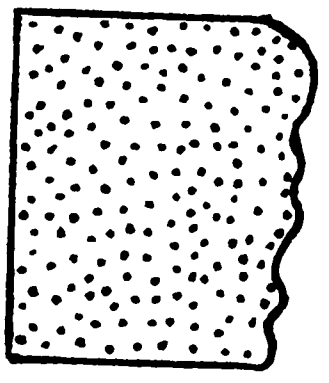

Figure B.13. Young Ranch Section 9.

APPENDIX C

POINT COUNT DATA

Table C.1. Antlers Point Count Data

Sample	Mono-S	Mono-U	Poly	Chert	OverGwth	Microqtz	Fe/other	Porosity	Total
LW-2-2	143	62	13	4	0	49	21	8	300
LW-3-1	141	60	18	6	45	9	3	18	300
LW-3-2	138	51	16	13	51	14	5	12	300
LW-3-3	135	68	17	8	46	0	10	16	300
LW-3-4	131	66	18	14	33	4	8	26	300
LW-3-5	159	54	18	15	33	3	1	17	300
LW-3-6	122	49	19	10	7	3	81	9	300
LW-3-7	114	96	21	0	41	10	2	16	300
LW-3-8	124	80	26	4	38	13	7	8	300
LW-3-9	103	23	68	34	19	3	50	0	300
LW-3-10	143	61	22	19	48	4	3	0	300
LW-3-11	115	84	12	23	0	64	2	0	300
LW-3-12	117	65	27	13	31	1	46	0	300
LW-3-13	109	71	15	13	29	2	61	0	300
LW-4-1	184	71	8	4	0	0	20	13	300
LW-7-1	144	54	15	3	39	2	26	17	300
LW-7-2	176	61	19	3	31	4	2	4	300
LW-7-3	137	49	38	19	31	6	3	17	300
LW-8-3	118	77	5	7	23	55	9	6	300
LW-9-1	142	62	5	11	38	0	32	10	300
LW-10-1	159	48	18	10	31	18	3	13	300
LW-10-2	138	39	18	15	2	34	12	42	300
LW-10-3	146	51	3	15	1	45	39	0	300
LW-10-4	165	89	15	9	12	2	0	8	300
LW-10-5	150	75	12	3	43	11	0	6	300
LW-10-6	133	71	20	13	39	0	4	20	300
LW-10-7	119	55	26	31	38	22	3	6	300
LW-10-8	140	73	14	3	46	19	3	2	300
LW-10-9	158	45	37	11	26	4	2	17	300
LW-10-10	133	88	19	2	41	6	2	9	300
LW-10-11	123	77	17	11	38	12	8	14	300
LW-12-1	144	63	27	4	48	0	0	14	300
LW-13-1	126	97	29	11	21	0	0	16	300
LW-13-2	118	90	21	9	42	7	5	8	300
LW-13-3	137	77	23	14	39	4	0	6	300
LW-13-4	113	76	33	21	45	2	1	9	300
LW-13-5	145	69	13	16	41	0	3	13	300
LW-13-6	123	65	27	19	26	9	17	14	300
LW-14-1	162	38	19	5	1	0	7	68	300
LW-14-2	151	73	14	8	7	0	1	46	300
LW-14-3	129	87	12	31	4	0	5	32	300
LW-14-7	144	34	23	11	0	67	2	19	300
LW-14-8	132	49	17	4	0	61	0	37	300
SUM	5883	2793	857	499	1174	569	509	616	12900
	0.456	0.217	0.066	0.039	0.091	0.044	0.039	0.048	1
	45.605	21.651	6.643	3.868	9.101	4.411	3.946	4.775	
		Percentage of each cement			0.674	0.326			
LW-7-4	146	41	26	1	0	0	81	5	300
LW-14-9	126	47	34	9	0	0	81	3	300
LW-14-10	123	39	31	12	0	0	78	17	300
LW-14-11	112	46	28	17	0	0	82	15	300

PERMISSION TO COPY

In presenting this thesis in partial fulfillment of the requirements for a master's degree at Texas Tech University or Texas Tech University Health Sciences Center, I agree that the Library and my major department shall make it freely available for research purposes. Permission to copy this thesis for scholarly purposes may be granted by the Director of the Library or my major professor. It is understood that any copying or publication of this thesis for financial gain shall not be allowed without my further written permission and that any user may be liable for copyright infringement.

Agree (Permission is granted.)

Student Signature Date

Disagree (Permission is not granted.)

Student Signature Date